UNIVERSITÀ DELLA CALABRIA

Dipartimento di Biologia, Ecologia e Scienze della Terra

Scuola di Dottorato: "Life Sciences"

CICLO XXVII

In co-tutela di tesi con
Flanders institute for biotechnology (VIB)-Department of Plant Systems Biology
University of Ghent- Belgium

Con il contributo di POR CALABRIA FSE 2007/2013
Settore strategico Polo di Innovazione regionale:
"Tecnologie per la gestione Sostenibile delle Risorse Ambientali"

The Elongator complex in plant: a study of its molecular network

Settore Scientifico Disciplinare BIO/01 Area 05

Direttore della scuola:

Prof. Marcello Canonaco

Supervisore:

Prof. ssa Maria Beatrice Bitonti

Co-Relatore:

Prof.ssa Mieke Van Lijsebettens

Dottoranda:

Dott.ssa Olimpia Gagliardi

Index

website:

http://arabidopsis.info/NASC
http://bar.utoronto.ca/efp
https://bioinformatics.psb.ugent.be/cornet

Abstract

The Elongator complex is a histone acetyltransferase complex associated with RNAPII to facilitate transcript elongation. It's composed of six proteins (ELP1-6). ELP1-3 form the Elongator core subcomplex, while ELP4-6 form the accessory subcomplex. Elongator complex, firstly identified in yeast, was later isolated from animals and plants and all its six subunits are evolutionarily conserved. The Elongator activity is conferred by ELP3 that targets specifically histons H3 (lysine-14) and H4 (lysine-12) by acetylating histone in order to facilitate the RNAPII progresses through the nucleosome. In yeast, mutations in Elongator subunits induce delay in growth due to a slowly adaptation to changing environmental conditions. In human, mutations in Elongator components affect neuronal development and this leads to neuronal disease. Whereas, in plant Elongator stimulates plant growth acting a positive regulator of cell proliferation. At the phenotypic level, Elongator mutants, called elongata, are known for narrow leaves and short root.

In the present work, by using the model plant *Arabidopsis thaliana*, we investigated some aspects of molecular networks underlying Elongator activity and its interaction with environmental factors, mainly focusing on light conditions. Based on previous unpublished data obtained through TAP analysis, in the first period of PhD project we focused the attention on the functional study of *Sec31* gene encoding a protein involved in cell secretory pathway, identified as a putative direct interactor of Elongator complex. To add information on this interaction we analyzed phenotypic and developmental characteristics of *sec31* mutants to compare with *elo3-6* mutant. The histological expression pattern of *Sec31* and *ELO3* transcripts in wild type seedlings was also investigated, through multiprobe *in situ* hybridization, to compare organ/tissue specific expression domains. The obtained results showed that expression pattern of the two genes is quite similar while *sec31* mutants do not resemble *elo3-6* phenotypes. Moreover further TAP experiments and in silico analysis of protein/protein interaction did not confirm previous data, thus excluding a direct interaction between ELO3 and Sec31.

However, expression analysis in *sec31* mutants of some Elongator-related genes, performed by qRT-PCR, showed that *Sec31* and *ELO3* share common downstream target genes and both seem play a role in auxin pathway. Future trascriptomic analyses on auxin mutants on one side, and the identification of possible interactors/players of both genes on the other side, could be useful to deepen if the molecular circuits, by which Elongator complex and the secretory machinery act on auxin pathway, show some cross-talk or they work in an independent manner.

A further aspect of Elongantor molecular network that we investigated deals with role of Elongator in the skoto/photomorphogenesis pathways. In particular we investigated the *elo3-6* mutant in darkness and under light condition (red, far-red and blue light) through microarray and

RNA-seq approaches. Gene ontology categories over representative in *elo3-6* seedlins, identified by BINGO analysis, allowed us to discover the putative targets of Elongator both in darkness and in light, and to understand the position of whole Elongator complex along either pathways. The results suggested that Elongator complex takes part in the skotomorphogenesis and photomorphogenesis and is dependent on photoreceptors PHYA and PHYB. Microarray, RNA-seq, qRT-PCR and ChIP-qPCR analyses displayed that Elongator regulates transcription of some genes both in light and in darkness. In the specific, results displayed that Elongator complex participates in the skoto/photomorphogenic pathways by binding target genes such as *HYH* and *LHY* in light and darkness condition, respectively. Whereas it can regulate the activity of other putative targets such as *Pifs* gene (*PIF4*) in darkness and *HY5* under light condition.

I° Chapter: General introduction

In all organisms the genetic information, that regulates their growth and development is stored in the DNA molecule. The eukaryotic cell developed a strategy to compact the long DNA molecule within the nucleus by wrapping it into a nucleoprotein complex which is referred as chromatin. Proteins that mediate the successive orders of DNA folding are represented by different histone classes: two copies each H2A, H2B, H3 and H4 histones form a protein core that wraps 146 base pairs of DNA tightly on its surface to form the core nucleosome (Kornberg & Lorch, 1999) (Figure 1). The linker histone H1 is not a part of core nucleosome but binds the DNA between two core particles and connects one nucleosome to the next one leading to the final chromatin structure. At the cytological level, in a non-dividing cell two different types of chromatin organization (i.e. decondensed or tightly dense) can be observed which correspond to different functional states (i.e. transcriptionally active or inactive DNA) an relate to a different DNA packaging and nucleosome arrangment: these two organization/functional states are indicated as euchromatin or heterochromatin (Jenuwein and Allis, 2001; Kouzarides, 2007; The ENCODE Project Consortium, 2007). Euchromatin is the region where DNA is accessible, representing an open conformation due to the relaxed state of nucleosome arrangement. The genomic regions of euchromatin are more flexible, and contain genes in active and inactive transcriptional states (Jenuwein and Allis, 2001; Kouzarides, 2007; The ENCODE Project Consortium, 2007; Koch, *et al*, 2007). Conversely, heterochromatin are areas where DNA is packaged into highly condensed forms that are inaccessible to transcription factors or chromatin-associated proteins (Jenuwein and Allis, 2001; Talbert and Henikoff, 2006; Huang, *et al*, 2004). The genomic regions within heterochromatin primarily consist of repetitive sequences and repressed genes associated with morphogenesis or differentiation (imprinting or X chromosome inactivation) (Reik, 2007; Feinberg and Tycko, 2004).
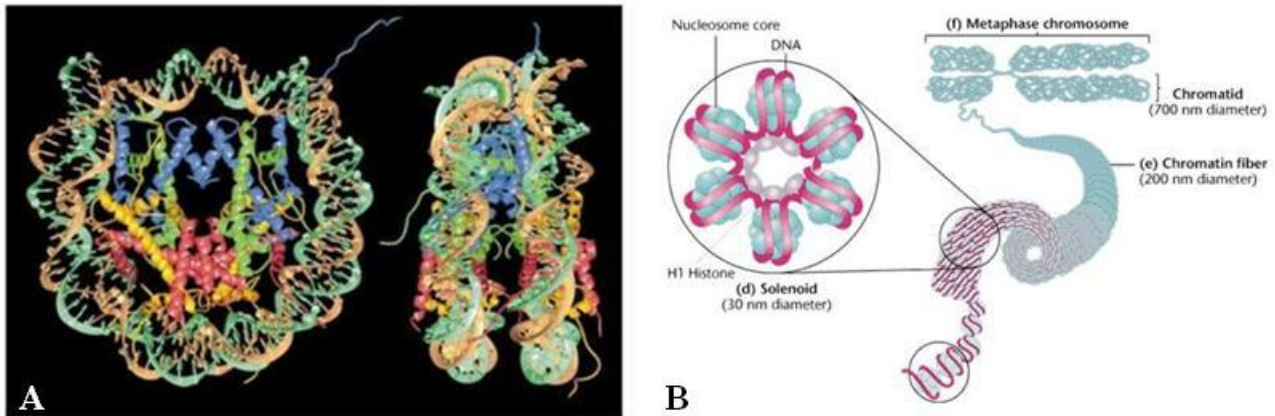
Figure 1. (A). Nucleosome core particle: ribbon traces for the 146-bp DNA phosphodiester backbones (brown and turquoise) and eight histone protein main chains (blue: H3; green: H4; yellow: H2A; red: H2B. The views are down the DNA superhelix axis for the left particle and perpendicular to it for the right particle. For both particles, the pseudo-twofold axis is aligned vertically with the DNA center at the top. **(B)** *Stabilization of the 30 nm chromatin by binding of the histone H1*
First picture from (Luger, *et al* 1997). Second picture from Klug & Cummings (1997 p542)

Thus beside packaging DNA into a smaller volume to fit into the cell, relevant functions of chromatin are to control DNA replication, chromosomal stability and gene expression. The dynamics of chromatin structure is tightly regulated through multiple mechanisms including histone modification, chromatin remodeling, histone variant incorporation, and histone eviction. In this chapter we want focus our attention on mechanisms of chromatin regulation and how such regulation controls gene expression during transcription.

Ia - The process of transcription in eukaryotic organism

Transcription is the process by which the information stored in the DNA double strand is copied into a new molecule of messenger RNA (mRNA). RNA synthesis involves separation of the DNA strands and synthesis of an RNA molecule from 5' to 3' direction by RNA polymerase, using one of the DNA strands as a template. Transcriptional regulatory mechanisms modulate the accurate recruitment and activation of RNA polymerase at different locations in the genome, such as gene promoters. Transcriptional regulators can be grouped into three types. First, the preinitiation complex (PIC) which binds at the core promoter and recruits RNAPII. Second, DNA-binding transcription factors which bind to sites such as proximal promoter elements and enhancers. Third, enzymes that modify the higher-order chromatin structure by promoting the physical movement of nucleosomes relative to the genome and post-translationally modify histone molecules to alter the stability and accessibility of chromatin RNA polymerases are large multi-subunit enzymes that

_____

perform transcription and thus produce all the RNAs in the cell from a DNA template. These complexes are assembled and tightly bound at the promoter of genes before initiating transcription. Different RNA polymerases identified in eukaryotic organisms are responsible for the synthesis of ribosomal RNA (RNAPI), pre-messenger RNA (RNAPII) and small RNAs including transfer RNA (RNAPIII) respectively (Cramer, 2002). Plants are unique in having evolved multisubunit RNA polymerases IV and V in addition to RNAPI, II, and III, the three ubiquitous nuclear DNA-dependent RNA polymerases of eukaryotes. RNAPIV and V synthesize noncoding RNAs for transcriptional silencing of transposons, repetitive elements, and a subset of genes (Haag and Pikaard; 2011; Herr *et al*., 2005; Kanno *et al*., 2005; Onodera *et al*., 2005; Pontier *et al*., 2005; Ream *et al*., 2014). The RNA polymerase structure is broadly conserved from prokaryotes to all eukaryotes (Saltzman and Weinmann, 1989). All RNA polymerase types are believed to have diverged from a common ancestral protein, as some subunits are shared between them. RNAPII uniquely possesses an extra C-terminal domain (CTD) on its largest subunit, it acts both in the recruitment of RNAPII to active promoters and as a binding platform for other proteins involved in transcription. Here, we will focus on RNAPII and its regulation, as it is at the origin of the production of all proteins in the cell. The transcription is divided into an initiation stage, during which transcription factors and RNAPII bind to promoter sites and RNA synthesis starts, followed by an elongation stage, during which RNAPII traverses along the DNA assembling an RNA transcript (Ponting, 2002).

Ia1. - Transcription initiation, elongation and termination

Transcription iniziation

The RNAPII arranges on the promotor region a complex formed by several proteins including factors. These proteins form the basis of the pre-initiation complex and they are responsible for the position of polymerase at the core promoter region as well as induce the separation of DNA helix to facilitate polymerase movement along DNA and allow transcription elongation. The promoter region includes a sequence called TATA-box (about 30 bp upstream from the transcription start site) that is recognized by a multisubunits protein complex called TFIID (Transcription Factor for polymerase II). One subunit of TFIID that binds TATA-box is called TBP (*TATA binding protein*), whereas the other subunits of this complex are called TAF (*TBP associated factors*). Some of the TAF proteins participate in the link whit the promoter and also control the

_____

dynamic of TBP connection at DNA. TBPs are associated with TAF and these last show a structural homology with histone proteins. Accordingly it was proposed that TAF proteins could link the DNA in the same manner as histones, although experimental evidences for that have not yet been provided. So far, it has been only shown that in *Drosophila* TAF42 and TAF6 form a similar structure as the H3·H4 tetramer. These histone-like TAF proteins are localized in the TFIID complex and associated to enzymes involved in histones modification such as the SAGA complex.

Currently, the role of the various transcription factors in directing transcription initiation is the subject of intense study. The TFIIB interacts directly with TBP, to form TFIIB-TBP-DNA complex, and with polymerase II. Therefore TFIIB, makes a bridge between TBP and polymerase II. While TBP and TFIIB play central roles in the nucleation of the transcription initiation complex, TFIIF, TFIIE, and TFIIH play roles at later steps. TFIIF interacts directly with RNA polymerase II and TFIIB and is required for stable assembly of RNAPII with the TATA-TBP-TFIIB complex. The factor TFIIE joins the complex TATA-TBP-TFIIB-RNA and this promotes the link with TFIIH. TFIIE and TFIIH promote melting and clearance through ATP hydrolysis. TFIID regulates the activities of TFIIH which possesses ATP-dependent helicase activity and also kinase activity which allows it to phosphorylate the C-terminal domain of RNAPII. Indeed the bigger subunit of RNAPII has a C-terminal domain (called CTD) which exhibits a tail rich in phosphorylation sites. In addition, TFIIE plays a direct role in promoter melting, perhaps by binding to the single-stranded region and thereby stabilizing the melted region of the promoter moreover it participates in the recruitment of TBP and TFIIA to the TATA box. The different GTFs together with the RNAPII complex form the "pre-initiation complex" (PIC) (Figure. 2).

In summary the activation of transcription by Polymerase requires DNA-binding by general transcription factors that form the PIC, so that transcriptional activator and co-activator then interact with the complex to initiate transcription.
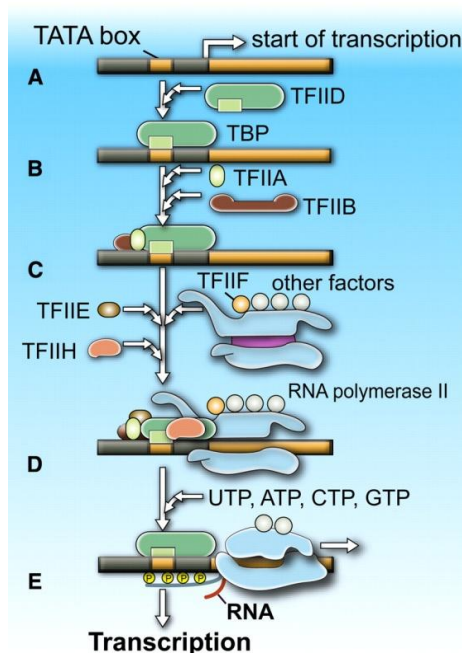
Figure 2. Transcription initiation in eukaryotes. To start transcription, eukaryotic RNA polymerase II requires the general transcription factors. These transcription factors are assembled around TATA-box sequence. TFIIH uses ATP to pry apart the double helix at the transcription start point, allowing transcription to begin. TFIIH also phosphorylates RNA polymerase II, releasing it from the general factors so it can enter the elongation phase of transcription. (Alberini, *2009, Physiol Rev*).

Transcription elongation

Following the transcription activation, elongation phase takes place when RNAPII get away from transcription initiation factors and moves into the (towards) coding region. This event triggers the recruitment of the elongation machinery, which includes the factors involved in polymerization, mRNA processing, mRNA export, and chromatin function (Hahn, 2004). Cells exploit a very sophisticated array of factors to control chromatin architecture during elongation, and the events and factors required at the beginning of the gene differ significantly from those required at the end (Li., *et al*, 2007). This is done not only to promote efficient RNA synthesis but also to ensure the integrity of the chromatin structure while RNAPII travels through the body of the gene. The transcription elongation requires new factors able to stimulate the elongation of RNAPII through phosphorylation of its CTD. The RNAPII CTD undergoes two major phosphorylation changes during elongation: Ser5 is phosphorylated by TFIIH at the 5' end of the ORF, and Ser2 is phosphorylated by the Ctk kinase as RNAPII transits toward the 3'end. These phosphorylation events appear to control the elongation processes and couple them with alterations in chromatin structure. One of proteins involved in the elongation of RNAPII is a kinase P-TEFb which phosphorylate the CTD of RNAPII on Ser5 and Ser7. Important components which bind RNAPII during elongation are SAGA, FACT, PAF, TFIIS, RAD6/Bre1, COMPASS, and many others (Figure 3). Most of these complexes play a function in relaxing the chromatin state to allow RNAPII passage during transcription but recently another level of transcriptional regulation has been identified during elongation.
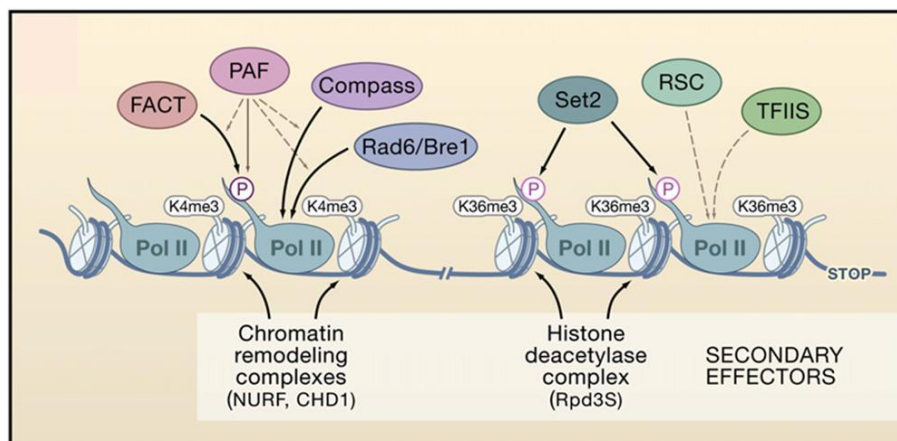

Figure 3. **Regulation of Nucleosome Dynamics during Transcription Elongation.**
The chromatin landscape during elongation is determined by the factors associated with different forms of RNAPII. PAF facilitates the binding of FACT, COMPASS, and Rad6/Bre1 to the Ser5-phosphorylated CTD. (Li., *et al*, 2007).

A series of discoveries suggest that many developmental and inducible *Drosophila* and mammalian genes, prior to their expression, contain RNAPII bound predominantly in their promoter proximal regions in a "stalled" state (Saunders, *et al.*, 2006; Sims, *et al.*, 2004) Genome-wide surveys of the phenomenon suggest that RNAPII stalling is likely to be a rate-limiting control on gene activation that poises developmental and stimulus-responsive genes for prompt expression when inducing signals are received. In addition, stalled RNAPII signals are associated with active histone modification marks, including trimethylation of lysine 4 on histone H3 (H3K4me3) and acetylation of H3 lysine 9 and 14 (H3K9ac and H3K14ac) (Guenther, *et al.*, 2007). Thus, RNAPII promoter-proximal stalling could help to provide an active chromatin environment and prepare developmental and stimulus-responsive genes for timely expression (Saunders, *et al.*, 2006; Lorincz and Schubeler, 2007). RNAPII promoter-proximal stalling was first described in *Drosophila* heat-shock-inducible *Hsp70* genes by using ultraviolet-crosslinking and chromatin immunoprecipitation (UV ChIP). RNAPII was found to be recruited to the promoter of the un-induced *Hsp70* gene, where initiates RNA synthesis but stalls after synthesis of 20-50 nucleotides of RNA (Saunders, *et al.*, 2006; Rasmussen and Lis, 1993). Heat-shock stimulation enabled RNAPII to escape from the Hsp70 promoter-proximal region and transcribe the full-length RNA. This suggests that regulation through pausing is a fundamental step for controlling developmental programs and enabling rapid reaction to environmental stimuli (Zeitlinger, *et al.*, 2007) Studies have revealed that TEFs regulate plant growth and development by modulating diverse processes including hormone signaling, circadian clock, pathogen defense, responses to light, and developmental transitions (Van Lijsebettens and Grasser, 2014). Indeed in plant the transcription of genes that are affected by the depletion of different TEFs can cause different types of growth and/or developmental defects.

Transcription termination

Termination occurs when RNAPII ceases RNA synthesis and both RNAPII and the nascent RNA are released from the DNA template. Transcription termination is important because it prevents RNAPII from interfering with downstream DNA elements, such as promoters, and promotes polymerase recycling. RNAPII termination can be elicited through different pathways, depending on the RNA 3′-end processing signals and termination factors that are present at the end of a gene (Richard & Manley, 2009; Lykke-Andersen & Jensen, 2007; Rondon, *et al*, 2008). Two models for transcription termination were proposed to explain the role of 3′-end processing. The first model, known as the allosteric or anti-terminator model, proposes that transcription through the

poly(A) site leads to conformational changes of the elongation complex (EC) by dissociation of elongation factors and/or association of termination factors (Logan, *et al*., 1987). The second model, the torpedo model, is based on the observed rapid degradation of the 3′ RNA after cleavage at the poly(A) site. Cleavage creates an entry site for a 5′–3′ exonuclease at the uncapped 5′-monophosphate, which degrades the RNA and, according to this model, in some way promotes RNAPII release upon "catching up" with RNAPII (Connelly and Manley, 1988). In summary, transcription takes place through the recruitment and action of multiple regulatory factors.

Ib1. - Role of chromatin state in the transcription

In eukaryotic cells the genomic DNA is packaged with histone proteins and this organization has double function, one is the need to compact 2 m of DNA into the small space of the nucleus and the other one plays a role in the gene transcription regulation. Decompaction of chromatin to facilitate access to DNA has been most widely studied for RNAPII-mediated transcription of protein-coding genes, a process that requires rapid access to genes for the response to environmental signals and programmed cellular events, but the underlying principles are equally applicable to any process requiring interaction with DNA (George Orphanides and Danny Reinberg, 2000). Recent reports confirm that eukaryotic cells are equipped with specialized proteins that help RNAPII pass through chromatin during transcription elongation. In order to facilitate the transcription of specific genes the chromatin must be available and this chromatin state is called "open chromatin" since the structure of chromatin is disrupted from the promoter region of the gene to the entire transcribed domain. During transcription the chromatin transcribed region reveals alteration at the level of histone proteins themselves. Indeed chromatin state undergoes many modifications through the action of many different proteins. by using a chromatin remodelling proteins complex such as ATP-dependent chromatin-remodeling complexes and covalent histone modifications. The ATP-dependent chromatin-remodeling complexes manipulate chromatin structure by using energy from ATP hydrolysis to disrupt chromatin and make DNA more accessible to DNA-binding proteins. The other class of histone modifications, covalent histone modifications, act on histone tails by modification of one or more amino acids that results in activation or repression of transcription. The activity carried out from the complexes involved in chromatin modification plays an important role during the life of an organism, because in that way they can regulate gene activity and expression during the phase of organism development and differentiation, or in response to environmental stimuli.

Ib1a - ATP-dependent chromatin-remodeling

The ATP-dependent chromatin-remodeling complexes. are conserved in evolution, and there is more than one type of complex in each cell All of the ATP-dependent chromatin-remodeling complexes contain an ATPase subunit that belongs to the SNF2 superfamily of proteins. Based on the identity of this subunit, they have been classified into two main groups, the SWI2/SNF2 group and the imitation SWI (ISWI) group (Eisen, *et al.*, 1995). Their mechanism of action is similar but the SWI/ SNF and NURF complexes utilize the energy of ATP hydrolysis to alter nucleosome structure, however, while the Swi2/ Snf2 ATPase of SWI/SNF is induced by either DNA or nucleosomes (Coˆteˊ, *et al.,* 1994). The SWI2/SNF2 group includes RSC that requires nucleosomes with intact histone amino-terminal tails for maximum stimulation. The results of Kasten *et al*, 2004, showed that Rsc4 is an integral and essential member of RSC preferential binding to the histone H3 peptide acetylated at Lys14 This means that both RSC and ATP-dependent chromatin-remodeling protein are involve the dynamic modification of chromatin architecture. In particular Rsc4 bromodomains recognize acetylated H3 Lys14 and cooperate with H3 Lys14 acetylation for their function. These results highlight the important role bromodomains play in the coordination of chromatin remodeling with histone acetylation in transcriptional regulation, and reveal new properties of tandem bromodomain function (Kasten, *et al*., 2004) The *Arabidopsis* genome encodes more than 40 different proteins belonging to ATP-dependent chromatin remodeling complexes, which can be grouped into three major types, namely SWI2/SNF2, ISWI and CHD based on the presence of other protein motifs in addition to the ATPase domain. Among them, only AtBRM, SPLAYED (SYD), PICKLE (PKL), DECREASE IN DNA METHYLATION (DDM1), MORPEUS MOLECULE (MOM), DRD1 and PHOTOPERIOD INDEPENDENT EARLY FLOWERING1 (PIE1) have been functionally characterized (Hsieh and Fischer, 2005).

In *Arabidopsis* SWI/SNF ATPases: SPLAYED (SYD) plays a specific role in maintenance of the stem cell pool in the shoot apical meristem, it's involved in floral transitino and ovule development. Whereas BRM is involved in the control of expression of two regulators of cotyledon separation: the CUP-SHAPED COTYLEDON genes CUC1 and CUC3 (Kwon, *et al.*, 2006). The *SPLAYED* (*SYD*) gene product acts as a LFY-dependent repressor of the meristem identity switch in the floral transition. SYD regulates flowering in response to environmental stimuli which in plant may be achieved in part by regulating transcription factor activity via alteration of the chromatin state. In addition *SYD* encodes a presumptive *Arabidopsis* homolog of the yeast Snf2p ATPase, which is implicated in transcriptional control via chromatin remodeling (Wagner and Meyerowitz, 2002).

In yeast and mammals, ATP-dependent chromatin remodelling complexes of the SWI/SNF family play critical roles in the regulation of transcription, cell proliferation, differentiation and development. Homologues of conserved subunits of SWI/SNF-type complexes, including Snf2-type ATPases and SWI3-type proteins, participate in analogous processes in *Arabidopsis* (Archacki, *et al*, 2009). This means that ATP-dependent chromatin remodelling complexes of the SWI/SNF family have a functional role in plant, yeast and mammals.

Ib1b- Covalent histone modifications

The chromatin modifications may affect higher-order chromatin structure by disrupting the contact between different histones in adjacent nucleosomes or the interaction of histones with DNA. Numerous studies have been performed to discover proteins catalysing histone modifications and understand their mode of action. Simplistically, the function of histone modifications can be divided into two categories: the establishment of global chromatin environments and the orchestration of DNA-based biological tasks. The histone tails are subject to a vast array of posttranslational modifications that include: methylation of arginine (R) residues; methylation, acetylation, ubiquitination, ADP-ribosylation, and sumolation of lysines (K); and phosphorylation of serines and threonines (Table 1). Modifications that are associated with active transcription, such as acetylation of histone 3 and histone 4 (H3 and H4) or di- or trimethylation (me) of H3K4, are commonly referred to as euchromatin modifications. Modifications that are localized to inactive genes or regions, such as H3 K9me and H3 K27me, are often termed heterochromatin modifications (Li.*, et al*, 2007). In the following section we discuss only about the function and role of "Histone acetylation" on transcription regulation because it is the histone modification around which this thesis has developed.

Table 1. Histone Modifications Associated with Transcription

Modifications	Position		Enzymes				Recognition Module(s)[a]	Functions in Transcription
			S. cerevisiae	*S. pombe*	*Drosophila*	Mammals		
Methylation	H3	K4	Set1	Set1	Trx, Ash1	MLL, ALL-1, Set9/7, ALR-1/2, ALR, Set1	PHD, Chromo, WD-40	Activation
		K9	n/a	Clr4	Su(var)3-9, Ash1	Suv39h, G9a, Eu-HMTase I, ESET, SETBD1	Chromo (HP1)	Repression, activation
		K27				E(Z)	Ezh2, G9a	Repression
		K36	Set2			HYPB, Smyd2, NSD1	Chromo(Eaf3), JMJD	Recruiting the Rpd3S to repress internal initiation
		K79	Dot1			Dot1L	Tudor	Activation
	H4	K20		Set9	PR-Set7, Ash1	PR-Set7, SET8	Tudor	Silencing
Arg Methylation	H3	R2				CARM1		Activation
		R17				CARM1		Activation
		R26				CARM1		Activation
	H4	R3				PRMT1	(p300)	Activation
Phosphorylation	H3	S10	Snf1				(Gcn5)	Activation
Ubiquitination	H2B	K120/123	Rad6, Bre1		Rad6	UbcH6, RNF20/40	(COMPASS)	Activation
	H2A	K119				hPRC1L		Repression
Acetylation	H3	K56					(Swi/Snf)	Activation
	H4	K16	Sas2, NuA4		dMOF	hMOF	Bromodomain	Activation
	Htz1	K14	NuA4, SAGA					Activation

[a] The proteins that are indicated within the parentheses are shown to recognize the corresponding modifications but specific domains have yet to be determined.

Table 1. Overview of different classes of modification identified on histones. The function have been associated with each modification are shown. (Li and Workman, 2007)

Histone acetylation

The acetylation and deacetylation are the most studied histone modifications, that play a role in gene activation and repression, respectively. The modification is reversible and is defined by a fine-tuned balance between the activity of histone acetyltransferases (HATs) and histone deacetylases (HDACs) to regulate gene expression. Histones are acetylated at N-terminal lysine residues. The source of the acetyl group in histone acetylation is acetyl-Coenzyme A and in histone deacetylation the acetyl group can be transferred back to Coenzyme A or to ADP-ribose by the NAD-dependent deacetylases (Denu, 2003). Histone acetylation neutralizes the positive charge of the target lysine residue, thereby changing the overall charge distribution of the histone tails and decreasing its affinity for DNA. The resulting change of nucleosomal conformation increases the accessibility of transcriptional regulatory proteins to the chromatin template, suggesting that histone acetylation is correlated with increased transcriptional activity. HAT activity is important for transcription initiation, in addition to a number of transcriptional coactivators. Several HAT

complexes can be recruited to promoter regions by direct interactions with DNA-binding activators, resulting in increased DNA accessibility and stimulation of transcription initiation (Utley, *et al*, 1998; Chan & La Thangue, 2001). Whereas the histone acetylation induces transcriptional activation, the Histone deacetylases (HDACs) in turn interact with transcriptional repressors, suggesting that deacetylation is involved in repression and silencing (Courey and Jia, 2001).

Based on the sequences outside the acetyltransferase domain, the HATs can be divided into four subfamilies: the Gcn5-related N-terminal acetyltransferases (GNAT), the MYST family, the CBP/p300 family, the family related to mammalian TAF250. Sequence and domain analyses of the *Arabidopsis* genome have revealed four families of HATs, and three families of HDAC, consisting of 12 genes and 18 genes respectively (Pandey, *et al*., 2002). The identification of plant-specific HD2 family of HDACs (Lusser, *et al*., 1997) provides an indication for functional diversification of histone-modifying proteins in plants. The N-terminal lysine residues of histone H3 (K9, K14, K18, K23, and K27) and H4 (K5, K8, K12, K16, and K20) are found to be acetylation/deacetylation targets in *Arabidopsis* (Zhang, *et al*., 2007; Earley, *et al*., 2007). This thesis focuses on the role of Elongator complex and their targets in plant development and their influence on the regulation on gene expression. Elongator complex is composed of six subunits (ELP1-ELP6), in particular Elp3 is a conserved member of the GNAT. Gcn5-related N-acetyltransferase) protein family, and recombinant Elp3 possesses acetyltransferase activity directed toward all four core histones (Wittschieben, *et al*, 1999). According to Winkler, 2002, both histones H3 and H4 are acetylated by holo-Elongator, the predominant site of acetylation *in vitro* is lysine-14 of histone H3 and lysine-8 of histone H4. Elp4, Elp5, and Elp6 subunits are required for Elongator HAT activity. As explained above the HAT group is divided into four types based on primary homology with yeast and mammalian. The GNAT (GCN5-related N-acetyltransferase) family is generally considered to comprise three subfamilies, designated GCN5 (General Control Nonderepressible protein5), ELP3 (a transcriptional Elongator complex Protein), and HAT1 in higher eukaryotes. In the *Arabidopsis* genome, a single homolog of each of the GCN5, ELP3, and HAT1 subfamilies (HAG1/AtGCN5, HAG3, and HAG2, respectively) has been identified (Pandey, *et al*., 2002) (Table 2) The *Arabidopsis* genome contains two MYST family genes (*HAG4* and *HAG5*), five p300/CBP genes (*HAC1*, *HAC2*, *HAC4*, *HAC5*, and *HAC12*), and two TAF1 genes (*HAF1* and *HAF2*).

HDAC gene family	Arabidopsis gene name	Gene code
RPD3/HDA1	HDA2	At5g26040
	HDA5	At5g61060
	HDA6	At5g63110
	HDA7	At5g35600
	HDA8	At1g08460
	HDA9	At3g44680
	HDA10	At3g44660
	HDA14	At4g33470
	HDA15	At3g18520
	HDA17	At3g44490
	HDA18	At5g61070
	HDA19	At4g38130
HD2	HDT1	At3g44750
	HDT2	At5g22650
	HDT3	At5g03740
	HDT4	At2g27840
SIR2	SRT1	At5g55760
	SRT2	At5g09230
HAT gene family	Arabidopsis gene name	Gene code
GNAT	HAG1/GCN5	At3g54610
	HAG2	At5g56740
	HAG3/ELO3	At5g50320
MYST	HAG4	At5g64610
	HAG5	At5g09740
CBP	HAC1	At1g79000
	HAC2	At1g67220
	HAC4	At1g55970
	HAC5	At3g12980
	HAC12	At1g16710
TAFII250	HAF1	At1g32750
	HAF2	At3g19040

Table 2. Genes encoding HAT and HDAC homologs in *Arabidopsis* (modified from Pandey, *et al.*, 2002).

The mechanism involved in histone modification influence many processes of plant development. Two HATs in plants, namely AtGCN5 and ELO3, have been analyzed functionally and have a significant effect on plant growth. They are both part of conserved complexes that have been studied primarily in yeast. The yeast GCN5 is part of the SAGA and ADA regulatory complex, where it serves as a nucleosomal HAT, capable of acetylating histone H3 (Bertrand, *et al.*, 2003). The *Arabidopsis* AtGCN5 has conserved HAT catalytic and bromodomains (Stockinger, *et al.*, 2001). The role of histone acetylation has been assigned to cell cycle, cell division, response to abiotic stimuli such as light and temperature and biotic signals linked to growth or to stress.

Removal of the acetyl group from the histones is mediated by HDACs, they consist of 3 families in plants: RPD3/HDA1 (histone deacetylase 1 protein), SIR2 (silent information regulator protein 2) and a plant-specific family of HDACs, HD2 which was discovered in maize. Exactly Four HD2 proteins are identified in Arabidopsis and they all contain a conserved N-terminus with the HD2-

type HDAC domain, a central acidic domain and variant C-terminal domain. By analyzing the sequence a single homologue is found in in the animal, fungi and Arabidopsis for all subfamilies (GCN5, ELP3, HAT1, HAG4 and HAG5) of the GNAT/MYST superfamily, suggesting that the plant proteins may form complexes similar to those formed in yeast and animals. In contrast the CREB-binding protein (CBP) and TAFII250 family of HAT proteins shows differences in domain architecture between plants and animals such as the absence of a bromodomain in the plant CBP-type HATs. The manner in which the chromatin organization influences the gene expression among different organisms depends on existing variety/diversity of enzyme involved in covalent modifications, suggesting that plants have developed mechanisms of global gene regulation related to their unique developmental pathways and environmental response.

Ib - The Elongator Complex

Ib1. - Identification of Elongator Complex in yeast, Drosophila and Human

In yeast

Studies suggested that in order to transcribe genes, the transcription machinery can recruit chromatin remodeling complex to facilitate the activation process. Among the chromatin remodeling complexes involved in post-transcriptional modification, the most prominent is histone acetyltransferase activity (HAT). It has been suggested that HATs might also assist RNAPII during transcript elongation through chromatin (Travers, 1992, Brownell and Allis, 1996; Cho, *et al*., 1998). The RNAPII isolated from native RNAPII/DNA/RNA ternary complexes in yeast chromatin is found tightly complexed with a novel multisubunit complex called Elongator. Elongator complex that was associated with the hyperphosphorylated form of RNAPII (Otero, *et al*., 1999). Holo-Elongator is an unstable six-subunit complex composed of two subcomplexes: core-Elongator, comprised of Elp1, Elp2, and Elp3 (Wittschieben, *et al*, 1999; Otero, *et al*, 1999; Fellows, *et al*, 2000), and a smaller three-subunit module composed of Elp4, Elp5, and Elp6 (Winkler, *et al*, 2001, Li, *et al*, 2001). The yeast Elongator complex consists of two WD40 proteins, Elongator factor protein 1 (ELP1) is involved in maintaining Elongator's structural integrity and ELP2 that mediate protein-protein interaction. The ELP3 subunit possesses a C-terminal histone acetyl transferase (HAT) and radical *S*-adenosylmethionine domains activity, whereas the three RecA-like proteins, ELP4, ELP5, and ELP6, which form a hexameric RecA-like ATPase, all of which are conserved.

The yeast ELP3 has motifs characteristic for the GCN5 family of HATs and acetylated in vitro histone H3 and H4 and all the core Elongator components are essential for in vivo histone acetylation (Winkler, *et al*, 2002). In nature the competition between organisms triggers different modes of action such as the secretion of toxic compounds that results in the killing or growth arrest of other species or genera. The yeast *Kluyveromyces lactis* secretes a toxin, called zymocin, which inhibits the growth of various sensitive yeast genera, including *Saccharomyces cerevisiae.* The native toxin is a heterotrimeric (αβγ) structure composed of three subunits, two of which are involved in facilitating toxin entry. Cytotoxicity resides solely within the γ subunit, and intracellular expression of this subunit alone in *S. cerevisiae* abrogates growth (Butler, *et al*, 1991). In particular the function of zymocin on *S. cerevisiae* is to inhibit the adenylate cyclase by the role of cAMP necessary for mitotic growth and cell division. Genetic screening for mutations that confer resistance toward the intracellular expression of the zymocin γ subunit identified genes that were named *TOT1–7* (toxin target) (Jablonowski, *et al*, 2001, Frohloff, *et al*, 2001). Interestingly, the initially isolated genes TOT1-7 shown to be allelic to the genes encoding the subunits of each yeast Elongator (Elp1/Tot1/Iki3, Elp2/Tot2, Elp3/Tot3, Elp4/Tot7, Elp5/ Tot5/Iki1, and Elp6/Tot6).

In addition, other genes in *S. cerevisiae* were identified which confer resistance to zymocin upon mutation, KTI11, KTI12, KTI13 and KTI14 (Fichtner, *et al*., 2002). The experimental results show that cells lacking *KTI12* or Elongator (*ELP*) genes are insensitive to the toxin zymocin. The deletion of *KTI12* doesn't affect the integrity of Elongator complex, whereas it strongly supported the idea that Kti12 is required for the normal (HAT) activity of Elongator complex *in vivo*. Based on the latter finding, Kitamoto, *et al.,* 2002 suggested that situations favoring histone hyperacetylation might reduce the cellular requirement for the HAT activity of Elongator and thereby reduce zymocin toxicity.The *S. cerevisiae* genome encodes other histone acetyltransferase (HAT) activities than the one associated with Elp3 (Tot3p) (Wittschieben, *et al*, 1999). Other HAT gene knockout, GNC5, HAT1, SAS3, HAPA3 were tested using zymocin eclipse assays, and only HAPA1 (isoallelic of TOT3/ELP3) remained zymocin sensitive. This lead to suppose that HAT activity appears to be required for zymocin action and in fact Elp3/Tot3p possess that activity (Figure 4). The Elongator mutants showed a resistance to zymocin but also a delay in growth. The slower adaptation is a consequence of decreased/delayed transcription of the GAL1-10 (galactose-inducible genes) transcripts.
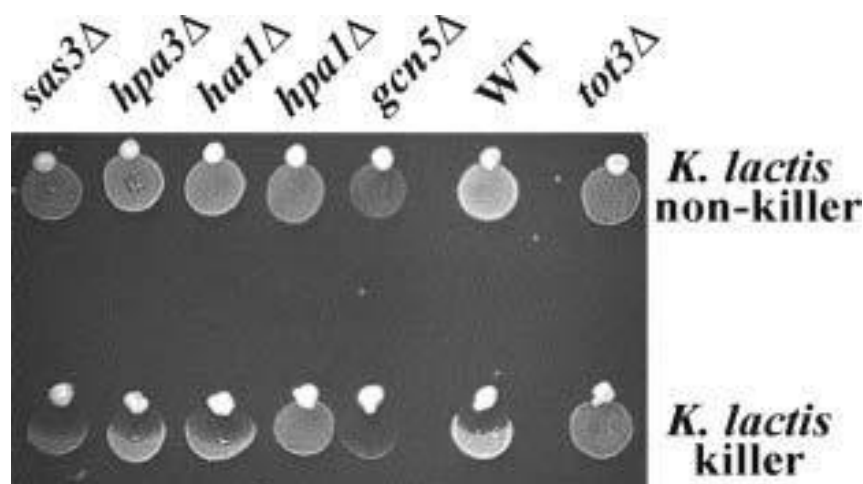
Figure 4. Effect of HAT gene deletions on zymocin sensitivity. Strains lacking non-Elongator HATs (*sas3Δ, hpa3Δ, hat1Δ, , hpa1Δ, gcn5Δ , WT, tot3Δ*) are subjecte to a killer eclipse assay. Deletion of TOT3/ELP3 confers zymocin resistance, whereas the other HAT gene deletions tested arrre zymocine sensitive.

In Human and Drosophila

Subsequently to yeast, the Elongator complex has been purified in human as a six-subunit complex and it is composed of the IKAP homologue of Elp1, hELP3, StIP1 homologue to yeast Elp2, hELP4 and two additional unidentified proteins. In human IKAP was located in the nucleus, the nucleoli and cytoplasm by immunostaining suggesting multiple roles in the cell.

In 2001, Slaugenhaupt, 2002 and Anderson *et al,* 2001 reported that mutation in *IKBKAP* (IKAP is the protein encoded by *IKBKAP*) are responsible for a syndrome called Familial dysautonomia (FD). This disease is an autosomal recessive disease resulting from poor development and progressive degeneration of the sensory and autonomic nervous system. The individuals with this disease have a low numbers of neurons in peripheral nervous ganglions. To better understand the role played by IKAP and Elongator complex during transcription and in the same time learn about the molecular defects underlying the FD, an RNA interference (RNAi) was used to deplete the IKAP protein in the human cells. In yeast the silencing of ELP1 (homologue of IKAP in human) destabilizes the ELP3 catalytic subunit and of course induces a change in the Elongator complex integrity. In order to identify genes that require IKAP for their transcription, a microarray analysis was performed that identified several genes involved in cell motility or actin cytoskeleton remodelling. The cell motility has an important role in the developing nervous system, therefore motility/migration assay demonstrated that the IKAP depletion has functional consequence, in fact IKAP-depleted cells showed defect in migration which may be linked to the neurodevelopmental disorder that affects FD patients. Chromatin immunoprecipitation analysis was performed to

investigate if or not the defects in cell migration resulted of impaired transcriptional elongation of IKAP-dependent genes. The results showed a decrease in histone H3 acetylation in the transcribed region of IKAP target genes and no defect in the recruitment of RNA polymerase II on the promoter region was observed. This indicates that IKAP/hELP1 has a specific effect on histone acetylation and on RNA polymerase across the target gene which is consistent with a direct effect of Elongator on transcriptional elongation *in vivo*. In human, the Amyotrophic lateral sclerosis (ALS) is a spontaneous, relentlessly progressive motor neuron disease, usually resulting in death from respiratory failure within 3 years. Mutation on *SOD1* gene remains the most common genetic cause of ALS (Simpson, *et al*, 2009). In the study of 1483 individuals, *ELP3* was associated with human motor neuron degeneration in the form of ALS (Amyotrophic lateral sclerosis, characterized by progressive motor disease, usually resulting in death from respiratory failure) in three different populations. In mammalian the regulation of cytoskeletal components such as microtubules assumes an important role in neuronal cell shape that are necessary in many aspects of cortical development. Indeed, mutations in α-tubulin or in the microtubule regulating proteins LISSENCEPHALY-1 (LIS1) and DOUBLECORTIN (DCX) result in neuronal migration defects in humans, thus pointing to a central role for microtubule regulation in neuronal migration (Wynshaw‐ Boris, 2009).

Post translational modification such as acetylation on microtubules and tubulin molecules influence their stability and interactions with other proteins. Creppe and colleagues supposed that depletion of ELP1 results in destabilization of ELP3 subunit of Elongator complex by short hairpin RNAs (shRNAs) reducing the migration speed of bipolar and multipolar cortical neurons in the mouse brain (Figure 5)Elongator acetylates histones in the nucleus but it also targets cytoplasmic proteins such as α-tubulin. In support of this hypothesis, SIRT2, a mainly cytoplasmic deacetylase, targets a-tubulin in this cell compartment but also moves into the nucleus once phosphorylated by cyclin‐dependent kinases in the G2/M phase of the cell cycle in order to target histone H4 (North and Verdin, 2007; Vaquero, *et al.*, 2006). The result obtained by Creppe, *et al,* 2009, showed that Elp3 in vitro promote the acetylation of α-tubulin, but not a HAT-defective Elp3 mutant, in contrast to the HDAC6-mediated a-tubulin deacetylation in HEK293 cells. Hence, Elongator in human binds to microtubules and promotes a-tubulin acetylation, a way in which it may regulate migration and maturation of cortical projection neurons.
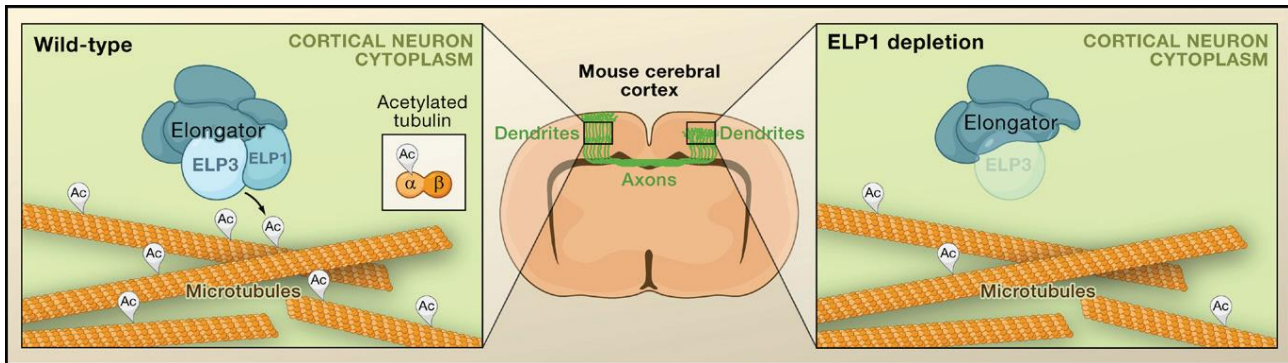
Figure 5. Modification of Elongator Complex subunit leads a reduction in migration and differentiation of projection neurons. (Left) Elongator may function in the cytoplasm of mouse neuronal cells to acetylate α-tubulin after microtubule polymerization, a modification that is associated with stable microtubules and is necessary for neuronal migration and differentiation. (Right) The depletion of ELP1 results in destabilization of ELP3, decreased tubulin acetylation in cultured cells, and defects in neuronal migration and branch formation in the developing mouse brain (Wynshaw-Boris, 2009).

The Elongator complex is conserved from yeast to humans and its biological activity was investigated also in *Drosophila melanogaster*. Deletion of the Elongator subunit *Elp3* induced larval lethality at the pupa stage. Moreover, larval growth is dramatically impaired during early development, with progression to the third instar significantly delayed and pupariation occurring only at day 14 after egg laying. Interestingly, melanotic nodules appeared in larvae after 4 days (Walker, *et al*, 2011). Microarray analysis of late-stage Elp3 mutant larvae shows that many stress-induced genes like some involved in oxidative stress response are upregulated. As explained above Elp3 mutation is associated with amylotrophic lateral sclerosis (Simpson, *et al*., 2009), a neurodegenerative disorder, which may be associated with oxidative damage induced by free radicals. In addition during larval stage of elp3 mutant melanotic nodules appear that indicates dysregulation of the innate immune system (Figure 6). The ability of cells to modulate their transcriptional program in response to physiological stimuli is vital for the proper development of eukaryotic organisms.
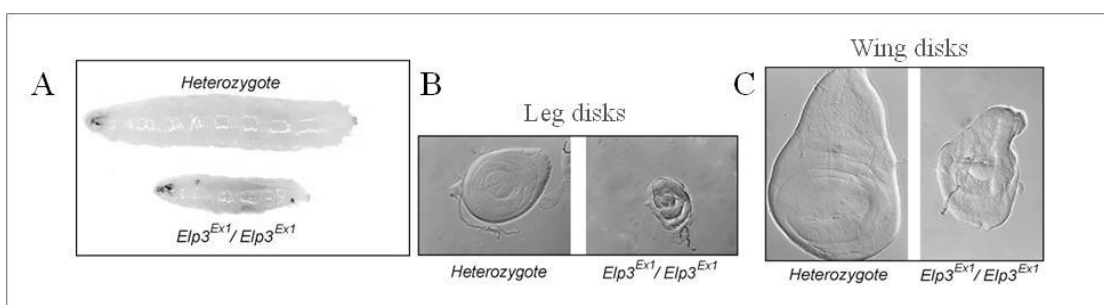

Figure 6. Phenotype of Elp3 mutant larvae. (**A**) Larvae at 5 days. Heterozygotes are at the wandering stage, but *Elp3* larvae remain in the food. Note at this stage the presence of melanotic nodules (blackspots). (**B** and **C**) Wandering stage Elp3 larvae show poorly developed leg and wing discs. (Karam, *et al*, 2010).

During the transcription process the serine residues on C-terminal end of RNA polymerase are differentially phosphorylated. In *Drosophila*, the phosphorylation of histone H3 at Ser10 (H3S10ph) was recently shown to be accompanied by the recruitment of members of the 14-3-3 protein family to specific genes upon induction (Macdonald, *et al*, 2005; Zippo, *et al*, 2009). Several members of the 14-3-3 phospho-binding protein family interact with H3 only when phosphorylated at Ser10 by the action of the JIL-1 kinase. JIL-1 and 14-3-3 are required for Elp3 binding to chromatin, and this was confirmed by a reduction of H3K9 acetylation level when both JIL-1 and 14-3-3 were absence. The 14-3-3 physically interact with the Elp3 subunit of Elongator and the data of this study suggested that 14-3-3 proteins mediate cross-talk between histone phosphorylation and acetylation during transcription elongation by creating a bridge between JIL-1 and Elp3 (Karam, *et al*, 2010). This general overview reveals important functions of Elongator complex both in human and Drosophila during embryogenesis where loss of ELP3 in the nervous system resulted in expansion of synaptic boutons in the larval fly neuromuscular junction and during development of the mammalian cerebral cortex in which misregulation of ELP3 can induce neuronal degenerative disease.

Ib1a. - Function of Elongator Complex

Function of Elongator complex in transcription

Eukaryotic gene expression is regulated at many consecutive stages and the phosphorylated state of RNA polymerase II change during transcription is hypo-phosphorylated during initiation and hyperphosphorylated during elongation. Thus the C-terminal domain of RNA polymerase (CTD) is differentially phosphorylated during the transcription cycle, but the interaction between Elongator complex and RNA polymerase is stabilized on the hyperphosphorylated CTD- RNAPII. This indicated that Elongator complex plays a role in transcription elongation. To investigate if Elongator is involved during transcription elongation, the resistance to the drug 6-azauracil (6-AU) was tested that inhibit enzymes implicated in the nucleotide metabolism pathway with the depletion of UTP and GTP in yeast cell. This compromises the activity of RNA polymerase during elongation. For example, the only phenotype of yeast strains lacking the gene *PPR2/SII*, which encodes RNAPII elongation factor TFIIS, is sensitivity to 6-AU (Hubert, *et al*., 1983). In contrast the elp1Δ cells were less sensitive to 50 mg/ml 6-AU, the siiΔ showed a moderate sensitivity at the same concentration of 6-AU. The phenotypic analysis of double mutant elp1ΔsiiΔ suggested a role

for Elongator in transcription elongator in vivo because the double mutant with their very small colonies confirmed the hypersensitivity to 6-AU. In order to detect if only the core-Elongator complex composed by ELP1, ELP2 and ELP3, were involved in facilitate with HAT activity the expression of some genes, were thus analyzed also the role of the other subunits ELP4, ELP5 and ELP6. At this aim by microarray on Elongator mutants were analyzed the expression level of a set of genes involved in different pathways and at least the expression level of 52 genes were reduced around 1,5 fold. The results clarified that the HAT activity resides in the catalytic subunit ELP3,indicating that core-Elongator and not the subcomplex is involved in histone acetylation but is required to form an active HAT. In the same microarray there were also genes that were up-regulated about 1,5 fold, so this means that in the Elongator mutant their expression increased. Most of these gene are involved in amino acid metabolism, and a similar subset of genes has previously been shown to be induced when S. cerevisiae cells were grown in the presence of carcinogenic alkylating agents, oxidizing agents, and ionizing radiation (Jelinsky, *et al*., 2000). In the beginning, the Elongator complex was considered to be involved in transcription because it co-immunoprecipitated with the elongating form of RNAPII. Moreover, in situ immunofluorescence of ELP1-ELP3 showed that Elongator is predominantly located in the cytoplasm and the authors suggest that Elongator may belong to a class of cytoplasmic, B-type histone acetyltransferases that are thought to catalyze acetylation events linked to transport of newly synthesized histone from the cytoplasm to the nucleus (Roth, *et al*., 2001). In conclusion it know the biological and molecular role of Elongator complex in the cell, though many are the questions that remains unclear such as the presence of this complex not only in the nucleo but also in the cytoplasm. Please phrase better To determine the nucleo-cytoplasmic distribution of Elongator was found that the nuclear localization sequence (NLS) in ELP1 subunit, may be essential for tRNA wobble uridine modification by acting as tRNA binding motif (Di Santo, *et al*, 2014)**.**

Elongator function in tRNA modification

Most cellular non-coding RNAs require the addition of post-transcriptional nucleoside modifications to be fully functional. The tRNA modifications in translation efficiency and fidelity assume importance as in the case of human where some human diseases are associated with malfunctioning of this process. Recently, it has become increasingly apparent that tRNA wobble modifications also provide cells with a powerful tool to regulate gene expression at the translational level (Gustilo, *et al*., 2008). In the cytoplasm of eukaryotic cells, amethoxycarbonylmethyl (mcm)

or carbamoylmethyl (ncm) group are added on side chains at position C5 of tRNA wobble uridine position. These modified nucleosides are important for efficient decoding during translation. Genes encoding the Elongator complex are required for an early step in the synthesis of mcm5U and ncm5U in the yeast *Saccharomyces cerevisiae* (Huang, *et al*., 2005). In *Saccharomyces cerevisiae*, mutations in any of the six Elongator protein subunit (ELP1–ELP6) genes or the three killer toxin insensitivity (KTI11–KTI13) genes cause similar pleiotropic phenotypes (Frohloff, *et al*, 2001). During tRNA modification all Elongator complex and also Kti11-Kti13 are required for the biosynthesis of modified uridine nucleosides present at the wobble position in tRNA. The new tRNA undergoes a set of post-transcriptional modification to generate a mature tRNA on four nucleoside such as: adenosine (A), guanosine (G), cytidine (C), and uridine (U). The group of Huang et al, 2005 have found that ELP1–ELP6 and KTI11–KTI13 genes are required for the formation of the modified nucleosides mcm ^{5}U, mcm ^{5}s ^{2}U, and ncm ^{5}U. Coimmunoprecipitation of Elp1 and Elp3 in vitro transcibed tRNAGlu UUC transcription indicated a direct involvement of Elongator in wobble uridine modification. The involvment of Elongator complex in tRNA modification was discovered by analysis of Elongator mutant elp1-elp6. In the beginning the study was focus on *elp3* -null allele where it suppressed the formation of mcm ^{5}s ^{2}U, mcm ^{5}U and ncm ^{5}U. All the elp deletion strains showed the same phenotype as *elp3*-null mutant. This demonstrated that all six subunits of the Elongator complex are required for the synthesis of mcm ^{5}s ^{2}U, mcm ^{5}U, and ncm ^{5}U. A mcm5 side-chain can be found in tRNA^{Glu}mcm^{5}s$^2_{UUC}$, tRNA^{Lys}mcm^{5}s$^2_{UUU}$, tRNA^{Gln}mcm^{5}s$^2_{UUG}$, tRNA^{Gly} mcm$^5_{UCC}$, and tRNA^{Arg} mcm$^5_{UCU}$ (Johansson and Byström, 2002) but only a reduction of tRNA^{Glu}mcm^{5}s$^2_{UUC}$ was found upon treatment with zymocin. These findings led to the hypothesis that zymocin may be an RNAse that specifically cleaves certain modified, but not unmodified, tRNAs (Lu, *et al*., 2005). It is known that elp1-elp6 and kti11-kti13 mutants show a resistance to K.lactis killer toxin. The linkage between transfer RNA and γ-toxin toxicity was first suggested based on the finding that elevated level suppresses the zymocicity (Butler, *et al*., 1994). The tRNA^{Glu}mcm^{5}s$^2_{UUC}$ has an anticodon sequence U $_{34}$ U $_{35}$ C $_{36}$ in which U $_{34}$ is modified to 5-methoxycarbonylmethyl-2-thiouridine (mcm^{5}s^{2}U). Interestingly, the Elongator mutants, which are class II zymocin resistant, are all defective in the formation of mcm^{5}s^{2}U in tRNA (Huang, *et al*., 2005). Furthermore, phenotypes in transcription and exocytosis observed in the Elongator mutants can be suppressed by overexpression of tRNAs that normally contain mcm^{5}s^{2}U. This suggests that these phenotypes are secondary and are caused by inefficient translation due to the tRNA modification defect (Esberg, *et al*., 2006). Taken together, class II zymocin resistance is linked to a

defect in mcm^{5}s^{2}U formation, suggesting that tRNAs containing this modified nucleoside could be the target of γ-toxin.

Ib2. - Identification of Elongator complex in plant

The existence of Elongator complex was investigated in *Arabidopsis thaliana*. The plant homologs of the yeast Elongator were identified through mutational analysis and BLAST. Tandem affinitty purification (TAP) with ELO1, ELO3 and AtELP5 as bait in cell suspension purified all the Elongator subunits. Hence, the plant Elongator complex consists of ELP1/ELONGATA2 (ELO2), ELP2, ELP3/ELO3, ELP4/ELO1, ELP5, and ELP6. In addition the *in silico* analysis showed that the functional domains of ELO2, ELO3, and ELO1 proteins were conserved between yeast and *Arabidopsis* (Nelissen, *et al*, 2003) (Table 3).

Human	**Yeast**	**Arabidopsis**	**AGI**
AAH12173	TOT4/KTI12	DRL1/ELO4	At1g13870
IKAP	TOT1/ELP1	ELO2	At5g13680
StIP1	TOT2/ELP2	ELP2	At1g49540
hELP3	TOT3/ELP3	ELO3	At5g50320
hELP4	TOT7/ELP4	ELO1	At3g11220
hELP5	TOT5/ELP5	ELP5	At2g18410
hELP6	TOT6/ELP6	ELP6	At4g10090

Table 3. Characterization of Elongator subunits in yeast, Arabidopsis and human.

Nelissen, *et al*, 2003 isolated a mutant with altered leaf size and shape, upon screening a Dissociation (Ds)-mutagenized Arabidopsis population for leaf mutants, which identified the DEFORMED ROOT AND LEAVES1 (DRL1) gene, a homolog of the yeast TOT4/KTI12 gene (Butler, *et al*., 1994; Frohloff, *et al*., 2001; Fichtner, *et al*., 2002). The drl1-2 was isolated as a mutant with narrow leaves (figure 7 (A) and 7 (B)) where the palisade cells were larger and more irregularly shaped than in the wild typ. In this mutant also lateral growth was reduced severely, the lamina was thicker, and the midvein was less pronounced (Figure 7 (C)) (Nelissen, *et al*, 2003). The DRL1 protein (AtDRL1) shares a high level of homology with the TOT4/KTI12 protein of yeast

(*Saccharomyces cerevisiae*) which is not a Elongator component but is associated with Elongator and regulated its function.An alignment presented by Fichtner, *et al*., 2002 showed the homology between the *S. cerevisiae, S. pombe, C. elegans, D. melanogaster, M. musculus*, *Arabidopsis*, and human sequences. Thus, DRL1 is not only conserved among eukaryotes: homologs also are found in archaea, suggesting that DRL1 is a universal and ancient protein (Nelissen, *et al*, 2003).

The drl1-2 mutant show meristematic defects such as significant reduction of leaf length, alteration in phyllotaxis and severel reduction of primary root growth. These results together with the finding of DRL1, and the putative homologs of the Elongator components ELP1-ELP6 in *Arabidopsis*, suggested that also in plant DRL1 can function as a putative regulator of Elongator.
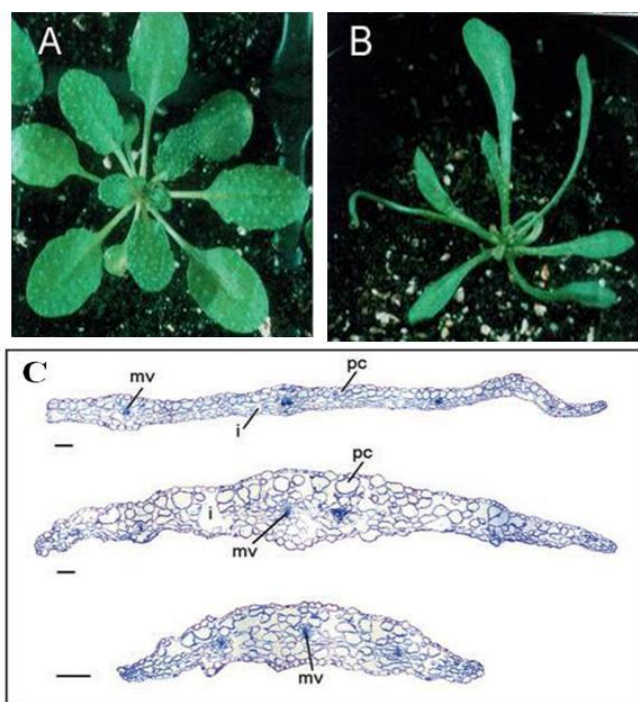

Figure 7. Leaf phenotype in *drl1-2* mutant. (A) and **(B)** Fully rosette of wild type and *drl1-2* mutant. **(C)** Transverse sections of wild-type (top) and drl1-2 (middle and bottom) plants. mv, midvein; pc, palisade cells (Nelissen H., *et al*, 2003).

The group of Bernà *et al*, 1999 were interested to study genes involved in the control of leaf morphogenesis in a model system such as Arabidopsis thaliana. The mutants were divided into different classes according to the shape and size of the leaves and divided into 94 complementation groups. The elongata class contains 4 members, *elo1-4*, with a reduced leaf lamina width. The *elongata* mutants exhibit a narrow leaf phenotype similar to the null mutant *drl1-2*. All *elo* mutants, *elo1*, *elo2*, *elo3* and *elo4*, have a delay in growth after germination, a reduction in leaf and root growth due to a reduced cell proliferation. These *elo* phenotype resamble the drl1-2 phenotype

Figure 8. Cell division activity is also decreased in the yeast Elongator mutants; the cells undergo a G1 delay and are often not able to continue the cell cycle (Fichtner, L. and Schaffrath, R., 2002).

Figure 8. Comparison of the *elo* and *drl1-2* mutant seedlings with L*er* (22 DAG). (Nelissen H., *et al*, 2005).

The mutant phenotypes suggested a positive role for Elongator in lateral leaf and primary root growth, which coincides with the expression of ELO genes in these organs. In addition the pleiotropic phenotypes in *elo* mutants suggested that Elongator regulates several, but distinct, developmental pathways (Van Lijsebettens *et al*., 2014). To know the existing genetic interaction between the different Elongator genes the elo and drl homozygotes were crossed. The *elo2elo3*, *elo4elo1*, and *elo2 drl1-2* DMs had phenotypes similar to those of *elo2*, *elo4drl1-4*, and *drl1-2*, respectively. Hence, DRL1 is epistatic to ELO2 and ELO1 in accordance with the proposed role for DRL1 as a regulator of the holocomplex (Fichtner et al.,2002). Furthermore, ELO1 was epistatic over ELO2 and ELO3, indicating the importance of the accessory subcomplex for the function of the core subcomplex. Finally, ELO2 was epistatic to ELO3, suggesting that the ELO2 scaffold protein is important for the maintenance of the integrity of Elongator as a HAT complex (Nelissen, *et al*, 2005). Elongator Complex and SUPPRESSOR OF Ty4 (SPT4)/SPT5 are RNAPII-associated transcript elongation factors that are implicated in chromatin dependent gene activation (Verséees, W.,*et al*. 2010; Hartzo, *et al*, 2013). The SPT4 and SPT5 genes are well studied in yeast and metazoa, indeed SPT5 is an essential gene in various organisms, whereas yeast cells lacking SPT4 are viable. In plants, the SPT4/SPT5 complex has been identified only recently, it pulled down the ELP3 subunit and subunit of RNAPII (Dürr, *et al*., 2014; Figure 9). The SPT5 is a nuclear protein

that occurs in the transcriptionally active euchromatin and colocalizes with transcribing RNAPII (Dürr, ,*et al*, 2014). In *Arabidopsis* the immunoblot and mass spectrometry analysis demonstrated that SPT4/SPT5 complex exists and is conserved (Figure 9). Leaves of SPT4-RNAi plants are clearly smaller compared with wild type, and also the rosette leaf venation pattern is altered. In addition, the transcriptomes of the SPT4-RNAi line and *elo3-1* mutants had common downregulated genes, including the auxin response and transport-related SHY2/IAA3 and LAX2, which are targeted by the Elongator complex for histone acetylation, transcription factors involved in cell elongation or organ morphogenesis, metabolic enzymes, membrane-located channels, and transporters (Van Lijsebettens, *et al*., 2014). In conclusion, the data suggest that Elongator and SUPPRESSOR OF Ty4 (SPT4)/SPT5 are transcript elongation factors may regulate the transcription of genes involved in the control of plant growth and development.
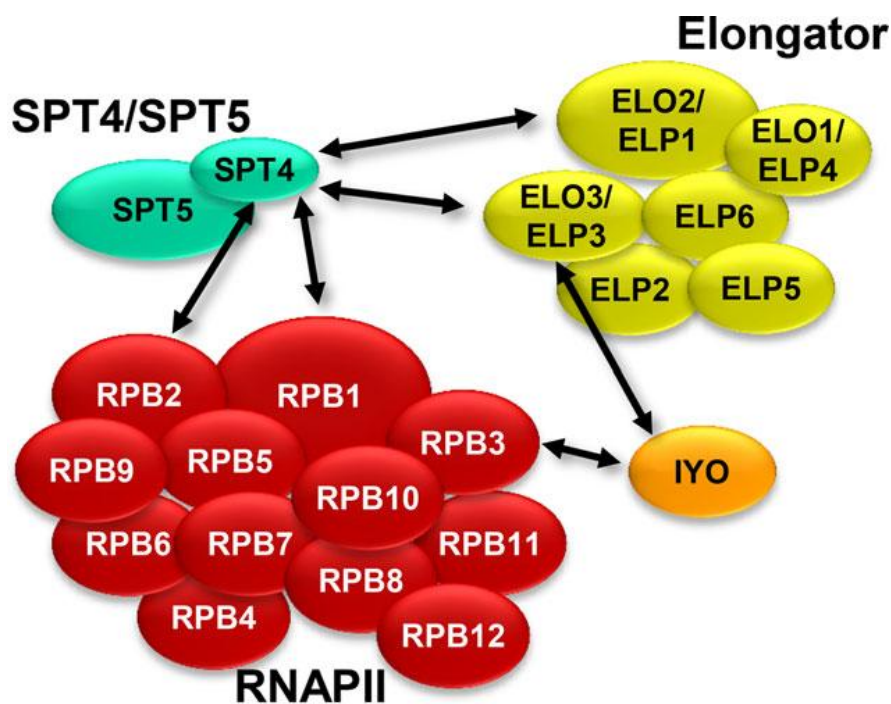

Figure 9. The structure of Elongator complex in Arabidopsis.
RNAPII subunits RPB1 and RPB2, all Elongator complex and the transcript elongation factor SPT4/SPT5 copurified with Elongator complex. Double-pointed arrows mark experimentally supported interactions between different protein (complexes), while interactions within complexes are not. (Van Lijsebettens, *et al*., 2014).

Ib2a. - Function of Elongator complex in plant

The phenotype of Elongator mutants are characterized by narrow and elongated leaves and petioles, short primary root, reduction in apical dominance defective venation patterning and altered phyllotaxis (Figure 10). In order to explain the phenotypes of the *elo* mutant microarray analysis identified a restricted number of significant GO categories (P < 0.001): chromatin assembly, pattern

specification, vascular tissue development, and response to auxin stimulus (Nelissen, *et al.,* 2010). Most of the down-regulated genes are involved in the auxin pathway such as: two SAUR, IAA14/SLR, IAA13, IAA11, ATHB8, IAA3/SHY2, IAA12/BDL, ARF10, ARF11, ARF18, ACL5, in addition to auxin biosynthesis (TAR2), and auxin transport (LAX2 and PIN4). All defects observed in *elo* mutants are connected to a defective auxin biology, indicating that auxin maxima are not properly established in elo mutants and suggesting a role for Elongator in auxin distribution or signaling. This suggested that Elongator likely controls plant development through its regulation of auxin-responsive genes. Indeed, the *elo* transcriptome identified a group of genes with a reduced expression level such as SHY2/IAA3 and BDL/IAA12 repressors, the ATHB8 auxin response gene the LAX2 influx carrier, the PIN4 efflux carrier, and the AP2/ERF ethylene response gene. Quantitative qPCR verified the down-regulation of these genes in the *elo* mutants. Chromatin immunoprecipitation (ChIP) were performed to investigate if the reduction in gene expression of some genes was related to reduced acetylation levels of histone H3 lysine-14 in their promoter and/or coding regions. Antibody against acetylated H3K14 or histone H3 and primers corresponding to the coding and 3′-untranslated regions showed reduced acetylation at the coding regions of the SHY2/IAA3 and LAX3 genes and confirmed that Elongator facilitates the expression of auxin-responsive genes by acetylation their coding region and thus facilitating the progress of RNA polymerase through the nucleosomes.
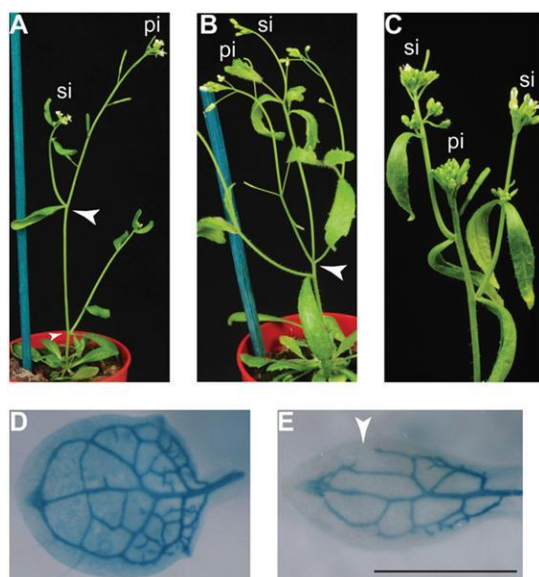
Figure 10. Auxin pathway is defective in *elo* mutant. **(A)**Wild-type inflorescence. **(B)** elo3-6 showing altered phyllotaxis of the secondary inflorescence branches (arrowheads). **(C)** elo1-1 showing reduced apical dominance. **(D)** Defective venation pattern visualized by X-Gluc histochemical assay of wild type. **(E)** elo3-1 mutant transformed with pATHB8-GUS showing open venation (arrowhead). (Nelissen, *et al.,* 2010).

Elongator complex plays many roles in plant in fact it is involved in abiotic stress responses, immune responses and in tRNA wobble uridine modification. Mutations in each subunit induced resistance to oxidative stress that is accompanied by increased expression of FSD1 (FE

SUPEROXIDE DISMUTASE 1), which converts the free radical superoxide into hydrogen peroxide and water and CAT3 (CATALASE 3), which decomposes hydrogen peroxide.(Nelissen, *et al*, 2005; Zhou, *et al.*, 2009). In a screen for drought-resistant mutants, the *abo1* mutation was isolated and it showed ABA hypersensitivity in the inhibition of seedling growth and the promotion of stomata closing. *abo1* is allelic to *elo2* and thus mutated in the gene coding for the largest subunit of the Elongator complex. The group of Zhou analyzed ABA sensitivity in seed germination and seedling growth for the *abo1/elo2/elp1*, *elp2*, *elp6* and *elp4/elo1* mutants and found that all these mutants were hypersensitive when grown on medium containing ABA.Micro-array analysis of genes affected by elp1 or elp4 mutation and subsequent analysis of specific genes in the four mutants showed that MYBL2 was downregulated and CAT3 was upregulated. MYBL2 is a single repeat MYB transcription factor with a suppressive role in the biosynthesis of anthocyanin (Dubos, *et al.*, 2008; Matsui, *et al.*, 2008).The *elo1*, *elp2*, *elp4* and *elp6* mutants contained about six or seven times more anthocyanin compared to wild type and this indicated that Elongator mutations negatively regulate the expression of genes in the anthocyanin biosynthesis pathway, probably by directly controlling the expression of the MYBL2 gene during transcription elongation (Figure 11).

Figure 11. Elongator mutants accumulated more anthocyanins than the wild type.
Anthocyanin accumulation in Elongator mutants and in the wild type in strong light. Four-week-old seedlings were treated with strong light for 2 days before they were photographed. (Zhou, *et al.*, 2009).

The plant reacts to pathogen infection through the accumulation of molecule salicylic acid (SA). This activity induces the expression of defense genes and the activation of systemic acquired resistance (SAR). Effective SA-mediated resistance requires the transcriptional co-activator NPR1, which regulates the activity of several transcription factors to modulate defense gene expression

(Cao, *et al.*, 1997, Dong, 2004). The role of ELO2 in the immune response to the hemibiotrophic pathogen *Pseudomonas syringae* was confirmed. As explained above NPR1is a transcriptional co-activator that regulates the cellular SA level in plant. Mutations in the NPR1 gene significantly block SA-mediated transcription reprogramming, compromise basal immunity, and render the plant completely defective in SAR (Wang, *et al.*, 2006). Indeed after infection, in *npr1* mutant the level of SA is high and this lead to cytotoxic effects and npr1 plants fail to develop beyond the cotyledon stage. Elongator is essential for this SA toxicity in npr1, as disruption of ELP2, (Defraia, *et al.*, 2010) as well as other subunits and DRL1 (Defraia, *et al.*, 2010), partially restore SA tolerance to *npr1*. Hence, Elongator complex has a role in the resistance of oxidative stress and on antioxidant genes activity can suggest its function in SA toxicity. Better phrasing please.The function of Elongator complex in tRNA modification in plants was tested. The RNA of *elo3* and wild type were isolated from leaves and degraded to nucleosides and analysed by HPLC. The elution profiles showed that for both the profiles were similar, except for the ncm^5U and mcm^5s^2U nucleosides that were absent in the elo3 mutant (Mehlgarten, *et al.*, 2010). These data support the idea that the plant Elp3/ELO3 protein is responsible for the early steps of the ncm^5U and mcm^5s^2U modification. In addition studies demonstrated that an *A. thaliana* Elongator mutant is lacking the very same tRNA modifications previously shown in yeast to be Elongator-dependent (Huang, *et al.*, 2005) and also in C. elegans Elongator mutants (Chen, *et al.*, 2009). According with these data indicated that also in the tRNA modification the role of Elongator complex is conserved in animals, fungi and plants.

Ic. - Objectives of present work

The main goal of the present research project was to dissect in the model plant *Arabidopsis thaliana* some aspects of molecular networks underlying the action of Elongator complex and its interface with environmental factors, mainly focusing on light condition.

The knowledge and expertise derived from such study will be essential to design efficient strategies for modulating the activity of Elongator complex and improving plant growth, first in *Arabidopsis thaliana* and then in other plant species. Therefore, according to the objectives of POR CALABRIA FSE 2007/2013- Action "Technologies for Sustainable Management of Environmental Resources", which founded this PhD research project, the long-term output of the present work will be to exploit the possibility to enhance biomass production, by engineering and /or modulating Elongator complex activity, in crop species particularly suitable for a green energy production.

In this context the attention was focused on:

A) **The study of *Sec31* gene encoding a putative Elongator's interactor**

Preliminary data, obtained by the group of Prof. M. Van Lijsbettens (personal communication) through a TAP analysis, indicated the Sec31 protein as a direct interactor of Elongator complex. In order to elucidate such interaction, in this section of PhD project we planned to investigate phenotypic and developmental characteristics of *sec31* mutants to compare with *elo3-6* mutant features, which are very well known by literature (Nelissen, *et al*., 2010). Attention was also addressed to co-localize *Sec31* and *ELO3* transcripts in *Arabidopsis thaliana* wild type seedlings, by multiprobe in situ hybridization (MISH) (Bruno *et al*., 2011), in order to compare cyto-histological expression domains of both genes, together with the analysis of the expression pattern of some Elo-related genes in *sec31* mutants.

B) **The study of Elongator-mediated gene expression under darkness and light qualities**

In this section we planned to study a specific gene category of Elongator network involved in response to light. In this case the aim was to verify whether Elongator works as interface between light signaling and gene expression during transcription elongation. Discovery of genetic interactions between Elongator and phytochrome light receptors and other components of light signaling will clarify the position of Elongator within the network of the light response pathway.

II° Chapter

Section A: Study of *Sec31* gene encoding a putative Elongator's interactors

IIa - Introduction

Eukaryotic cells contain a number of different membrane compartments that play specialized roles. Relevant among these roles is the secretory pathway which allows the proper intracellular distribution of a wide range of proteins, complex carbohydrates and lipid. Trafficking in the secretory pathway is highly dynamic and responsive to specific cellular functional demands. Delivery proceeds through a series of events, including directed membrane translocation, membrane budding and membrane fusion, leading to the formation of a transport vesicle that guides secretory cargo to its ultimate destination. Endomembranes involved in this process belong to several cellular compartments such endoplasmic reticulum (ER), the Golgi stacks, the cell-delimiting plasma membrane (PM), various endosomal compartments and a vacuole/lysosome equivalent (Brandizzi and Barlowe, 2014).

Formation of a transport vesicle is not a simple event. A mechanism for cargo selection and concentration is required to decide what must be carried in the vesicle (Sanderfoot and Raikhel, 2003). Some signal must be sent from the lumen to the cytoplasm, where a coat must form, to indicate a site for vesicle formation. This is accomplished through a large collection of proteins that are referred to as "coatomer" or coat proteins. Each type of coat is distinct, though some are related, and a particular coat is responsible for vesicle formation at a particular type of organelle.

So far, the best studied traffic pathways are those that use carrier vesicles coated by the coatomer named coat protein complex I and II (COPI, COPII), or clathrin and its partners (Kirchhausen, 2000) (Figure 1). The COP I and II operate in the bidirectional traffic between ER and Golgi: in particular COPII operates in the major biosynthetic route, named anterograde pathway, which flows from the ER to Golgi, while the COPI operates in the route known as retrograde pathway which flows from Golgi to ER. Clathrin and its partners are involved in two routes, one from the plasma membrane to endosome, and the other one from the Golgi to endosome.
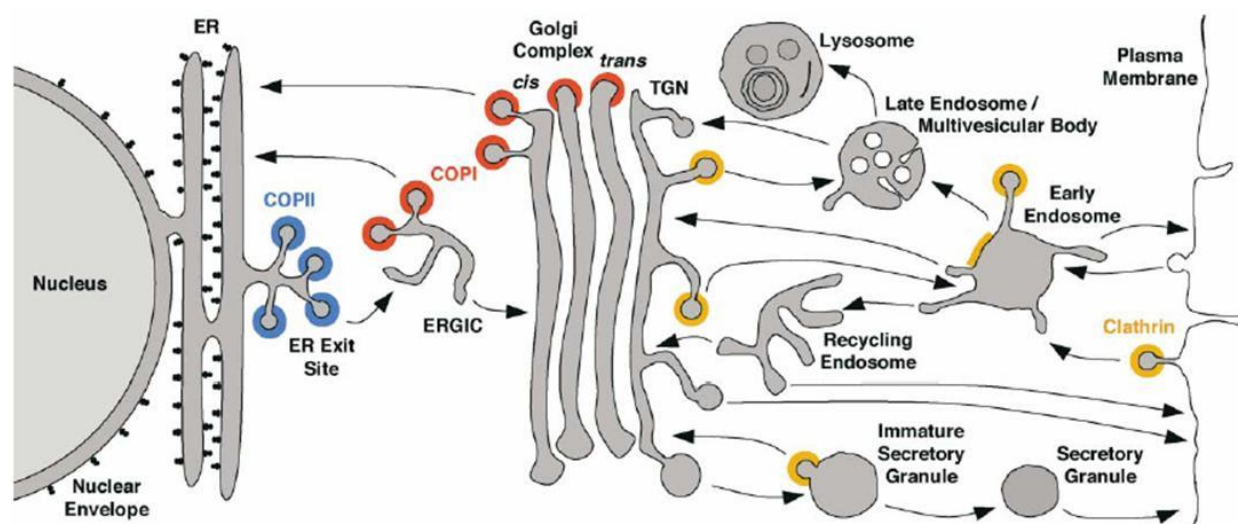
Figure 1. The major membrane traffic pathways that use carrier vesicles coated with COPI, COPII and clathrina in eukaryotic cells. The scheme depicts the compartments of the secretory, lysosomal/vacuolar, and endocytic pathways. Transport steps are indicated by arrows. Colors indicate the known or presumed locations of COPII (blue), COPI (red), and clathrin (orange). (Bonifacino and Glick, 2004)

COP I-coated vesicles were first identified from an intra-Golgi transport assay (Balch, *et. al.*, 1984). COPI coatomer consistes of 7 polypeptides (α /Rer1p, β/Sec26p, β'/Sec27p, γ/Sec21p, δ/Ret2p, ε/Sec28p, and ζ/Ret3p; listed in the mammalian/yeast nomenclature) that are conserved across eukaryotes, plus the small GTP binding protein ARF1 that is not part of the coatomer itself. It is subdivided in two main subcomplexes: a tetrameric complex (γ-COP–δ-COP–ζ-COP–β-COP) forming the inner layer core and a trimeric (α-COP–β´-COP–ε-COP) complex which constitutes the inner layer core.

The COPII coat was first identified in yeast *Saccharomyces cerevisiae* and is conserved in all eukaryotes (Novick, *et al* 1980, 1981; Antonny and Schekman, 2001). It is made of five cytosolic proteins and having been first described in yeast, the components are typically referred to according to the yeast nomenclature: Sar1p , Sec13, Sec31p , Sec23 and Sec24p (Antonny and Schekman, 2001). In yeast there is only one protein of each family, except for Sec24 which has two additional Sec24-like proteins(Roberg, et al,1999; Kurihara, et al, 2000). In metazoan, each COPII subunit has two isoforms, except Sec13, which has none, and Sec24, which has four termed Sec24A, B, C and D (Robinson, *et al*., 2007; Marti, *et al*., 2010).

In higher plants the cell secretory pathway has been deeply investigated mainly in the model system *Arabidopsis thaliana* (Snderfoot & Raikhel, 2003) and similarities with and some relevant differences from other organisms have been detected. Concerning COPI coat, it is formed by the seven component listed by mammalian/yeast nomenclature which in *Arabidopsis* are encoded by multiple genes (except for γ and δ) (Table 1). Concerning COPII coat machinery, like in other organisms it consists of five cytosolic proteins: Sar1, Sec23, Sec24, Sec13 and Sec31. Also in this

35

case, *Arabidopsis* coatomer subunits are each encoded by multiple genes (Table 2), though whether this indicates redundancy has not yet been fully investigated.

```
--------------------------------------------------------------------
Sar1-like GTPases (COP-II)
                          At4g02080, At3g62560,
                          At1g56330, At1g09180,
                          At1g02620
Sar1-GEF
Sec12                     At2g01470, At5g50550

ARF-like GTPases (COP-I, Clathrin, etc.
                          ; see Vernoud et al.,2002)
                          At2g47170, At3g62290,
                          At1g10630, At1g70490,
                          At1g23490, At5g14670,
                          At5g67560, At3g22950,
                          At5g52210, At5g17060,
                          At2g15310, At2g18390,
                          At3g03120, At3g49860,
                          At5g37680, At3g49870,
                          At1g02430, At1g02440,
                          At5g37680, At3g49860,
                          At3g49870, At5g67560,
                          At5g52210, At2g18390

ARF-GEF
Sec7/BIG-Type:            At4g35380, At4g38200,
                          At1g01960, At3g60860,
                          At3g43300
GNOM-Type:                GNOM(At1g13980),
                          At5g39500,
                          At5g19610
ARNO-Type:                None found
--------------------------------------------------------------------
```

Table 1. Coat GTPases and their Effectors

Coat proteins of COPII						
	Subunits					
Proteins Complex	**Mammals**	**Yeast**	**Arabidopsis**	*****	**Size**	**Feature**	**Interactions**
Sec13 complex	hSec13p	Sec13p	AtSec13p*	2	33 kDa	WD-40 repeats	
	hSec31p	Sec31p	AtSec31p*	2	150 kDa	WD-40 repeats	
Sec23 complex	hSec23p	Sec23p	AtSec23p	5	85 kDa	GAP for Sar1p	Bos1p,Bet1p
	hSec24p	Sec24p	AtSec24p*	5	105 kDa		
Sar1	hSar1p	Sar1p	AtSar1p	4	21 kDa	GTPase	Bos1p

Table 2. Coat proteins of COPII vesicles (*Arabidopsis isoforms) (Adapted from Wieland and Harter1999 with modification

In particular, in plants, there are even more predicted isoforms of *Sec24* than in metazoan, rendering their systematic analysis very complicated and raising also questions about possible overlapping functions, tissue specificity of certain complexes and the rules of subunit association (Robinson, *et al.*, 2007; Marti, *et al.*, 2010) (Figure 2).
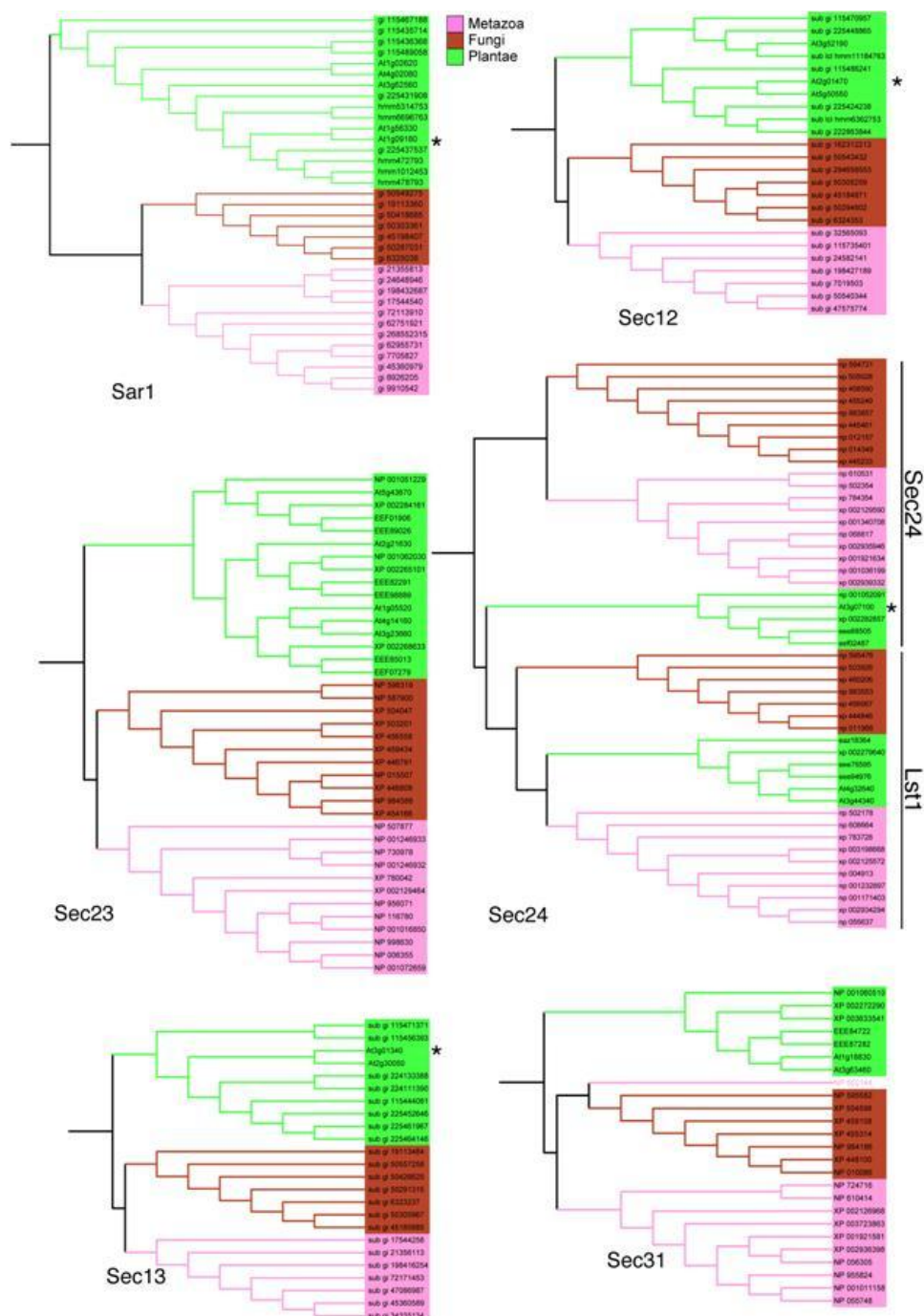

Figure 2. Phylogeny of Sec12, Sar1, Sec23, Sec24, Sec13 and Sec31 proteins from the Metazoa, Fungi and Plantae phyla. (De Craene, *et al.*, 2014).

Moreover, while the coat-GTPase Sar1p in yeast is encoded by a single copy gene, in plants like in mammals there are multiple Sar1p homologues (Table 1).

As far as protein assembly is concerned for COPI it is depicted in Figure 3. Once activated by ADP-ribosylation factor (ARF) guanine nucleotide exchange factors (GEFs) containing a conserved SEC7 domain, myristoylated membrane-anchored ARF GTPases recruit COPI to Golgi membranes. The coatomer subunits α-COP, β′-COP, γ-COP and δ-COP recognize sorting motifs on the cytosolic domain of membrane cargo and mediate cargo incorporation into nascent COPI vesicles[127]. ARF GTPase-activating proteins (GAPs) bind cytoplasmic signals on cargo proteins, γ-COP and β′-COP subunits as well as active ARFs. Stimulation of the GTPase activity of ARFs by ARF GAPs leads to the release of ARF from the complex and ARF GAP and coat dissociation (Szul, & Sztul, 2011; Shiba, & Randazzo, 2012).
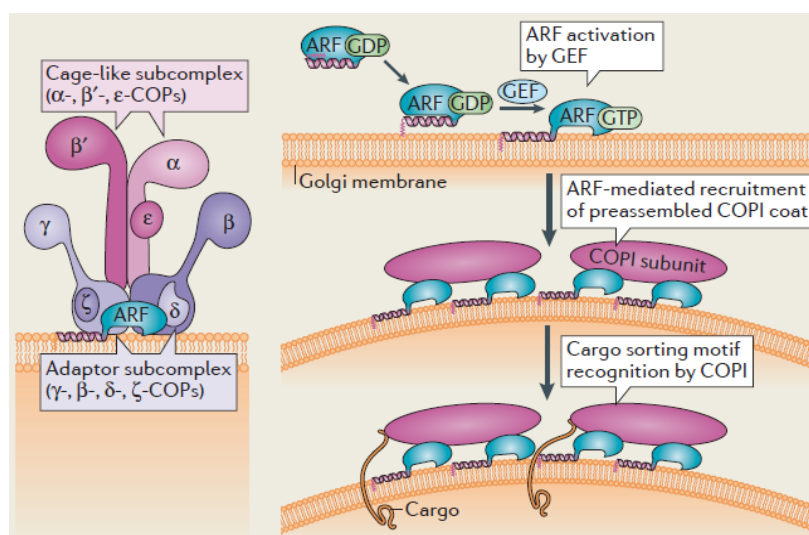

Figure 3. The COPI coat complex and retrograde transport.

For COPII the sequence of protein assembly has been established by sequential addition of yeast COPII components to an *in vitro* ER vesicle budding assay and subsequently was confirmed in mammalian cells (Barlowe *et al*., 1994; Kuge *et al*., 1994; Aridor *et al*., 1995; Lee, *et al*., 2004). According to this order of assembly, Sar1 is the first COPII component recruited to the ER membrane and it begins the process of vesicle formation. Sar1 is a small GTPase, whose activity, similarly to that of other small G proteins, is controlled by the state of the nucleotide to which it is bound (Pucadyil and Schmid, 2009). In its GDP-bound state, Sar1 is cytosolic and dormant, but when bound to GTP, Sar1 activates by exposing an amphipathic N-terminal α-helix, which embeds into the ER membrane (Lee and Miller, 2007; Bielli, *et al*., 2005). This activity is restricted to the

ER membrane, because Sec12, the guanine nucleotide exchange factor (GEF) that activates Sar1, is only found at the ER (Weissman, *et al*., 2001). This coat-GTPase differs depending on the particular coat proteins, and may be a member of the ARF-family or of the Sar1plike family of small G-proteins. The coat-GTPase for the COP-II coat is called Sar1p. Once activated Sar1p-GTP recruits two coatomer protein complexes from the cytosol: the Sec23/24p and the Sec13/31p complexes. The Sec23–Sec24 heterodimer complex arrives at the scene by the direct interaction between Sar1 and Sec23 (Bi, *et al*., 2002). This interaction plays not only a structural role in assembling the inner coat complex on the membrane, but also a catalytic role. Namely, Sec23 is a GTPase activating protein (GAP) for Sar1, accelerating the poor intrinsic GTPase activity of Sar1; full GTPase activity, however, is not realized until the complete COPII coat is assembled following the arrival of the Sec 13-31 heterotetramer complex (Yoshihisa, *et al*., 1993; Antonny, *et al*., 2001). The Sec13/Sec31 subcomplex is the last of the COPII components to be recruited onto membranes before vesicle formation and forms the outer coat. (Figure 4).
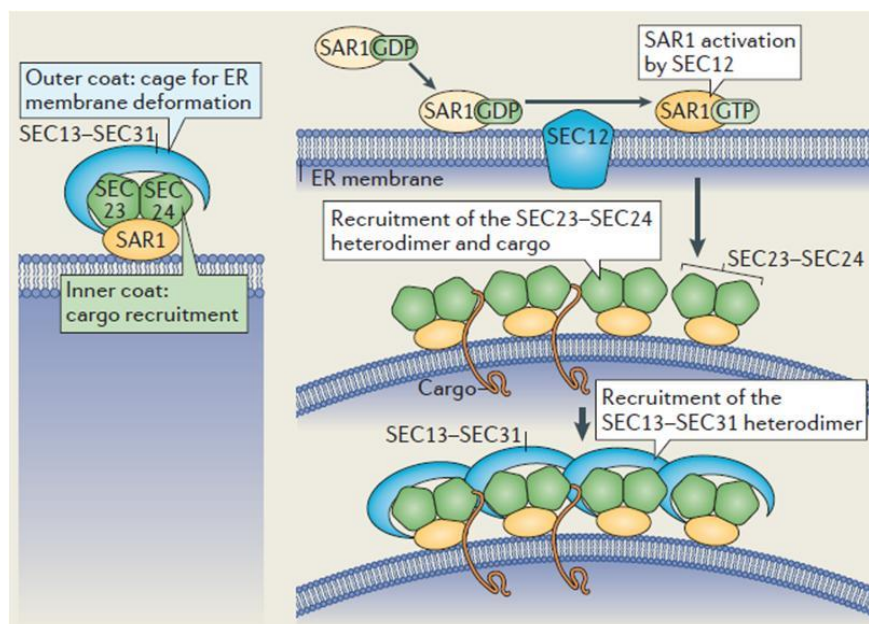

Figure 4. The coat complex II (COPII). The core machinery of COPII recruitment to membrane, coat polymerization, vesicular budding. (Brandizzi and Barlowe, 2013).

The Sec13–Sec31 outer coat may be linked to components of regulatory mechanisms that govern ER exit, acting as a scaffold to collect cargo and direct vesicle budding (Figure 4). It has been demonstrated in rat liver that the depletion of cytosolic proteins, which could potentially interact with the C-terminal fragment of Sec31A, is defective in ERGolgi transport (Tang *et al*., 2000). This observation indicates that a cytosolic factor(s) sequestered by the C-terminal fragment of Sec31A is likely important for ER export

Although in some organisms like *Saccharomyces cerevisiae*, the entire ER membrane seems capable of acting as ER-exit sites (Rossanese *et al.*, 1999; Glick, 2001), in most organisms ER-exit sites are discrete points along the ER membrane (Bannykh and Balch, 1997; Rossanese *et al*., 1999) and in mammalian cells the COPII vesicle budding is restricted to distinct domains of the ER known as ribosome-free transitional ER (tER) or ERexit sites (ERES) (Palade, 1975; Orci *et al.*, 1991; Rossanese *et al.*, 1999). The COPII coated vesicles are quite unstable, in fact these vesicle quickly fuse with each other into larger vesicles, which either fuse with the cis-Golgi (or form a *de novo* cis-Golgi stack in cisternal maturation models) or with a compartment, called the ERGolgi Intermediate complex (ERGIC), found in most mammals.

Although the dynamic and aim of cell secretory pathway is conserved in all eukaryotic organisms, the early phases of this pathway in plants is organized differently from animal and yeast, undoubtedly as a consequence of the different physiology of the plant cell. Firstly, important differences are related to the function and appearance of ER and Golgi apparatus. Indeed, in plants, the ER is at least partially a storage organelle, whereas the Golgi stacks have devoted a major part of their existence to the creation of cell wall precursors. The vacuole, beside the role of "garbage dump" assigned to the homologous organelles in other eukaryotes, has also a major role in the storage of ions and various metabolites. Moreover, in literature it's possible find some differences between plants and other eukaryotic organisms both in the process of coat complex formation and during the vesicular transit.

In more details, in plants the transport between the ER and the Golgi apparatus does not involve a mobile, microtubule-dependent intermediate (ERGIC) compartment (Brandizzi, *et al*., 2002; Brandizzi, *et al*., 2003), because the ER and Golgi are in close proximity and COPII vesicles quickly reach the Golgi membrane (Robinson, *et al*., 2007); In contrast, the mammalian ERGIC represents a long-range cargo carrier in ER to Golgi transport (Stephens and Pepperkok, 2001) (Figure 6).

According to this assumption, in plants ER-Golgi protein traffic is quite similar in cells depleted of actin and in cells depleted of both actin and microtubules (Brandizzi *et al.*, 2002).
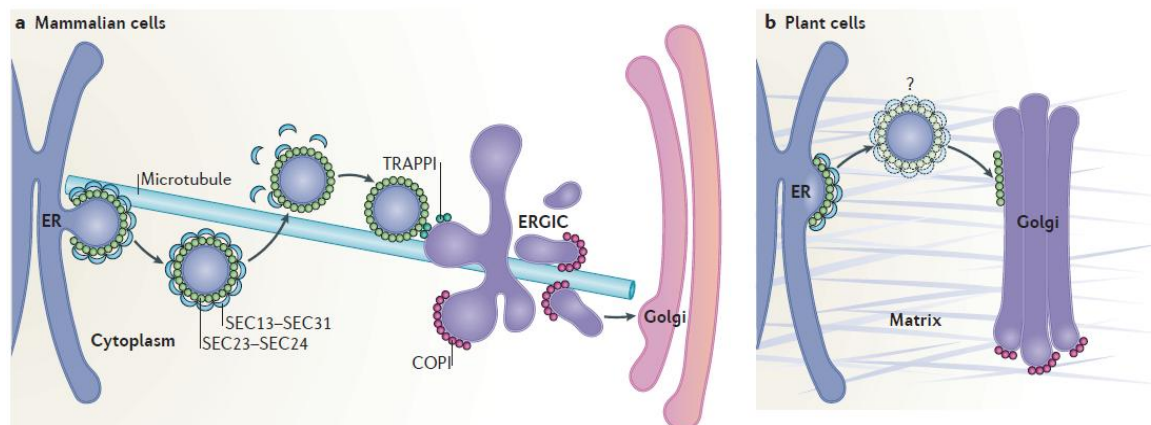
Figure 6. The ER–Golgi interface and ERES have a distinct organization in mammals and plants. (a) In mammalian cells, ER exit sites (ERES) are orientated towards a juxtaposed endoplasmic reticulum (ER)–Golgi intermediate compartment (ERGIC). (**b**)In plant cells, ERES and Golgi are closely associated, possibly through a matrix (indicated in grey) that holds the ER and the Golgi together

Thus, the ER export in plant cells occurs through a unique mechanism in which a specialized subdomain of the ER and an associated Golgi stack acts as a secretory unit and COPII carriers are formed and quickly released at the ER subdomain and partially coated COPII carriers then associate with the Golgi (Figure 6).

As previously mentioned, in yeast there is only one protein of each family of coat protein complexes to fulfill all the described functions, except for Sec24 which has two additional Sec24-like proteins involved in the active recognition of the different sorting signals found on cargo proteins. While in metazoan and mainly in plants there are multiple isoforms (Kurihara, *et al.*, 2000; Marti, *et al.*, 2010; Roberg, *et al.*,1999; Robinson, *et al.*, 2007, Wendeler, *et al.*, 2007). The presence of multiple isoforms in higher organisms brings about combinatorial diversity for COPII vesicle formation, indicating a greater range of complexity in the regulation of COPII-mediated protein export.

In the context of this complex regulation, in the present work which aims to elucidate the Elongator molecular network, we focused the attention on a gene encoding a component of cell secretory pathway, such as Sec31, because TAP analysis, previously performed by M. Van Lijsbettens's research group, identified such protein as a putative interactor of Elongator complex.

Therefore, one section of this PhD research project was addressed to study at functional level the *Sec31 gene* encoding such protein, with the aim to add information useful to confirm and elucidate such interaction. In particular we investigated whether: i) at the phenotypical level *sec31* mutant resembles *elo3* mutant; ii) cytohistological expression domains of *ELO3* and *Sec31* genes overlap; iii) the two genes shares some common downstream target genes.

IIb - Materials and Methods

Plant material and growth conditions

Two mutant lines of *Sec31* gene, selected on the basis of a T-DNA insertion, were used: *salk_012544C* and *salk_035921C* by NASC (http://arabidopsis.info/NASC). Both T-DNA insertion are localized in the first exon of *Sec31* gene (see figure 5, reported in IIa paragraph). *elo3-6* mutants (GABI-KAT collection code GABI555_H06) and seedlings of *Arabidopsis thaliana* Columbia (Col-0) obtained from the Nottingham Arabidopsis Seed collection, were also used for the comparison and as control, respectively. Both the mutants lines for *Sec31* gene and *elo3-6* mutants are in Col-0 background.

Seed were sterilized in 5% bleach (v/v) in water with 0.05% Tween 20, for 10 min. and washed in water five times for 5 min. Seeds were germinated in rockwool soil and watered every two days; plant growth was performed at set conditions: 16 h/8 h (day/night) with white light (neon tubes, cool white), 100 µmolesm-2s-1 light intensity, and 21°C., and 50% relative humidity.

In vitro plant growth conditions

After sterilization at the above described conditions seeds were sown in on one-half-strength MS medium (Murashige and Skoog, 1962) with 1% of sucrose on Petri dishes and vernalized for 48h. Thereafter the Petri dishes were transferred in the growth chamber room at set conditions: 16 h/8 h (day/night) with white light (neon tubes, cool white), 100 µmolesm-2s-1 light intensity, and 21°C, and 50% relative humidity.

For root growth analysis seedlings were grown as above described on vertical Petri dishes

Phenotype analysis

For the morphological analysis of aerial part, plants grown on soil at the above described set conditions were used. Observation were performed periodically from cotyledon stage (about one week) until complete development (eight weeks). Each vegetative stage was photographed to better analyze the differences between wild type and *salk_012544C* and *salk_035921C* mutant lines. The observations were performed on three independent replicates and in each replicate 30 plant for each sample were monitored.

For the root growth analysis, seedlings grown in vitro on vertical plate, as above described, were used. Primary root length was marked every 2 days for 16 days and the plates were scanned and root length was measured by Image J software. Measurements were carried out on three independent replicates and in each replicate 30 seedlings for each sample were used. Data were statistically analyzed through Student's t-test.

Root meristem size evaluation

Six-days old seedlings grown *in vitro* on vertical plate, as above described, were used. Whole seedlings were fixed in 50% methanol and 10% acetic acid in water and shaken at 48°C for at least for12 h. The samples were washed in distilled water and stained by using the pseudo-Schiff propidium iodide (mPS-PI) staining Technique (Haseloff, 2003; Moreno *et al*., 2006; Truernit *et al*., 2006).

The mPS-PI staining technique is based on the covalent labeling of cell wall material with fluorophors and the subsequent clearing of the tissue with chloral hydrate. Fixed plant tissue is treated with periodic acid, which leads to the formation of aldehyde groups in the carbohydrates of cell walls. These aldehyde groups can then react covalently with fluorescent pseudo-Schiff reagents, such as propidium iodide, resulting in samples with highly fluorescent cell walls that are well suited for confocal microscopy (Haseloff, 2003; Moreno *et al*., 2006; Truernit *et al*., 2006).

Therefore, after washing, samples were a incubated in 1% periodic acid at room temperature for 40 min., rinsed again with water and incubated in Schiff reagent with propidium iodide (100 mM sodium metabisulphite and 0.15 N HCl; propidium iodide to a final concentration of 100 mg/mL was freshly added) for 1 to 2 h or until samples were visibly stained. The samples were then transferred onto microscope slides and covered with a chloral hydrate solution (4 g chloral hydrate, 1 ml glycerol, and 2 ml water). Slides were kept overnight at room temperature in a closed environment to prevent drying out (Truernit *et al*., 2006). The images of roots were captured by a Leica TCS SP2 (Spectral Confocal and Multiphoton System) laser scanning confocal microscope. The excitation wavelength for PS-PI stained samples was 488 nm, and emission was collected at 520 to 720 nm. Morphometrical analysis was performed by ImageJ tool on 20 seedlings and data were statistically evaluated through Student 's t-test.

RNA extraction and purification

RNA extraction was performed by using Kit RNeasy Plant Mini Kit (RNA isolation and cleanup) (QIAGEN). About 100 mg of tissues were placed in liquid nitrogen and ground thoroughly with a mortar and pestle. The tissue powder was transferred in 2 ml microcentrifuge tube, before cooled with liquid-nitrogen, where 450 μl Buffer RLT t were added. The sample was subjected to vigorous vortex and transferred to a QIAshredder spin column (lilac) placed in a 2 ml collection tube and centrifugated at 13,000 rpm for 2 min. The supernatant of the flow-through was carefully transferred to a new microcentrifuge tube without disturbing the cell-debris pellet in the collection tube. The supernatant was precipitated by adding 0.5 volume of ethanol (96–100%) and mixed immediately by pipetting. The sample (about 650 μl) was transferred into RNeasy spin column (pink) placed in a 2 ml collection tube (supplied in the kit) and centrifugated for 15 sec. at 10,000 rpm. 700 μl Buffer RW1 were added and then the sample was centrifuged for 15 sec. at 10,000 rpm to wash the spin column membrane. To purify the RNA, Buffer RPE was used twice to centrifuge the sample at 10,000 rpm once for 15 sec. and in the second time for 2min. In order to remove residual ethanol which may interfere with downstream reactions a centrifugation at full speed for 1 min. was applied. The RNeasy spin column was transferred into a new 1.5 ml collection tube (supplied) and 30 μl RNase-free water were added directly on the spin column membrane and the sample was centrifugated at 10,000 rpm for 1 min to elute the RNA. The integrity of extracted RNA was assayed through electrophoresis on agarose gel (1%) in TBE 0.5X (5.4 g L-1 of Tris base, 2.75 g L-1 of boric acid, 2 ml L-1 of EDTA pH 8.0) at 80V.

To eliminate a possible contamination by genomic the extracted RNA was purified through a DNase treatment using a DNase I recombinant / RNase-free Kit (Roche) in which enzyme concentration is 10 unit/μl. 1μl of enzyme was used to digest 5μg of sample using te reaction mix reported in (Table 3).

Table 3. DNase mix

Reagent	Volume
RNA	5 μl
DNase I	1 μl
Buffer 10X	5 μl
H_2O DEPC	39 μl

The mix reaction was incubated at 37°C for 15 min. Afterward 5 µl di NaAc 3M and 2 volumes of Et-OH 100% were added to the mix and the sample was stored at -20°C. At the moment of use the sample was centrifuged at 13,000 rpm at 4°C for 30 min. After having discarded the supernatant and were added 1ml of Et-OH 80%, the sample was again centrifuged at 13,000 rpm at 4°C for 20 min. Again the supernatant was discarded and the pellet was dried. Finally the sample was re-suspended in 10 µl of H_2O DEPC and stored at -20°C.

cDNA synthesis: First strand cDNA Synthesis (SuperScript™ III Invitrogen USA)

To perform reverse transcription and synthesize ssDNA, 1 µg of RNA was added to the reaction mix containing 1ml of Primer Oligo (dT)20 (50 µM), 1 µl dNTP Mix (10 mM) and 8 µl H2O DEPC and 10 µl of cDNA Synthesis Mix (Table 4). The sample was incubated at 50°C for 50 min., then at 85°C for 5 min. and at the end put on ice for 4 min. In the last step, to digest the heteroduplex, 1 µl of RNase H was added and the sample was incubated at 37°C for 20 min.

Table 4. cDNA synthesis mix.

Reagent	Volume
RT Buffer 10x	2 µl
$MgCl_2$ 25 mM	4 µl
DTT 0,1 M	2 µl
RNasi Out (40U/µl)	1 µl
SuperScript III RT	1 µl
Volume finale	**10 µl**

Multi probe whole mount RNA/RNA in situ hybridization

The in situ hybridization (ISH) allows the localization of specific sequences of DNA or RNA directly on the tissues or organs of interest. The ISH is based on the principle that complementary nucleotide sequences are able to pair up with each other in particular experimental conditions. The specific labelling of one of the two sequences (probe) allows to localize the target

sequence to which it will bind, where there is (*in situ*). Depending on the molecule to be located and the chosen probe, it is possible perform a hybridization: DNA / DNA, DNA / RNA or RNA / RNA. The RNA-RNA in situ hybridization (ISH) is a powerful technique that enables the localization of the transcripts of the gene at the cellular level. Multi probe whole mount RNA/RNA in situ hybridization (MISH) is an upgraded technique by which, using probes differentially labeled, is possbible to simultaneously localize different transcripts in the same sample (Bruno, *et al*., 2011). The procedure included several steps:

Fixation and Dehydration of the plant material

Seedlings grown in vitro as above described were collected at 4DAG and fixed, under vacuum pump, with a solution containing 4% (w / v) paraformaldehyde, in 1X PBS (PBS 10X: 1,3 M di NaCl, 70 mM Na_2HPO_4 * $2H_2O$ and 30 mM KH_2PO_4, pH 7,4 with1 M KCl). Cuvette containing samples were gently shaked on an orbital platform at 60-80 rev / min, at 4°C, overnight. Thereafter fixative was removed and in order to remove the chlorophyll, the samples were washed with methanol twice for 5 min and then in 100% ethanol three times for 5 min, gently shaking at 4°C. Samples were stored in 100% ethanol, at -20°C, overnight.

RNA probe synthesis

For ELO3 (At5g50320) genes, specific PCRragments (GSTs) were amplified through PCR reaction using specific primers (Table 5) and the amplicon was cloned in pGEM-T Easy (Promega)

Table 5. Sequence of primers used in the PCR reaction

Gene	Primer	Sequence	Amplicon (bp)
ELO3	FW	5'-TGAAGATACACGCCAGGACA-3'	
ELO3	BW	5'-CACCAGAAATCACACCGATT-3'	310

Amplified fragment was linearized by using restriction endonuclease such as SpeI and NcoI and then used as template for the *in vitro* transcription of riboprobes; for riboprobe synthesis fluorescent labeled nucleotides Digoxigenin-11-UTP, Biotin-16-UTP and RNA polymerase T7 o SP6 (DIG, Biotin, FITC RNA labeling Mix,Roche) were used (Hejatko, *et al*., 2006; Traas , 2008).

For *Sec31* (At3g63460) genes, specific gene fragment was was obtained by PCR synthesis using specific primers which exhibit sequences for both T7 and SP6 polymerase (Table 6).

_____

Table 6. Sequence of primers used in the PCR reaction

Gene	Primer	Sequence	Amplicon (bp)
Sec31	FW T7	5' CCAAGCTTCTAATACGACTCACTATAGGGAGAACCAGCAAGTCCTCCAAC AC-3'	350
Sec31	BW Multipro	5'- CTCCGCTGTTGAGTTTCACA- 3'	
Sec31	FW Multipro	5'- ACCAGCAAGTCCTCCAACAC- 3'	350
Sec31	BW T7	5'- CCAAGCTTCTAATACGACTCACTATAGGGAGACTCCGCTGTTGAGTTTCAC A-3'	

The fragment was isolated, purified and used as a template for the next *in vitro* transcription, performed as above described.

Hybridization step

Whole mount fixed seedlings were permeabilized by immersion in new absolute ethanol for 30 min., washed twice in absolute ethanol for 5 min. and gradually rehydrated in 75% ethanol (v / v in water), 50% and 25% ethanol (v / v in PBS 1X) for 10 min. each. The samples were re-fixed in fixative solution above described at room temperature (RT) for 20 min., washed twice in PBT (1X PBS plus 0.1% (v / v) Tween-20) for 10 min. and then incubated with 20 µg ml-1 proteinase K (Roche) in 1X PBS for 15 min. The digestion was stopped by incubating the samples in 1X PBS plus 0.2% glycine for 5 min. and then washed twice in PBT for 10 min. The samples were refixed for 20min. at RT, washed twice in PBT for 10min and once in hybridisation solution of 50% (v / v) formamide in 5X SSC (20X SSC: 3 M NaCl, 300 mM sodium citrate, pH 7.0 with 1 M HCl), 0.1% (v / v) Tween-20 and 0.1 mg ml-1 of heparin (Sigma) for 10 min, and then pre-incubated in the same solution, at 50°C, for 1 h. Hybridization was performed overnight at 50°C by incubating the samples in integrated hybridization solution (modified with the addition of 10 g ml-1 salmon sperm

DNA for hybridization solution) containing the labeled RNA probes, previously denatured by incubation at 80°C for 2 min. The optimal hybridization temperature was 50°C, which ensured a sufficient specificity of hybridization.

Post-Hybridization and Fluorescence detection

The samples were washed: three times (10 min., 60 min. and 20 min.) in a solution of 50% (v / v) formamide, 2X SSC and 0.1% (v / v) Tween-20 at 55°C, once for 20 min. in 2XSSC, 0.1% (v / v) Tween-20 at 55°C; twice for 20 min. in 0.2X SSC, 0.1% (v / v) Tween-20 at 55°C; three times for 10 min. in PBT at room temperature, once for 30 min. in PBT plus 1% BSA (Roche). Subsequently, the samples were incubated with a mixture of primary antibodies selected (anti-digoxigenin sheep, Roche, anti-biotin mouse, Roche); diluted (1: 500) in (PBT + BSA), overnight at 4 ° C under stirring. The next day, samples were washed three times for 10 min. in PBT, once for 30 min. in PBT plus BSA and then incubated with a mixture of secondary antibodies (Alexa Fluor 555 dye Donkey Anti-Sheep, Invitrogen, Alexa Fluor 488 dye Donkey Anti-Mouse, Invitrogen) diluted (1: 500) in PBT plus BSA kept in the dark at RT for 2 h. After incubation, the samples were washed twice for 15 min. in PBT agitated gently in the dark. In all stages of the multi-probe method, the procedure has been adopted to ensure complete immersion of the samples in the solutions applied (using 0.5 ml of solution in an eppendorf tube containing 2 ml). The samples were mounted on a microscope slide with a 1:1 solution of 1X PBS and glycerol for the detection.

Confocal analysis

The samples were analyzed with a Leica TCS SP2 (Spectral Confocal and Multiphoton System) laser scanning confocal microscope. The simultaneous detection of the dyes Alexa Fluor (AF) 488, AF555 was performed by combining the settings indicated in the sequential structure of the scanning microscope, as instructed by the manufacturer. The dye conjugates were excited at 488 nm, 555 nm, respectively, from a Ar / He / Ne laser. The fluorescence emission was collected for 488 nm to 517 nm, 555 nm to 569 nm using a Leica HC PL fluotar 10x0.3 NA lens. In these conditions was not detected autofluorescence.

Quantitative qRT- PCR analysis

For qRT-PCR, RNA was extracted from three weeks old seedlings (rosette stage), according to the procedure previously described with the addition of a purification step after the treatment with RW1 Buffer. Purification was performed through a treatment with Rnase-free DNase using a RQ1 RNase-free DNase Promega Kit. The digestion mix is reported in Table 7:

Table 7. Dnase digestion mix

Reagente	Volume
RQ1 Buffer	8μl
DNase	8μl
Rnase free water	64μl

A second purification was performed before cDNA synthesis to make pure samples that will be used for qRT-PCR. The digestion was conducted using the RQ1 RNase-Free DNase kit of Promega (Table 8).

Table 8. Dnase digestion mix

Reagente	Volume
RNA	1-8μl
RQ1 Rnase-Free Dnase 10X Reaction Buffer	1μl
RQ1 Dnase-Free Dnase	1u/μg RNA
Nuclease-free water to Final Volume	10μl

Samples were incubated for 30 min. at 37°C in the digestion mix, then RQ1 DNase Stopsolution was added at a concentration equal to 1/10 of final volume and samples were incubated at 65°C for 10 min.

In this case for cDNA synthesis the iScripttm cDNA Synthesis Kit was used. 1μg of total RNA was used for reverse transcription and mixed with 4 μl of 5X iScript reaction mix, 1 μl iScript reverse transcrptase and nuclease-free water to reach a final volume of 20μl. The sample was incubated in a reaction cycle characterized by: 5 min. at 25°C, 30 min. at 42°C and 85°C 5min.

Specific primers were designed for each of selected genes (Table 9). qRT-PCR reactions were performed using the LightCycler thermal cycler (Roche) with Power SYBR® Green PCR

Master Mix and 0,5 μM primers. The conditions of the PCR were: 95.0°C for 10 min. followed by 40 cycles at 95.0°C for 10 sec. and 60.0°C for 30 sec. The results of two biological replicates and three technical replicate, were analyzed using the qBase PLUS software (Hellemans, *et al*., 2007).

Table 9. List of Primers used for qPCR

Name	Primer	Sequence
PIN1	FW	TACTCCGAGACCTTCCAACTACG
PIN1	RW	TCCACCGCCACCACTTCC
PIN2	FW	TTTCTCCACGCAAATTCTTTG
PIN2	RW	GCTGCTCTTCCTCAAGGAATC
PIN3	FW	GAGGGAGAAGGAAGAAAGGGAAAC
PIN3	RW	CTTGGCTTGTAATGTTGGCATCAG
PIN4	FW	GATGCTGGTCTTGGAATGG
PIN4	RW	CCTGAACGATGGCTATACG
PIN7	FW	CTTGGTATGGCAATGTTCAG
PIN7	RW	CACACGCAATAGGTCTC
ARF7	FW	AGAAAATCTTTCCTGCTCTGGAT
ARF7	RW	TGTCTGAAAGTCCATGTGTTGTC
IAA3	FW	TTAACCTCAAGGAAACAGAGCTG
IAA3	RW	TTAACCTCAAGGAAACAGAGCTG
LAX3	FW	TCACCATTGCTTCACTCCTTC
LAX3	RW	AAGCACCATTGTGGTTGGAC
ABI1	FW	GATCAGATTGGGTAAAGGTTACTG
ABI1	RW	CCAGAAACAGAGCATGATGAAG
ABI1_3	FW	CGGGATCAGATTGGGTAAAGG
ABI1_3	RW	CAGAAACAGAGCATGATGAAGTC
PLY1_2	FW	CTCAACACTCCATCACCAAAC
PLY1_2	RW	GTCTCACCACGGACCATAC
PLY1_1	FW	CAACACTCCATCACCAAACC
PLT1_1	RW	CTCACCACGGACCATACTG

The expression levels were normalized with CT values obtained using the reference gene previously tested using the standard curve. For this type of analysis were tested fifteen reference gene (Table 10) (Tomasz C. et al., 2005), among which only. *PP2A* and *SAND* have been used to normalize the results obtained by qBasePLUS (Hellemans, *et al*., 2007).

Table 10. List of Primers of reference gene tested in qRT-PCR

Name	Primer	Sequence
GAPDH	FW	TTGGTGACAACAGGTCAAGCA
GAPDH	RW	AAACTTGTCGCTCAATGCAATC
AT2G32170	FW	ATCGAGCTAAGTTTGGAGGATGTAA
AT2G32170	RW	TCTCGATCACAAACCCAAAATG
PTBP	FW	GATCTGAATGTTAAGGCTTTTAGCG
PTBP	RW	GGCTTAGATCAGGAAGTGTATAGTCTCTG
UBQT	FW	TTCAAATACTTGCAGCCAACCTT
UBQT	RW	CCCAAAGAGAGGTATCACAAGAGACT
AT4G26410	FW	GAGCTGAAGTGGCTTCCATGAC
AT4G26410	RW	GGTCCGACATACCCATGATCC
AT4G33380	FW	TTGAAAATTGGAGTACCGTACCAA
AT4G33380	RW	TCCCTCGTATACATCTGGCCA
YLS8	FW	TTACTGTTTCGGTTGTTCTCCATTT
YLS8	RW	CACTGAATCATGTTCGAAGCAAGT
AT5G12240	FW	AGCGGCTGCTGAGAAGAAGT
AT5G12240	RW	TCTCGAAAGCCTTGCAAAATCT
FBOX	FW	TTTCGGCTGAGAGGTTCGAGT
FBOX	RW	GATTCCAAGACGTAAAGCAGATCAA
PPR	FW	AAGACAGTGAAGGTGCAACCTTACT
PPR	RW	AGTTTTTGAGTTGTATTTGTCAGAGAAAG
CA	FW	TCGATTGCTTGGTTTGGAAGAT
CA	RW	GCACTTAGCGTGGACTCTGTTTGATC
SAND	FW	AACTCTATGCAGCATTTGATCCACT
SAND	RW	TGATTGCATATCTTTATCGCCATC
PP2A	FW	TAACGTGGCCAAAATGATGC
PP2A	RW	GTTCTCCACAACCGCTTGGT
UBC	FW	CTGCGACTCAGGGAATCTTCTAA
UBC	RW	TTGTGCCATTGAATTGAACCC
TIP41	FW	GTGAAAACTGTTGGAGAGAAGCAA
TIP41	RW	TCAACTGGATACCCTTTCGCA

IIc. - Results

in silico analysis of *Sec31* gene

In the beginning we performed *in silico* analysis of *Sec31* gene which corresponds to At3g63460 (AtSec31A) paralog gene identified in *A.thaliana* genome (Robinson, *et al*., 2007). Gene sequence is 6701 bp long and includes 21 introns and 22 exons (Figure 7). The full-length cDNA of this gene has a open reading frame (ORF) of 3315 bp. The deduced protein consists of 1104 amino acids, has a molecular mass of 119873.6 kDa and an isoelectric point of 4.755 (Figure 7). T-DNA insertions, causing the two mutant genotypes *salk_012544C* and *salk_035921C* analyzed in the present work, are localized in the first exone (Figure 7).
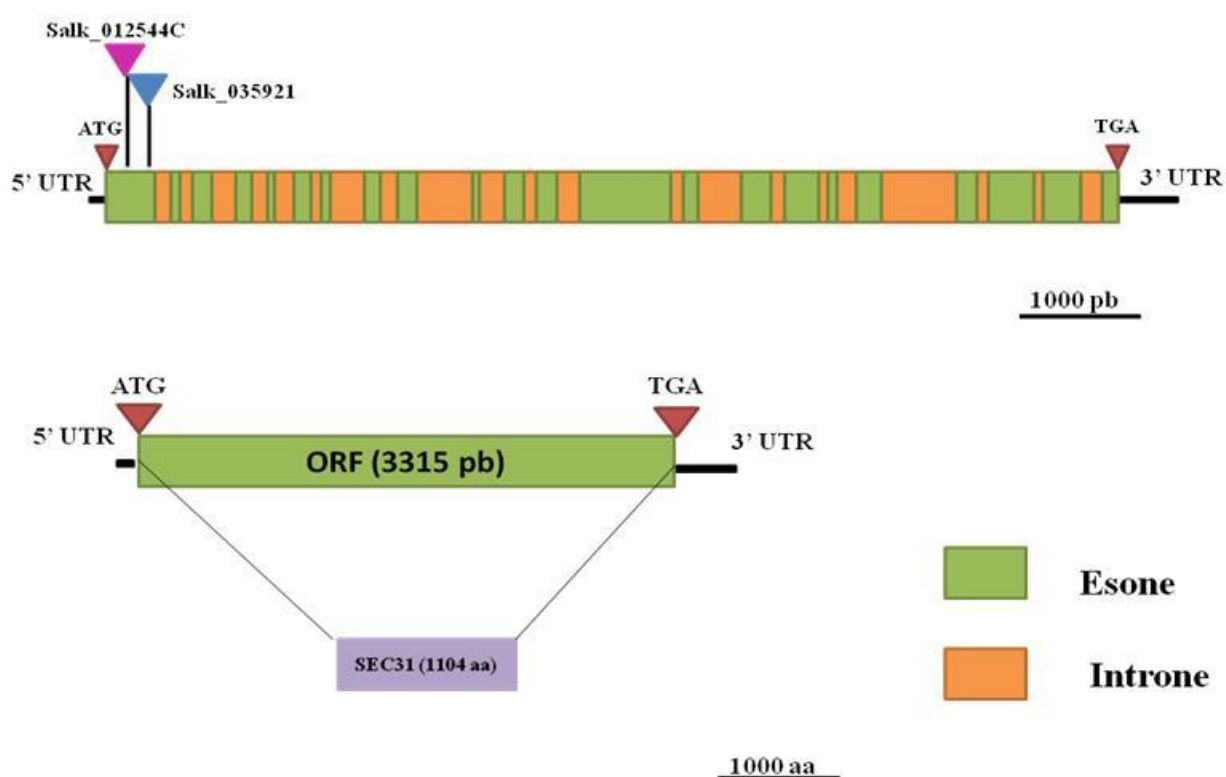
Figure 7. Graphic representation of *Sec31* (At3G63460) gene and corresponding encoded protein. The green and orange boxes indicate exons and introns respectively, whereas the purple and blue triangles represent the sites of T-DNA insertions leading to *salk_012544C* and *salk_035921C* mutant genotypes.

The *in silico* analysis of *Sec31* gene expression clearly shows that this gene is expressed in all organs and developmental stages although at different levels. In particular, the strongest expression is detected at the early phase of seed germination and in the male organ (stame and pollen) of flower; expression is spread in all the young seedling while in adult plant it is high in the

shoot apex, mainly during the transition from the vegetative to inflorescence phase, but absent in the root;, in the leaf, gene expression increases in relation to organ senescence (Figure 8).
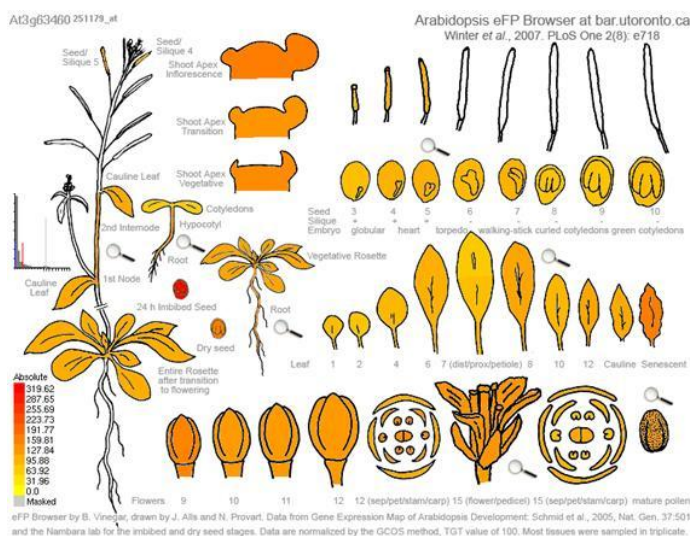
Figure 8. Expression level of *Sec31* gene in different tissues and at specific stages of plant development deduced by using the database (http://bar.utoronto.ca/efp).

IIc1. - Phenotypical analysis of *sec31* mutants

Stem growth

We then analyzed the phenotypic characteristics of two *sec31* mutant genotypes (*salk_012544C* e *salk_035921C*) to compare with those of *elo3* mutant (Figure 9) well described in the literature (Nelissen, *et al*., 2010). Seedlings of *Arabidopsis thaliana* Columbia (Col-0) were used as control. The development of plants, grown on soil in growth chamber with septate conditions of light, humidity and temperature, was monitored periodically. The analysis encompasses the entire lifecycle of plant, starting from the rosette stage, after three week, and including the study of the plant architecture, the structure of floral and reproductive organs, the development and organization of silique (Figure 10). As it possible to observe in Figure 10 A, at the rosette stage *sec 31* mutant lines are quite comparable to the wild type Col0 and do not exhibit narrow leaf phenotype which is distinctive of *elo3* mutant (Nelissen, *et al*, 2010). Moreover, no alterations are reported for the *sec31* mutants compared to the control with respect to the length of the stem, phyllotaxis (Figure 10 B), number of reproductive organs and floral structure (Figure 10 C, D, E), as well as to number and size of siliques (Figure 10 F, G, H).
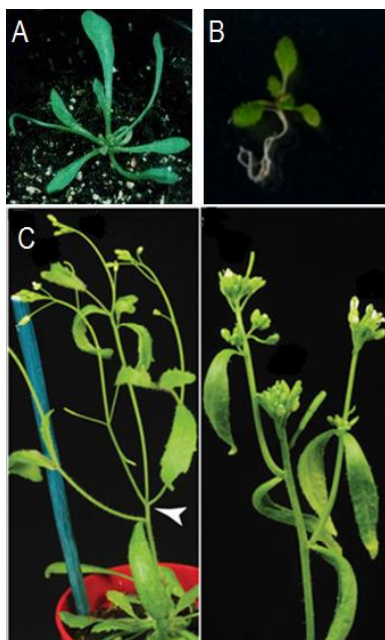
Figure 9. Figure 2. Distinctive traits of elo3-6 mutant: A narrow leaf; B reduced root growth, C altered phyllotaxis (arrowheads) **and apical dominance (Nelisse H.,** *et al*, **2010).**
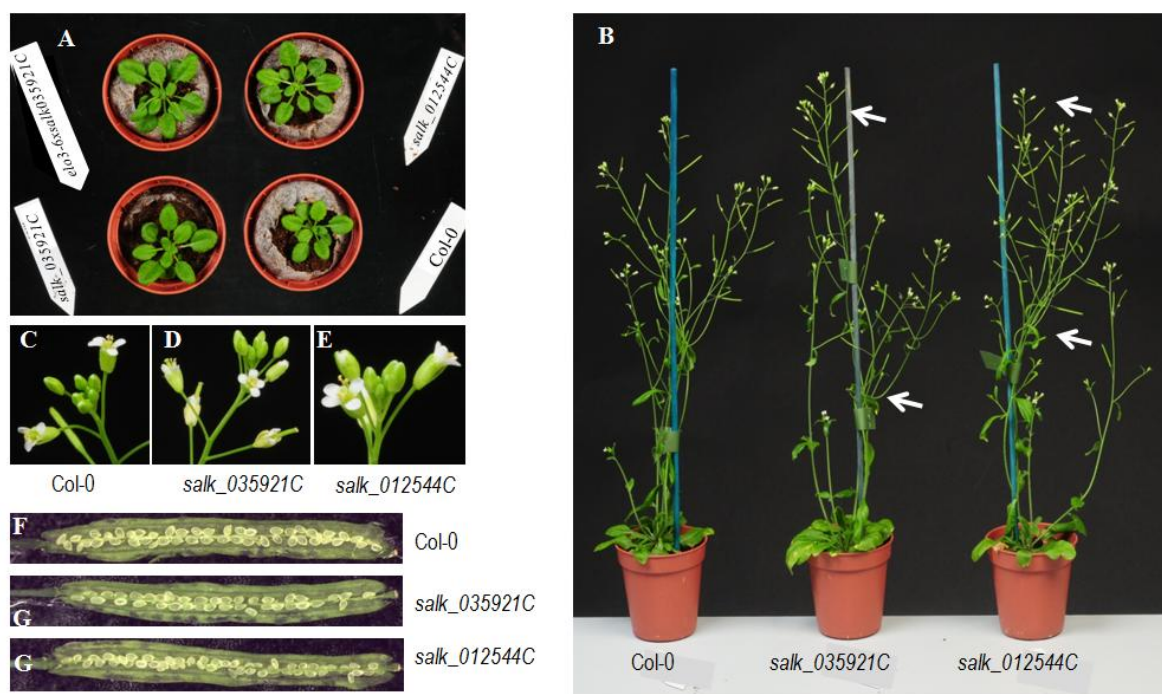

Figure 10. Plants of *Arabidopsis thaliana* **wild type (Col-0) and** *salk_012544C* **and** *salk_035921C* **mutants.** (**A**) rosette stage (three weeks). (**B**) Fully developed plant (seven weeks). (**C, D, E**) Flower magnification. (**F, G, H**) Siliqua. Arrows indicate correct phyllotaxis and apical dominance in *sec31* mutant . The pictures are representative of the results derived from three independent biological replicates.

Root growth and organization

To analyze root phenotype, seeds of *sec 31* mutants were germinated on culture medium in growth chamber with septate conditions of light, humidity and temperature. Root growth was monitored up to 16 days after germination (DAG) by measuring root length every two days using ImageJ software (Figure 11). The obtained results reveal that, with the exception of earliest germination phases and until the fourteenth DAG, the mutant lines *salk_012544C* and *salk_035921C* presents a root significantly smaller compared to the wild type. However, at the sixteenth DAG such difference is no more evident and root length is quite similar in all the three analyzed phenotypes.
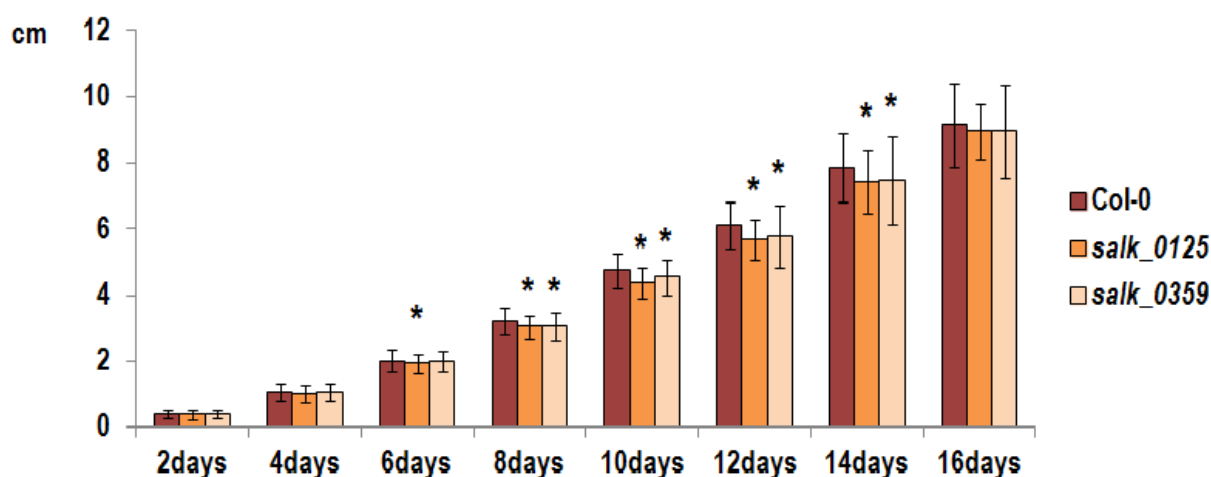

Figure 11. Root length of *Arabidopsis thaliana* wild type seedlings (Col-0) and *salk_012544C* and *salk_035921C* mutants at different days after germination The results represent to the mean value (± standard deviation) of three independent biological replicates. The data were analyzed by Student's t-test; asterisk * indicates the statistically significant difference between the mutant and Wt ($P \leq 0.05$).

Therefore, the *sec31* mutants show only a delay in the growth rate, in contrast to the strong reduction of root development exhibited by *elo* mutants (Figure 9) (Nelissen, *et al*., 2010).

To add information on root organization of *sec31* mutants, we performed also a study of proximal meristem (PM) size (Figure 12 A-E) by using the method described in Dello Ioio, *et al*. (2007).
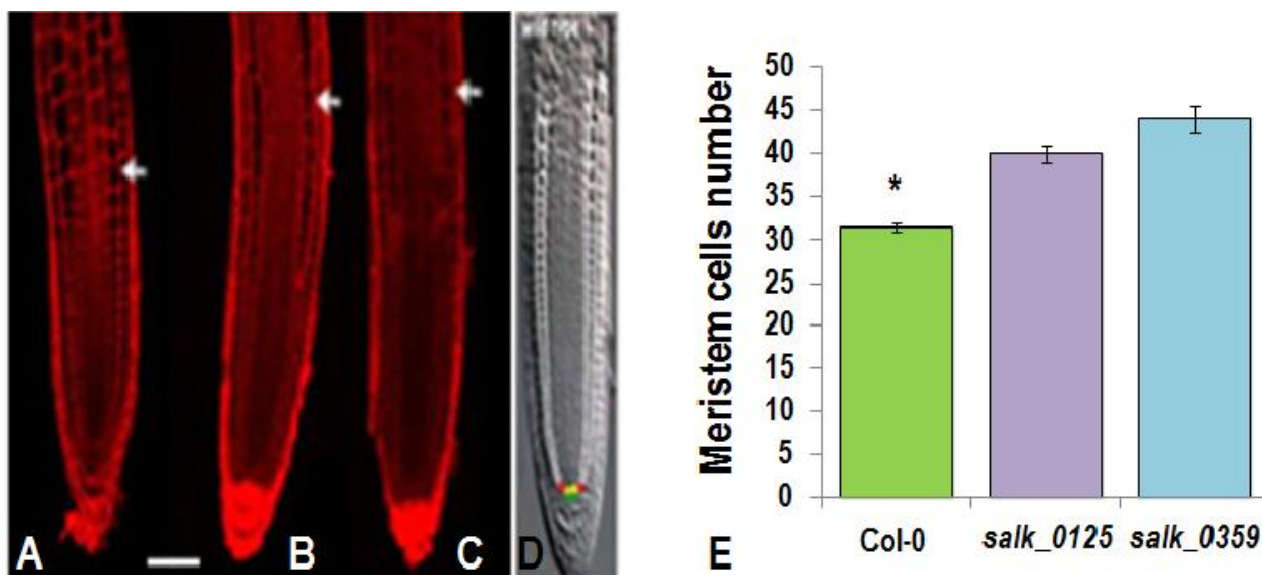
Figure 12. Root meristem size in *Arabidopsis thaliana* wild type (WT) seedlings and in the two *sec31* mutant lines *salk_012544C* e *salk_035921C* at 6 DAG.
A-C: mPS-PI–Stained whole-mounted roots of (**A**) wild-type Columbia ecotype, (**B**) mutant line *salk_012544C*, (**C**) mutant line *salk_035921C*. **A-C** images were obtained through confocal microscope and white arrows indicate TZ where cells leave the meristem and enter the (EDZ). Scale bar size is 100µm
D: Longitudinal section of the *Arabidopsis* root meristem, where the quiescent center is marked in yellow, initial cortical cells in red, a cortex cell file of PM in white, and a cortex cell file of the elongation. **E**: Average cell number along the cortex cell file in the PM. The results represent the mean value of 20 analyzed roots. The data were analyzed by Student's t-test; asterisk * indicates the statistically significant difference between the mutants and Wt (P≤0.001).
DAG= days after germination; **TZ**= transition zone; **EDZ**= elongation- differentiation zone; **PM**= proximal meristem

In root, PM extends until the transition zone (TZ) where cells leave the meristem and enter the elongation /differentiation zone (EDZ) (Fig. 12 A, D). Through the above mentioned method it has been defined that at six DAG *Arabidopsis thaliana* seedlings exhibit a PM with a fixed size: in particular it has been proved that the cortex cell file, before leaving the TZ and enter the EDZ, is formed by 30 cells (Dello Ioio, *et al*., 2007).

We analyzed *sec31* mutants at this stage and we observed that the mutants have more than 30 cells along the cortical cell line in the PM, while wild-type exhibits a typical organization (Figure 12 E). Such difference is accompanied by difference in PM length and width. Namely, in the WT the average length and width of the PM are 213.4µm ±0.23 and 58.8µm±0.23 respectively, while in *salk_012544C* mutant the average length is 220µm±0.06 and the average width is 65.7µm±0.06 and in *salk_035921C* mutant the average length is 231µm±0.23 and the average width is 71.8µm±0.08 (Fig.10 a). Since a longer meristematic zone causes a delay in root cell elongation and differentiation (Moubayidin, *et al*., 2010), these results are consistent and could explain the initial delay of root growth in the *sec31* mutants compared with the control.

In summary, overall the results obtained from the morphological analysis and the evaluation of plant growth parameter do not show similarities between *sec31* mutants and *elo3-6* phenotypes.

IIc2 - Multitprobe in situ hybridization of *ELO3* and *Sec31* in wild type *Arabidopsis* seedlings

As largely known, the definition of organ/tissue-specific gene expression provide additional information on gene functional role. Therefore, based on the putative interaction between Sec31 and ELO3 we also investigated whether the corresponding genes exhibited similar expression domains at the cyto-histological level. The analysis was performed on WT seedling at 4 DAG by using multi probe whole mount *in situ* hybridization method (MISH), which allows to simultaneously localize different transcripts in the same sample (Bruno, *et al.*, 2011). The results show a perfect co-localization of *Sec31* and *ELO3* messengers at the level of shoot apical meristem and differentiating procambial strands (Figure 13 A, B). A clear even if partial overlapping was also observed at the level of root apical meristem; indeed *ELO3* transcripts are spread throughout the whole PM while for *Sec31* they mainly localized in the eumersitem, along the epidermis and in the cortex, while signal appeared faint in the stele (Figure 13 C, D).
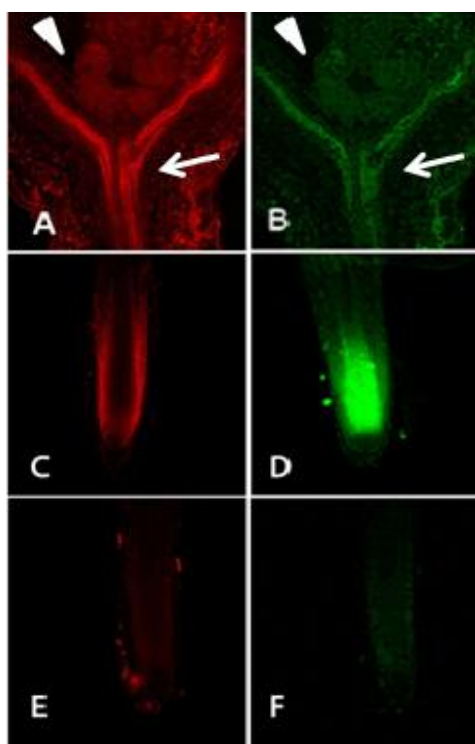

Figure 13. Multi probe whole mount *in situ* hybridization of *Sec31* and *ELO3* genes performed on wild type (Col-0) Arabidopsis seedlings at 4 days after germination (DAG). (A, C) In red the localization of *Sec31* transcript in the shoot and root meristem, respectively. **(B, D)** In green the localization of *ELO3* in the shoot and root meristem, respectively. **(E, F)** Root controls hybridized with sense probe of **(E)** *Sec31* and **(F)** *ELO3*. Scale bar size is 70µm. The arrowhead indicates the shoot apical meristem whereas the arrow indicates the differentiating procambial strands.

Therefore, for both genes the depicted expression patterns are consistent with data in literature and *in silico* analysis (Nelissen, *et al*., 2010; http://bar.utoronto.ca/efp).

IIc3 - *In silico* analysis of protein-protein interactions between ELO3 and secretory pathway proteins

All together the results above described (absence of phenotypic similarities vs similar gene expression pattern) do not support a clear interaction between Sec31and ELO3 proteins. This prompted us to perform an in silico analysis of protein/protein interaction by using CORNET software to predict interaction between ELO3 and either Sec31 or other proteins of the secretory pathway (Figure 14). Based on these results no direct interaction of ELO3 with Sec31 or other components of the secretory pathway could be predicted although some proteins were found in between and more information on this aspect is reported as supplemental data (appendix Table S1). Simultaneously, TAP analysis was replicated by the research group of Prof. M. Van Ljisbettens and did not confirm the previous data,thus excluding a direct interaction between Sec31and ELO3.
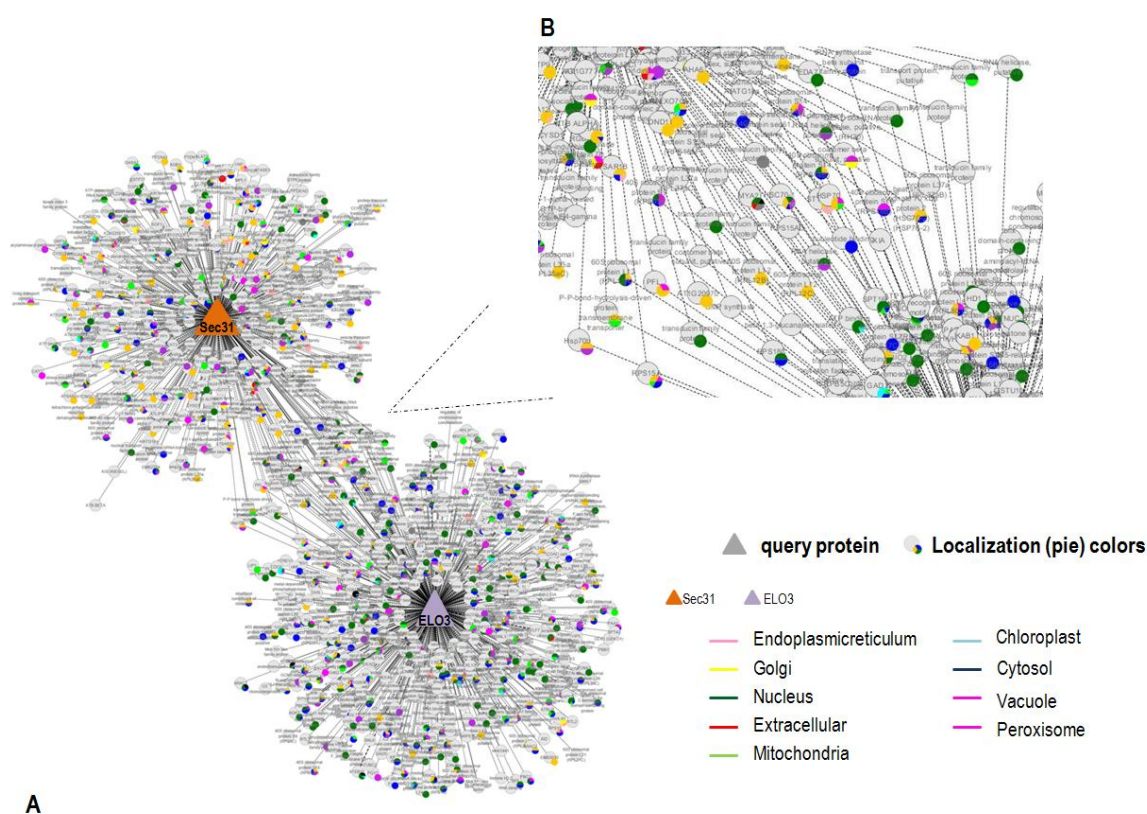

Figure 14. *In silico* analysis of protein network of Sec31 and ELO3 by using the protein-protein interaction NETworks tool (CORNET 2.0, https://bioinformatics.psb.ugent.be/cornet, De Bodt *et al*., **2012). (A)** Protein interacting with Sec31 and ELO3. **(B)** Higher magnification illustrating protein interacting with both SEC31 and ELO3

IIc4 - qRT-PCR expression analysis of Elongator-related genes in *sec31* mutants

Notwithstanding, it seemed interesting and useful to analyze in *sec31* mutants the expression pattern of some direct or indirect target genes of Elongator action. In particular, among these targets we selected genes involved in the metabolism, transport and signaling of auxin hormone which were found to be differentially expressed in the *elo* mutant through both microarray (Nelisse, *et al.*, 2005) an transcriptomic analysis (in progress). The rational for selecting these specific genes relied on literature data showing that alterations in the secretory pathway are responsible of altered/reduced translocation and signaling of auxin, due to an incorrect location of the transporter proteins of these hormones (Kleine-Vehn, *et al.*, 2009).

Therefore, we planned to investigate in the *sec31* mutant the expression level of some of these auxin-related genes, in order to add some information about the convergent action on the same hormonal pathways . In particular we selected by GENEVESTIGATOR the *PIN1-4, PIN7* and *LAX3* genes involved in auxin transport and the *LAX3, IAA3* and *ARF7* genes involved in auxin signaling (Figure 15).
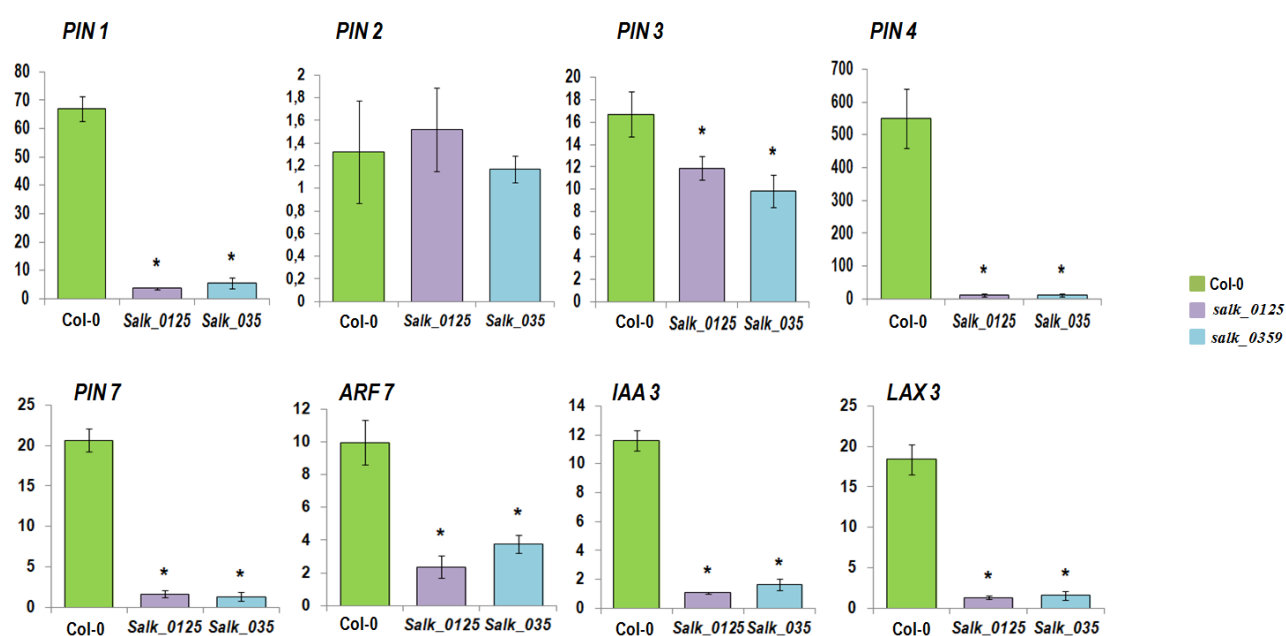

Figure 15. Gene expression levels estimated by RT-qPCR in *sec31* mutants. The RT-qPCR data were normalized using a housekeeping genes and analyzed by qBasePLUS software. The asterisk * indicates the statistically significant difference between the mutant and Wt (P≤0.05) estimated on three biological replicates.

The obtained results show that, with the only exception of *PIN2* gene, selected genes are significantly down-regulated in both *sec31* mutant lines analyzed (Figure 15). In details, transcript

levels in the mutants is about 4 times lower than in the control in the case of *PIN3* and strongly reduced (about 100 times lower) in the case of all other genes.

IIId. - Discussion

Morphological analysis and growth parameters evaluation performed on *sec31* mutants showed that both analyzed genotypes do not exhibit phenotypic alterations but only a delay in root growth. At this respect it is worthy noting that *Arabidopsis thaliana* genome encodes two *Sec31*paralogs At3g63460 (AtSec31A), At1g18830 (AtSec31B) (Robinson, *et al*., 2007). Therefore this result could be related to a compensatory effect, due to the redundancy of *Sec31* genes in the *Arabidopsis* genome. On the other hand, it is well known that the redundancy of genes encoding components of secretory pathway, which occurs in higher organism due to duplication events, is related to a greater complexity of regulatory mechanisms that govern this pathway (Marti, *et al*., 2010).Thus, the absence of phenotypic alteration could be also related to an un-preeminent role of Sec31 protein in cell secretory pathway

Concerning the expression pattern of *Sec31* gene, according to in silico analysis, we observed that in young seedling it is expressed in both shoot and root apical meristem. Moreover, a clear overlapping was also observed when comparing the expression domains of *Sec31* and *EL03*. Therefore, as known for ELO3 (Nelissen, *et al*., 2010), a putative role for *Sec31*gene in meristem activity/organization could be hypothesized, as also supported by the alteration detected in proximal mer size of mutant lines (Figure 12). However, in absence of phenotypic similarities between *sec31* and *elo-6* mutants, this result does not provide useful information about the functional relationship between the encoded protein and the related action. On the other hand, replicated TAP analysis and *in silico* analysis of protein-protein interaction did not confirm previous result, thus excluding a direct interaction between ELO3 and Sec31.

Finally, we analyzed in *sec31* mutants the expression pattern of some genes modulated by Elongator complex. The genes selected for this analysis encode either auxin carriers or proteins involved in auxin signaling and all were found down-regulated in *sec31* mutant. As previously mentioned, it is known that alterations in the secretory pathway are responsible of altered/reduced translocation and signaling of auxin, due to an incorrect location of the transporter proteins of these hormones (Kleine-Vehn, *et al*., 2009). The downregulation of analyzed genes in *sec31* mutant is not surprising since the transcription of genes encoding auxin carriers is influenced by auxin itself, an action that is only a component of the fine-tuning mechanism by which auxin acts as one of the key regulators of its own transport (Vieten et al. 2007; Petràsek and Frimml 2009). Therefore, reduced

60

gene expression could be related to a kind of feedback mechanism in response to the defect on transporters dislocation and auxin transport and accumulation (Kleine-Vehn, *et al.*, 2009).

In conclusion and very interestingly, despite the absence of a direct interaction, trough this analisys we demonstrated that *Sec31* and *ELO3* share common downstream target genes and both seems play a role in auxin pathway. Future transcriptomic analyses on auxin mutants on one side and the identification of direct interactors or related players of both genes on the other side, could be useful to deepen if the molecular circuits through which Elongator complex and the secretory machinery act on auxin pathway exhibit a cross talk or they work in an independent manner.

III° Chapter

Section B: Study of Elongator-mediated gene expression under darkness and light qualities

IIIa. - Introduction

In plants, the growth and final architecture are defined by spatial and temporal regulation of cell division and expansion that are steered by endogeneous, hormonal, and environmental stimuli leading to transcriptional change and the onset of specific developmental program. Plants are sessile organisms that evolved a high degree of plasticity to optimize their growth and reproduction in relation to fluctuating environmental conditions such as light, salinity, humidity and temperature. The efficient perception, interpretation, and transduction of such signals allow plants to synchronize their development with seasonal change. In fact the plants use a wide range of sensory systems to perceive and transduce specific environmental signals. Light is one of the key environmental signals that influences plant growth and development. In addition to being the primary energy source, light also controls multiple developmental processes in the plant life cycle, including seed germination, seedling de-etiolation, leaf expansion, stem elongation, phototropism, stomata and chloroplast movement, shade avoidance, circadian rhythms, and flowering time (Deng and Quail, 1999; Wang and Deng, 2003; Jiao et al., 2007). In addition, plants have the capacity to monitor different characteristics of light such as quality, quantity, duration and wavelength, because they posses four classes of photoreceptors, the phytochromes (phys), that absorb red (R) and far-red (FR) wavelengths (600-750 nm), and three types of photoreceptors that absorb the blue (B)/ultraviolet-A (UV-A) region of the spectrum (320-500 nm), i.e. cryptochromes (crys), phototropins (phots), and three newly recognized LOV/F-box/Kelch-repeat proteins ZEITLUPE (ZTL), FLAVIN- BINDING KELCH REPEAT F-BOX (FKF), and LOV KELCH REPEAT PROTEIN 2 (LKP2) (Li, *et al*., 2011). In addition, UV RESISTANCE LOCUS 8 (UVR8) was recently shown to be a UV-B (282-320 nm) photoreceptor (Rizzini, *et al*., 2011) (Figure 1).
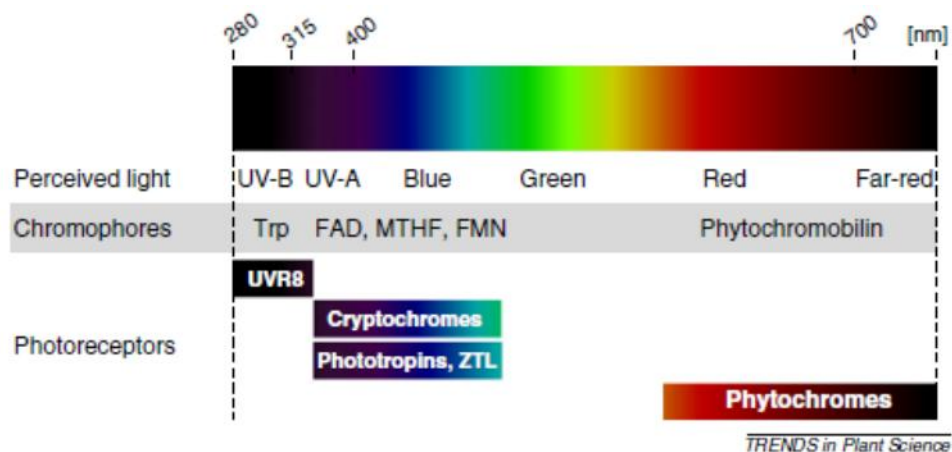
Figure 1. Photoreceptors mediate the light perception in plants. (*UV-B photoreceptor-mediated signalling in plants Heijde and Ulm, 2012*).

The phytochromes were discovered by Butler *et al*., 1959, and are a superfamily of photoreceptors in higher plants and many prokaryotes and fungi. In plants, phytochromes regulate the germination of seeds, stem growth and flowering time and other important functions by providing a link between light and plant development. The phytochrome is a soluble protein, it exists as homodimer and is formed by two equivalent subunits with a total weight of 250 kDa. Each subunit is composed of two components: a pigment that absorbs the light called chromophore and an apoprotein, both chromophore and apoprotein arrange the holoprotein. Phytochrome apoproteins are synthesized in the cytosol, where they assemble autocatalytically with a linear tetrapyrrole chromophore, phytochromobillin (PΦB) (Li, *et al*., 2011). Phytochrome domains have different functions, essential for the photoreceptor activity, i.e. a N-terminal photosensorial region (~70kDa) and a C-terminal regulatory region (~55 kDa), connected by a flexible hinge region. The N-terminal domain can be further divided into four consecutive subdomains: N-terminal extension (NTE), Per-Arnt-Sim (PAS), GAF, and PHY, while the C-terminal domain can be divided into two subdomains: the PAS-related domain (PRD) containing two PAS repeats, and the histidine kinase-related domain (HKRD) (Li, *et al*., 2011) (Figure 2).
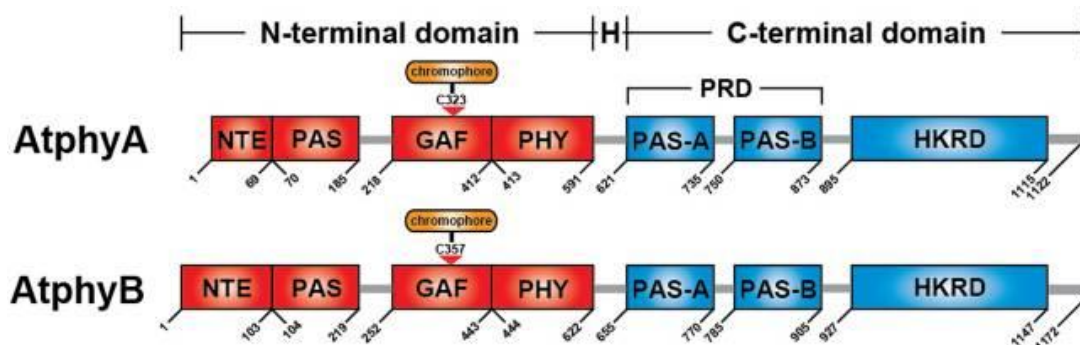
Figure 2. The domain structure of Arabidopsis phyA and phyB molecules. (Li, *et al*., 2011).

In the C-terminal domain there is a sub-domain called Nuclear Localization Signal (NLS) necessary to import the phytochrome molecule from cytosol to the nucleus. The intrinsic photochemical activity of the phytochromes resides in the photoreversibility of their molecular structure, because the phytochromes exist in two reverse forms, one biologically inactive Pr and the other biologically active Pfr. Indeed the phytochromes are synthesized in the cytosol in the Pr conformation that absorbs maximally at 660 nm (red light) converting Pr in Pfr which absorbs maximally at 730 nm (far-red light). When the phytochrome molecule arrives in the nucleus, it interacts with different regulators of transcription that modulate changes during gene transcription.

IIIa1. - Skoto and Photomorphogenesis pathways

In plants, the light pathway starts by the perception of a light signal and it proceeds through a modulation of transcription and it terminates with a consequent variation on plant growth and development. Light regulates the translocation of the photoreceptors from the cytoplasm into the nucleus and this represents the key event in the phytochrome signaling cascade that induces the transcription of genes involved in plant photomorphogenesis program. The light signaling pathway downstream from photoreceptors is able to converge the light signal to a conserved protein complex, COSTITUTIVE PHOTOMORPHOGENIC/DE-ETIOLATED/FUSCA (COP/DET/FUS also known as CDD), which integrates the different light signals and modulates a considerable number of signaling intermediates such as a large number of transcription factors. Phytochrome-INTERACTING FACTOR 3 (PIF3), PIF4, PIF3-LIKE 5 (PIL5) / PIF1 and LONG POCOTYL 5B HY5 (HY5), are the key components of the light signaling pathway. Indeed they link light signals to developmental programs such as the circadian clock, flowering time, phytohormone regulation and photomorphogenesis. Through molecular and genetic approaches it was observed that in plants the light induces a strong reprogramming of the transcriptome which was demonstrated by gene

expression studies that highlight the existence of different levels of expression in seedlings grown in the presence of light or grown in darkness (Yuling, *et al*., 2007). Plant can undergo two different developmental programs, skoto- and photomorphogenesis, depending if they grow in the absence or the presence of light. Light affects many developmental and physiological responses, in fact light exposure triggers several major developmental and physiological events. These include: growth inhibition and differentiation of the embryonic stem (hypocotyl), maturation of the embryonic leaves (cotyledons), and establishment and activation of the stem cell population in the shoot and root apical meristems (Arsovski, *et al*., 2002). Seedlings grown in darkness, show a completely different phenotype, characterized by long hypocotyl, closed cotyledons, apical hook and development of protoplastids into etioplasts (Figure 3). In the two separate programs of plant development, the phytochromes play a key role,i.e. phytochrome A (PHYA) and phytochrome B (PHYB), act to suppress two main branches of light signaling such as COP1-TFs (*CONSTITUTIVE PHOTOMORPHOGENESIS 1*) and PIFs-TFs, promoting the transcription of a diverse range of genes involved in the photomorphogenesis process, whereas in darkness Pifs-TFs and COP1-TFs target several photomorphogenesis-promoting transcription factors as HY5, HYH, HFR1 and LAF1 and both phytochromes for degradation, this is required to start the skotomorphogenesis program (Figure 3).
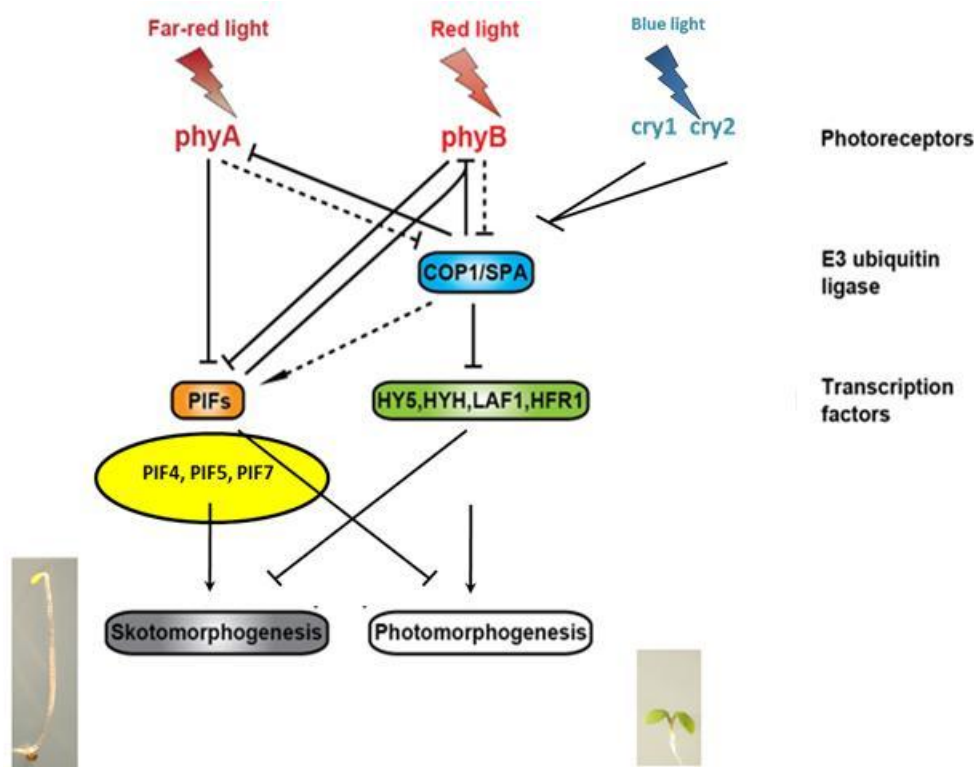

Figure 3. A simplified model of phytochrome signaling pathway. (Li, *et al*., 2011).

The transition from dark to light induces a rapid change in plants and restoration of the development program. Generally the mutants that in the presence of light show a etiolation phenotype identify positive regulators of photomorphogenesis. These mutants, isolated by Koornneef *et al.* 1980 were denominated *long hypocotyl* or *hy* and are characterized by the lack of capacity to perceive light, such that, in the presence of light they show a typically etiolation phenotype, that is characterized by a long hypocotyl. The transcription factor HY5, a bZIP DNA binding protein, promotes photomorphogenesis in all light qualities regulating the transcription of genes involved in the photomorphogenetic program. While in the dark, COP1 interacts with HY5, inducing ubiquitination of this transcription factor resulting in the degradation. Therefore, in the presence of light HY5 will accumulate inducing a rapid photomorphogenic response resulting in the inhibition of the hypocotyl elongation. Obviously, the mutants *hy5* under light conditions are characterized by a long hypocotyl, that represents a typical defect in the light signaling pathway. The development of a long hypocotyl in plants is a strategy to escape from the darkness condition and grow towards the light source, essential for their survival. In *Arabidopsis thaliana* the hypocotyl is composed by rows of 22-25 cells and this number does not change, if the plant grows under continuous exposure or in darkness (Takase, *et al.*, 2003). This indicates that the hypocotyl elongation, as morphological response to the dark condition is caused by a longitudinal expansion of the cells of the hypocotyl, and does not result from cell division activity. Recent studies have shown that through phytochrome-INTERACTING FACTOR 3 (PIF3), PIF4, PIF3-LIKE 5 (PIL5) / PIF1 and LONG POCOTYL 5B HY5 (HY5), the light signaling and the hormone signaling (gibberellic acid (GA), acid abscisic acid (ABA), auxin (IAA) and ethylene (ETH)) converge in a program of development and growth such as photomorphogenetic program. The hormones in fact are involved in the process of cell expansion along its longitudinal axis, and maybe they are active during the process of hypocotyl elongation.

Light signaling and hormone activity: a coordinated network

The phenotype of a plant that is grown under light condition or in darkness is the result of a coordinated activation / inhibition of transcription factors, belonging to the pathway of the light signaling, as well as to an integrated physiological activity of hormones. The light acts by reducing the levels of gibberellin in the *Arabidopsis thaliana* and HY5 induces the expression of *giberellins-2-oxidase* acting negatively on the gibberellin pathway. In the dark, however, the levels of gibberellin are high, then the protein DELLA, inhibitor of the GA in presence of light, undergoes

degradation, thereby releasing PIF3, which induces the expression of genes involved in skotomorphogenesis, while the gibberellin in cross talk with other hormones, promotes hypocotyl elongation, the formation and maintenance of the vegetative hook called "apical hook". In plants the "apical hook" develops soon after germination and its function is to create a protection of the shoot apical meristem, during the passage through the soil to reach the light. The coordinated actions of gibberellins, ethylene and brassinosteroids control asymmetric auxin distribution to allow the correct development of the hook in darkness (Mazzella, *et al.*, 2014). From literature it's known that in seedlings grown in darkness the establishment of hook structure is due first to an auxin gradient above the optimum, able to inhibit the growth at the inner side of the hook and then to gibberellin that determine the speed and degree of the hook formation by promoting cell elongation and cell division at the outer side at the hook. (Figure 4).
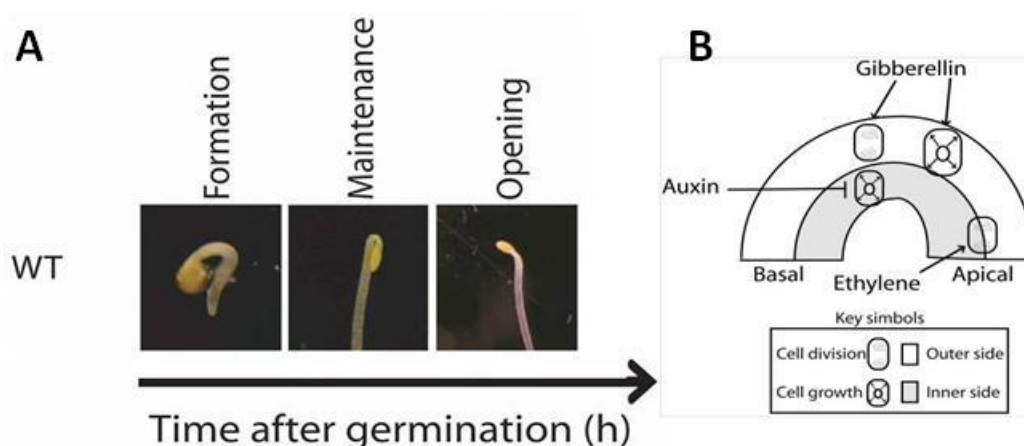

Figure 4. Development of apical hook. (**A**) Apical hook development in dark grown seedlings, the photographs were taken 24 h after germination for the formation phase, 48 h after germination for the maintenance phase and 84 h after germination for the opening phase. (**B**) Primary action of auxin (inhibition of cell expansion at the inner side), gibberellins (promotion of cell division and expansion at the outer side) and ethylene (enhanced cell division at the top) during apical hook development. Arrows: Positive regulation; T-bars: Negative regulation (Mazzella, *et al.*, 2014).

Mutants defective in brassinosteroid synthesis such as *det2* (*dee-tiolated* 2) lack an apical hook in darkness (Choryetal.,1991). Brassinosteroids enhance the activity of the kinase BIN2 (BR-INSENSITIVE 2) that phosphorylates ARF2 and reduces its activity, leading to the enhanced expression of auxin responsive genes (Vert, *et al*., 2008). It has been proposed that brassinosteroids affect auxin distribution through PIN modulation (De Grauwe, *et al*., 2005), however further work is necessary to define the points of regulation of brassinosteroids in the network signaling that leads to apical hook formation. A low light intensity stimulates the plant to orient upward both cotyledons and mature leaves, thus strengthening the extension of the petiole and reducing the expansion of the

leaf lamina. The bending upwards of the leaves, caused by a rapid growth of the lower part compared to the upper side, is called hyponasty. The hyponasty is a rapid response, in order to increase the probability of reaching the light and get out of the shade condition. These rapid plant responses coincide with the decrease in the chlorophyll content in the leaf tissues. This physiological process is regulated by hormones such as ethylene, gibberellic acid, which regulate the asymmetric distribution of auxin that leads to an increase of cell proliferation between the adaxial and abaxial side of the leaf as well as to an asymmetric elongation of mesophyll cells. The curvature of the leaf downwards, which occurs when the upper part of the lamina grows faster than the lower part, is defined epinasty. The ethylene and the high concentrations of auxin induce epinasty and it is noticed that the auxin acts indirectly inducing the production of ethylene.

IIIa2. - The Elongator Complex takes part in regulation of Skoto/Photomorphogenesis

In *Arabidopsis thaliana*, there are five phytochromes, designated phytochrome A (PHYA) to PHYE. They are encoded by five distinct members of the phytochrome gene family and are classified into two groups according to their stability in light (Sharrock and Quail, 1989). PHYA is a type I (light labile) phytochrome, and PHYB to PHYE are all type II (light stable) phytochromes. Hence PHYA is most abundant in dark and far-red grown seedlings, whereas its level drops rapidly upon exposure to R or white (W) light. In light-grown plants, PHYB is the most abundant phytochrome, whereas PHYC-PHYE are less abundant (Clack, *et al*., 1994; Hirschfeld, *et al*., 1998; Sharrock and Clack, 2002). Phytochromes play many roles in the regulation of plant architecture, and indeed it's clear now that they perform specific and overlapping roles during all life cycle of a plant. This means that phytochromes are involved in seed germination, seedling de-etiolation, shade avoidance, flowering time and regulation of circadian clock system. The first phytochrome deficient mutants in *Arabidopsis* were a series of *phyB* alleles in the Landsberg *erecta* (*Ler*) background (*phyB-1* to *phyB-8*), *phyB-9* and *phyB-10* were identified in the Columbia (Col) and L*er* backgrounds, respectively. Mutants deficient in PHYA were isolated by exploiting the signalling behaviour of PHYA in the HIR mode to identify mutants displaying an etiolated appearance in continuous far-red light. Multiple *phyA* alleles were isolated through these screens; *phyA-1, phyA-2, phyA-201, phyA-202, phyA-203, phyA-204, phyA-205, phyA-206, phyA-207and phyA-208* in L*er* (Whitelam *et al*., 1993, Reed, *et al*., 1994), *phyA-101–phyA-103* in RLD (Parks and Quail, 1993; Dehesh *et al*., 1993), and *phyA 209–phyA-211* in Col-0 (Reed *et al*., 1994). The *Arabidopsis phyA*

mutant displays a wild-type phenotype under white and red light exposure. Whereas when it is grown in continuous far-red light, the *phyA* mutant shows a skotomorphogenic phenotype, that confirmed it role as a primary photoreceptor involved in the perception and mediation of responses to far-red light. It should be noted that *phyA* mutants also display elongated hypocotyls in continuous blue light (Whitelam *et al.*, 1993; Neff and Chory, 1998), suggesting that PHYA also plays a pivotal role in perceiving and transducing blue light. By contrast PHYB is the predominant phytochrome that regulates the de-etiolation under white and red light, indeed mutants deficient in PHYB display a significantly elongated petiole, reduced leaf area and increased apical dominance. Moreover, the long hypocotyl and reduced cotyledon expansion phenotypes were enhanced in *phyA phyB* double mutants relative to *phyB* monogenic mutants in red light, revealing a role for PHYA in responding to red light which is normally masked in the presence of PHYB (Neff and Van Volkenburgh, 1994; Reed *et al.*, 1994; Casal and Mazzella, 1998; Neff and Chory, 1998). The choice to analyze the role of Elongator in relation to the light pathway is based on previous studies which proved that the photomorphogenetic process is altered in Elongator mutants. In fact, by comparing the phenotype of the *elo* mutants with the phenotype of the *phy* mutants it is possible to observe that the *elo* mutants show morphological features similar to those present in *phy* mutants, such as leaf hyponasty long petioles and narrow leaf laminas (Figure 5).
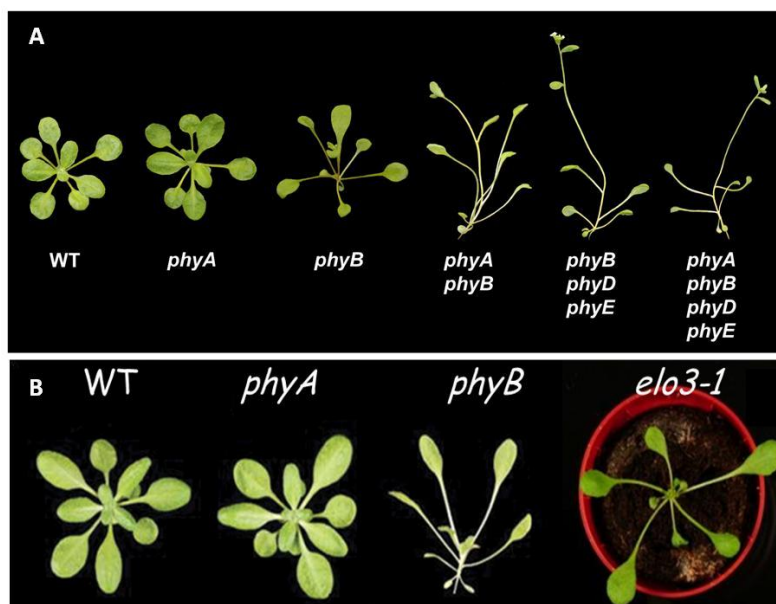

Figure 5. Comparative analysis between phytocrome mutants and *elo* mutant. (A) Phenotypes of 3 week-old wild-type (WT), *phyA*, *phyB*, *phyA phyB*, *phyB phyD phyE*, *phyA phyB phyD phyE* plants grown under white light conditions (16-h light/8-h dark). **(B)** WT, phyA, phyB plants grown in 8 h photoperiods of white light at 120 μmol m^{-}2 s^{-}1. Scale bar represents 10 mm.

Furthermore, the analysis of the *elo* mutants under different light qualities (red, far-red, blue) showed a longer hypocotyl than the WT, thus highlighting hyposensitivity to light. This

morphology suggests that the *elo* mutants are defective in light perception, they are still shorter in light than they are in darkness. This suggesting that the Elongator complex is involved in the photomorphogenesis process and that it plays an important role in the light-signaling pathway in which the two principal phytochromes (PHYA and PHYB) are involved. Discovery of genetic interactions between Elongator and phytochrome light receptors and other light signaling components will clarify the position of Elongator within the network of the light response pathway.

IIIb. - Materials and Methods

The experimental work was focused on identification of putative target genes of the Elongator complex in a model plant *Arabidopsis thaliana*. In order to understand if Elongator works as interface between light signaling and gene expression during transcription elongation, a set of experiments were carried out in the lab of Mieke Van Lijsebbettens, Ghent (Belgium), to investigate whether Elongator can regulate plant development under light and in darkness. The experiments required growth chambers equipped with light lamps allowing to obtain red, far-red and blue light. These facilities are available in the laboratory of Prof. Dominique Van Der Straeten and Filip Vandenbussche (Department of Molecular Genetics, Unit Plant Hormone Signalling and Bio-imaging, Ghent University).

Plant material and plant growth in soil

Seedlings of *Arabidopsis thaliana* Columbia-0 (Col-0), of Landsberg erecta (Ler), and of all mutants analyzed, were grown for upscale in growth chamber in half-strength Murashige and Skoog medium (Murashige and Skoog, 1962), supplemented with 1% sucrose under a 16-h day (110 μmol m^{-2} s^{-1}) and 8h night regime. Seed sterilization was performed in 5% bleach (v/v)in water with 0.05% Tween 20 for 10 min. and washed in water five times for 5 min. Plants were germinated in rockwool soil and watered every two days and grown at 21 ºC, 100 mol m^{-2} s^{-1} photosynthetically active radiation in a 16-h light regime, and 50% relative humidity.

In vitro plant growth conditions

The seedlings of *Arabidopsis thaliana* Columbia-0 (Col-0) and of Landsberg erecta (Ler) were obtained from the Nottingham Arabidopsis Seed collection. The *elo3-6* mutant (GABI-KAT collection code GABI555_H06) and phyB-9 were in Columbia-0 (Col-0) background whereas the *elo3-1* mutant (Nelissen H., *et al*, 2005) and phyA-201 were in Landsberg erecta (Ler) background. For *in vitro* plant growth the seeds of all these mutants and of both wild type after sterilization were sown in on one-half-strength MS medium (Murashige and Skoog, 1962) without sucrose. Subsequently a period of vernalization lasted for 48h, the seeds were subjected to a treatment of 6h under white light, 16 h/8 h (day/night) with white light (neon tubes, cool white), 100 μmolesm^{-2}s^{-1} light intensity, and 21°C, to stimulate the germination and then transferred in a growth chamber for

4days under continuous light conditions (red, far-red and blue) (10 µmol.m^{-2}.s^{-1}). Whereas the seeds used for the experiments in darkness, were exposed for 6h to white light to stimulate the germination, but after that for they were grown in the growth chamber room inside a special light-proof envelopes for 2 to 6 days. For each experimental replicate.

Hypocotyl assay

Sterilized seeds were sown in 0.5x Murashing and Skoog (MS) plus vitamine and without sucrose, incubated at 4°C for 48h. After the vernalization they were transferred to growth chamber for 6h (16h/d) under white light to stimulate the germination an then transferred to growth chambers and grown under continuous red, far-red or blue light (10µmol.m^{-2}.s^{-1}) until for 2 to 6 days. The hypocotyl lengths were measured using ImageJ software and the Student's test was performed to determine whether the difference between two samples was significant at $\alpha = 0.05$ (5%).

RNA extraction

The total RNA extraction was performed using the kit RNeasy Plant Mini Kit (RNA isolation and cleanup) (QIAGEN). Up to 100 mg of tissue was homogenized in liquid nitrogen and transferred into pre-cooled eppendorf, 450 µl of buffer RLT was added, the sample was vortexed and transferred into the QIAshredder spin column placed in a 2 ml eppendorf and centrifuged at 14000 rpm for 2 min. at 20-25 ° C. The supernatant obtained was transferred to a new Eppendorf tube, then precipitated with the addition of 0.5 volume of 100% ethanol. The sample was transferred to a new column RNeasy spin column, inserted into a collection tube and then centrifuged at 10,000 rpm for 15 sec at 20-25 °C. In this column were added 350 µl of Buffer RW1, centrifuged at 10000 rpm for 15 sec at 20-25 °C, the eluate thus obtained was eliminated. 80 µl of DNase were added on the membrane mix (prepared previously), the tube was ? at room temperature for 15 min. After the incubation period, were added a 350 µ of Buffer RW1, centrifuged at 10000 rpm for 15 sec at 20-25 °C, the eluate thus obtained was eliminated. In order to purify the RNA were added to 500 µ of Buffer RPE to wash the membrane and the column and then was centrifuged at 13000 rpm for 15 sec at 20-25 °C. I deleted the flowthrough and repeated the same steps again, changing only the spin centrifugation and time, then 50 sec at 10000 rpm. I delete the supernatanat and added 350 µl of Buffer RPE at 10000 rpm for 20 sec. This step was repeated a second time to purify the sample and then was deleted the flowthrough and repeated the same steps again, changing only the centrifugation time, 2 min at 10000 rpm. To remove any traces of ethanol, the column "RNeasy spin

column (pink)" was transferred into a new centrifuge for 2 min and column. at 14000 rpm. Finally, the column "RNeasy spin column (pink)" was transferred into a 1.5 ml eppendorf are added directly to the silica membrane of 50μl of RNase-free H20 to eluate the RNA, the sample was incubated for 5 min at room temperature environment and centrifuged for 1 min. at 10000 rpm.

Treatment with Rnase-free DNase

To eliminate a possible contamination by genomic DNA digestion with DNase is applied during the extraction of RNA by using RQ1 RNase-free DNase Promega. The mix for the sample shown in Table 1 includes:

Table 1. Dnase digestion mix

Reagente	Volume
RQ1 Buffer	8μl
DNase	8μl
Rnase free water	64μl

cDNA synthesis: iScripttm cDNA Synthesis Kit

Before cDNA synthesis was carried out on RNA samples a DNA digestion, this to make pure samples that will be used for qRT-PCR. The digestion was conducted using the RQ1 RNase-Free DNase kit of Promega (Table 2).

Table 2. Dnase digestion mix

Reagente	Volume
RNA	1-8μl
RQ1 Rnase-Free Dnase 10X Reaction Buffer	1μl
RQ1 Dnase-Free Dnase	1u/μg RNA
Nuclease-free water to Final Volume	10μl

Samples were incubated for 30 min at 37 °C. Then was added μl of RQ1 DNase Stop and subsequently samples were incubated at 65 °C for 10 min. The iScripttm cDNA Synthesis Kit was used for the synthesis of cDNA, 1μg of total RNA was used for reverse transcription, and mixed with 4 μl of 5X iScript reaction mix, 1 μl iScript reverse transcrptase and nuclease-free water to reach a final volume of 20μl. The whole was incubated in a reaction cycle characterized by: 5 min at 25 ° C, 30 min at 42 ° C and 85 ° C 5min.

qRT-PCR analysis

qPCR reactions were performed using the LightCycler thermal cycler (Roche) with Power SYBR® Green PCR Master Mix and 0,5 μM primers (Table). The conditions of the PCR are: 95.0 °C for 10 min followed by 40 cycles at 95.0 °C for 10 sec and 60.0 °C for 30 sec. The results of two biological replicates and three technical replicate, were analyzed using the qBase PLUS software (Hellemans, *et al*., 2007).

Table 3. Primers used in q-PCR

Name	Primer	Sequenza
PIF3	FW	CCCTCCCTTGATGGATATTG
PIF3	RW	CAGCAGGAGCTGATTCATTG
PIF4	FW	AGGGAAACAGAAATGGAACAG
PIF4	RW	AGCCACCTGATGAGGAACTT
PIF5	FW	CAGAACCATCCCGGTTTAGTA
PIF5	RW	CGAGCTGCTCCGATAAGATT
PIF7	FW	CTTGCAACAATGGCAAGAAT
PIF7	RW	TGGTGCAGTCTCTGTTACCC
HY5	FW	TCAGAACGAGAACCAGATGC
HY5	RW	GAAGGAGATCAAAGGCTTGC
HYH	FW	CAATGACCAGCTCGAAGAGA
HYH	RW	CACTGAACAATGGATTAAAGGG
HFR1	FW	TCATCTCCGATATCTCTTTAACTAACA
HFR1	RW	TAGACGATCTTCATCACTTCTTGC

EID1	FW	GTTTGTGCGATGAGACTTGG
EID1	RW	TAAAGCAGTCCAAGCACCAG
LHY1F2	FW	GAGACAGACAGGATTTAAGCCA
LHY1R2	RW	GAAGCTTCTCCTTCCAATCG
SPA1	FW	TGGAGGTAGGGATTCGAAGA
SPA1	RW	CTGGATTACGTGCATCAACC
TOC1	FW	TCGAATATCGAGTTGTCTCTAAGG
TOC1	RW	AAGCTAAACCCAATGAGAGCTT
CCA1F3	FW	CCATGGAAGCCAAAGAAAGT
CCA1R3	RW	GGAAGCTTGAGTTTCCAACC
PPR7	FW	AATGCATGAAGATGGAGGCT
PPR7	RW	TCCACGTGCATTAGCTCTTC
PRR5	FW	CGGGACAGAGTTCATACCCT
PRR5	RW	CTAACGGAACTAGGGCTTGG
PRR8	FW	AGTGATGCAGGATGGACTCA
PRR8	RW	GGCGAGATCGGTGAATATCT
PRR9	FW	CAATGGATTTGATTGGTGGA
PRR9	RW	TGCTTGCTTTCATCTTGGTT
AS1	FW	AGAGGCCAAAGACCAGAAAC
AS1	RW	CTGCAACCCATTTGTTGTTC
REV	FW	GCTTGCCTTCAGGAATCTGT
REV	RW	ATGCAGCAAACACTTTCCAA
PHAV	FW	ATATGTGTGTCGAGCATGGG
PHAV	RW	AGCAGTGGTTTGATTCGTTG
HEMA1F2	FW	TCCTATAGCGATGGATCTATTTGA
HEMA1R2	RW	CACTCGAGTCTATGAAGCAACA
STH	FW	AAGTTCCCGAGCTTTCCTTT
STH	RW	CAAGCCTCTGCTTCTTGTTG
GNC1	FW	ACCAAGACTCCTCTTTGGCG
GNC1	RW	TTGCCGTATACCACATGCGT
GNC2	FW	CGAAGACCAACCCCATCCTC
GNC2	RW	AACCGCATCTTTGGGGACAT
CGA1	FW	CCAGAGCAACTCCACGATGT

CGA1	RW	TTCCGTGCGATAGAGCCATT
CGA2	FW	CCCACCGGTCATGAAGAAGA
CGA2	RW	AATCCTCGGCTAATGCGGTC

The expression levels were normalized with CT values obtained using the reference gene previously tested using the standard curve. For this type of analysis were tested fifteen reference gene (Table 4) (Tomasz, *et al*., 2005), among which only. *PP2A* and *SAND* have been used to normalize the results obtained by qBasePLUS.

Table 4. Primers list of reference genes used for qRT-PCR.

Name	**Primer**	**Sequenza**
GAPDH	FW	TTGGTGACAACAGGTCAAGCA
GAPDH	RW	AAACTTGTCGCTCAATGCAATC
AT2G32170	FW	ATCGAGCTAAGTTTGGAGGATGTAA
AT2G32170	RW	TCTCGATCACAAACCCAAAATG
PTBP	FW	GATCTGAATGTTAAGGCTTTTAGCG
PTBP	RW	GGCTTAGATCAGGAAGTGTATAGTCTCTG
UBQT	FW	TTCAAATACTTGCAGCCAACCTT
UBQT	RW	CCCAAAGAGAGGTATCACAAGAGACT
AT4G26410	FW	GAGCTGAAGTGGCTTCCATGAC
AT4G26410	RW	GGTCCGACATACCCATGATCC
AT4G33380	FW	TTGAAAATTGGAGTACCGTACCAA
AT4G33380	RW	TCCCTCGTATACATCTGGCCA
YLS8	FW	TTACTGTTTCGGTTGTTCTCCATTT
YLS8	RW	CACTGAATCATGTTCGAAGCAAGT
AT5G12240	FW	AGCGGCTGCTGAGAAGAAGT
AT5G12240	RW	TCTCGAAAGCCTTGCAAAATCT
FBOX	FW	TTTCGGCTGAGAGGTTCGAGT
FBOX	RW	GATTCCAAGACGTAAAGCAGATCAA
PPR	FW	AAGACAGTGAAGGTGCAACCTTACT
PPR	RW	AGTTTTTGAGTTGTATTTGTCAGAGAAG
CA	FW	TCGATTGCTTGGTTTGGAAGAT

CA	RW	GCACTTAGCGTGGACTCTGTTTGATC
SAND	FW	AACTCTATGCAGCATTTGATCCACT
SAND	RW	TGATTGCATATCTTTATCGCCATC
PP2A	FW	TAACGTGGCCAAAATGATGC
PP2A	RW	GTTCTCCACAACCGCTTGGT
UBC	FW	CTGCGACTCAGGGAATCTTCTAA
UBC	RW	TTGTGCCATTGAATTGAACCC
TIP41	FW	GTGAAAACTGTTGGAGAGAAGCAA
TIP41	RW	TCAACTGGATACCCTTTCGCA

Chromatin immunoprecipitation (ChIP)

Chromatin immunoprecipitation (ChIP) is a powerful technique to study interaction between DNA and protein *in vivo*. In particular we would like to investigate the interaction between Elongator and specific regions of DNA. This technique was performed by making some changes to protocol of Bowler *et al*. (2004). Seedlings were harvested after 4 days and fixed in 1% formaldehyde for 10 min in a vacuum and neutralized by 0.125 M glycine for 5 min. The samples after cross-linking were washed and put in liquid nitrogen. Samples were ground in liquid nitrogen and nuclei were isolated and lysed in the presence of protease inhibitors. The isolated chromatin was sonicated 3 times of 30 sec. with a pause of 60 sec. in a Bioruptor. The anti-histone H3K14Ac antibodies for immunoprecipitation were purchased from Upstate Biotechnology (07-353). Immunoprecipitated DNA was de-crosslinked and purified with MinElute PCR Purification Kit (Qiagen) and dissolved in 50 μl elution buffer supplemented with RNase A 10μg/ml. The concentration of each ChIP sample was measured by Qubit® 2.0 Fluorometer Invitrogen, and analyzed by real-time PCR (Roche LC480). A qPCR was performed as a measure of the amount of acetylated H3K14 level. The qPCR results were normalized with two reference genes: UBQ5 and ACT2. The table below shows the primers used and their sequence (Table 5 (A, B)). To perform a qPCR the specific primers were designed homologous to the promoter region, coding region and 3'untranslated region of a set of genes selected for our experiments.

Table 5A. List of genes housekeeping and sequence

Name	Primer	Sequenza
UBQ5	FW	GACGCTTCATCTCGTCC
UBQ5	RW	GTAAACGTAGGTGAGTCCA
ACT2_new	FW	ACGAGCAGGAGATGGAAACC
ACT2_new	RW	TCCATTCCCACAAACGAGGG

Table 5B. List of genes used for ChIP assay

Name	Primer	Sequenza
LHY1 UP	FW	TTGCAACTAAGCTCTGCTCC
LHY1 UP	RW	AGATTCCAGCTTACAACTGTGT
LHY1 Prom	FW	GCGTAAAAGTGAGGCCCATA
LHY1 Prom	RW	TGGTGGTCCACAATTGCTTA
LHY 2C	FW	CCGAAAAATTCGGGTCAGTA
LHY 2C	RW	GGCGGAATTTCTATGTCCAA
LHY 3C	FW	GCCATTGGCTCCTAATTTCA
LHY 3C	RW	TCGAAGCCTTTTGCAGACTT
HYH UP	FW	AGGGGTCCCTTGAGTGATACA
HYH UP	RW	GTGGCATATCGACCGACCAA
HYH Prom	FW	AAACACAGATACACACCATTGGA
HYH Prom	RW	CACTCAAAGTCTGCAACTCGT
HYH F2	FW	GTTGATGGTTCCTGACATGG
HYH F2	RW	AAGCTCCGGATTGTTGACTC
HYH F3	FW	CAATGACCAGCTCGAAGAGA
HYH F3	RW	CACTGAACAATGGATTAAAGGG
PIF4 Promo	FW	GCAAGCTTTCCTAGATTGCCA
PIF4 Promo	RW	AAGCAAGTCCATGAGTCCGT
PIF4 Ex3	FW	TTTGCAGGCAATCGGTAACA
PIF4 Ex3	RW	AACTTCAGCTGCTCGACTCC

PIF4 Ex5	FW	GTGATGTGGATGGGGAGTGG
PIF4 Ex5	RW	GGTTGAACTCCGGGGAACAT
PIF4 Ex6	FW	ATTTAGTTCACCGGCGGGAC
PIF4 Ex6	RW	AGTGGTCCAAACGAGAACCG

IIIc. - Results

The skoto/photomorphogenic response of elo3-6 mutant in darkness and in different light qualities

The plants orient their growth in relation to the light direction to optimize the exposure of photosynthetic organs towards the light source. The phototropism is a highly organized growth process in which the plants exposed to the shade exhibit a higher cell elongation rate in the hypocotyl compared to plants exposed directly to the light. The typical leaf phenotype of Elongator mutants characterized by narrow leaf lamina, increased petiole length, shows a high resemblance to *phy* mutants and this suggested that *elo* mutants are not able to perceive correctly the light signal. According to these results the *elo3-6* mutant and wild type plants were grown for four days under different light qualities, in order to study the photomorphogenic response (Figure 10). After four days in all light qualities, the *elo* mutant (*elo 3-6*) shows a longer hypocotyl as compared to the wild type (Col-0). These results strongly support the hypothesis that the Elongator complex is involved in the light response pathway.

Figure 10. Skoto and Photomorphogenetic phenotype of *elo3-6* mutant. Seedlings of 4 days old of wild type (Col-0) and *elo3-6* mutant grown in darkness, in red, far-red and blue light ($10\mu mol.m^{-2}.s^{-1}$).

After four days in darkness, *elo3-6* mutants display a shorter hypocotyl, an apical hook, in which the angle of curvature is much sharper, a pair of yellow cotyledons that are closed and bigger than Col-0. These phenotypes could be related to hormone activity, indeed, gibberellic acid stimulates the maintenance of apical hook and auxin inhibits cell proliferation induced cell differentiation. Hence, the skotomorphogenic phenotypes are compromised in the *elo3-6* mutant. In continuous red, far-red and blue light, double phenotypic effects were found in *elo* mutants, one is related to the length of hypocotyl that in all light condition is longer than wild type, and the other one is the leaf tropism known as hyponasty. Whereas in the wild type that also showed phototropic response in all light condition, under far-red light the phototropic response is clearly observed by an orientation of the cotyledons downward. The downward bending of the leaf, which occurs when the upper part of the petiole grows faster than the lower one, is defined as epinasty. The light induces a reprogramming on different levels to perform plant adaptation and it is interesting to understand which genes drive these biological events.

The root analysis of elo3-6 mutant in darkness and in different light qualities

The skoto and photomorphogenesis developmental program in plant doesn't influence only its photosynthetic part but it can condition the root growth. Indeed the root length changes from darkness to light but also within the different light qualities (Figure 11).
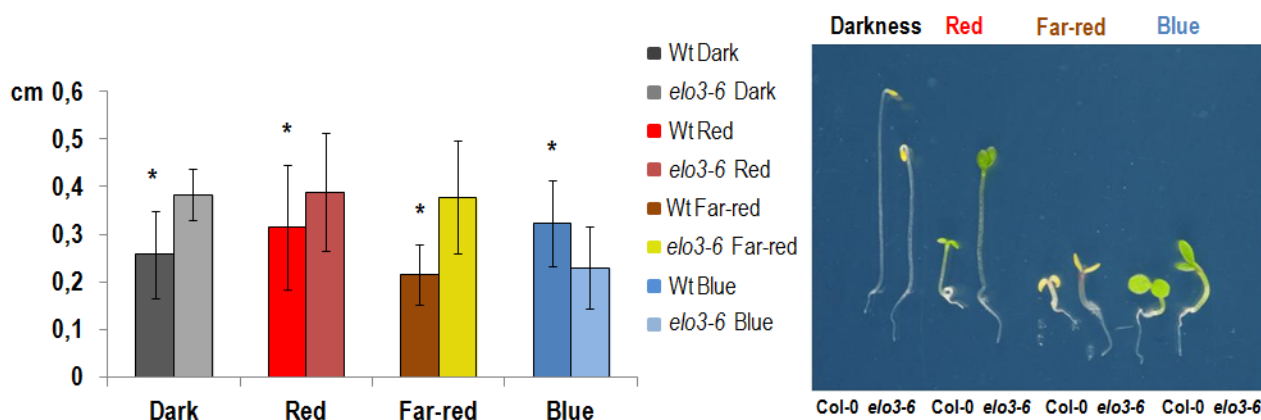

Figure 11. Root length of *elo3-6* in dark and in different light conditions. Seedlings of 4 days old wild type (Col-0) and *elo3-6* mutant grown in darkness, in red, far-red and blue light ($10\mu mol.m^{-2}.s^{-1}$). Error bars represent SD (Standard Deviation) values of at least three repetitions. *, significant difference between wild-type and mutant according to *t*-test (p≤0.05).

A root analysis was performed on seedlings of *elo3-6* and Col-0 grown for four days in continuous dark, red, far-red and blue light (Figure 11). The results of this analysis demonstrate that in darkness, red and far-red light the *elo3-6* root growth is significantly stimulated in contrast to what is seen in blue light condition. Hence, in the *elo3-6* mutant processes related to the regulation of primary root growth are affected both in the dark and in response to light.

elo3-6 in darkness: rate of germination and hypocotyl elongation

In order to interpret better the data obtained in darkness by the hypocotyl assay, it was necessary to determine the rate of germination of *elo3-6* and Col-0 in dark from 0 hour until 40 hours. The aim of this experiment was to understand if the shorter hypocotyls of *elo3-6* plants grown in darkness were related to a defect in the genes involved in the first phases of plant development or linked to a delay in germination. The germination is a biological process which consists of three phases: a rapid imbibition of the seed, the rupture of the tegument called "testa rupture" and finally ends with the protrusion of the root called "endosperm rupture". For many species, including *Arabidopsis,* testa rupture and endosperm rupture are two sequential steps during germination (e.g. Karssen 1976, Hepher and Roberts 1985; Leubner-Metzger *et al*., 1995; Krock *et al*., 2002; Petruzzelli *et al*., 2003; Leubner-Metzger, 2003; Liu *et al*., 2005). Each single germination phase was analyzed in order to identify difference between *elo3-6* mutant and wild type. Between the WT and *elo3-6* there was a delay of 3 hours in germination, because 50% of Col-0's seeds were germinated after 19 hours in darkness whereas 50% of *elo3-6* seeds were germinated after 22 hours (Figure 12). It can be concluded that the reduced rate of hypocotyl elongation in the dark in *elo3-6* is not the consequence of a delay in seed germination.
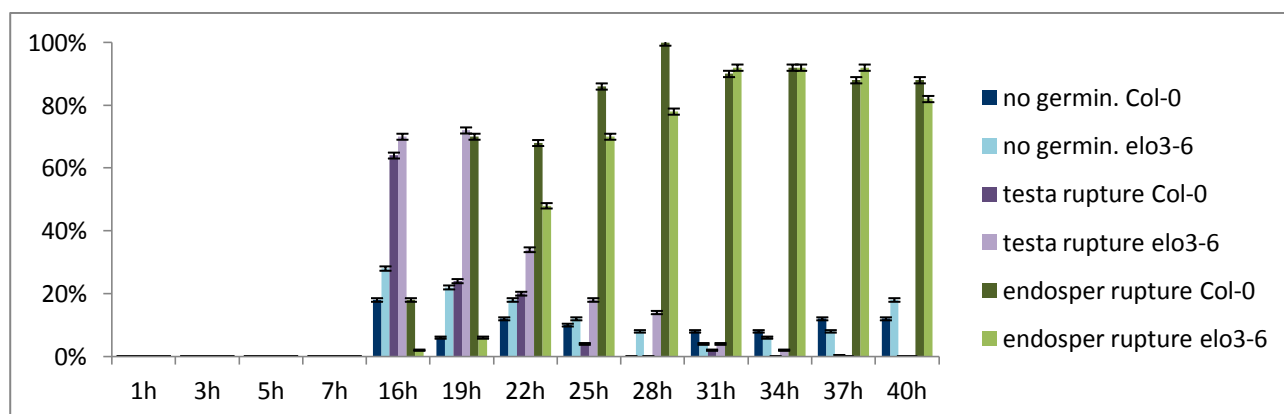

Figure 12. Germination rate of elo3-6 in darkness. Seedling grown in darkness until 40 hours. t_{50} is the time required to obtain 50% of germinated seeds. Testa rupture and endosperm rupture are two sequential steps during germination. Error bars represent SD (Standard Deviation) values on 100 seeds.

Magdalena Woloszynska performed an hypocotyl assay on seedlings of *elo3-6* and wild type that were grown from three to seven days in darkness, red, far-red and blue light. The hypocotyls of the darkness grown *elo3-6* mutant were significantly shorter compared to wild type seedlings grown from 3 to 6 days. This suggested to investigate the hypocotyl length of *elo3-6* after two and three days in darkness (Figure13).
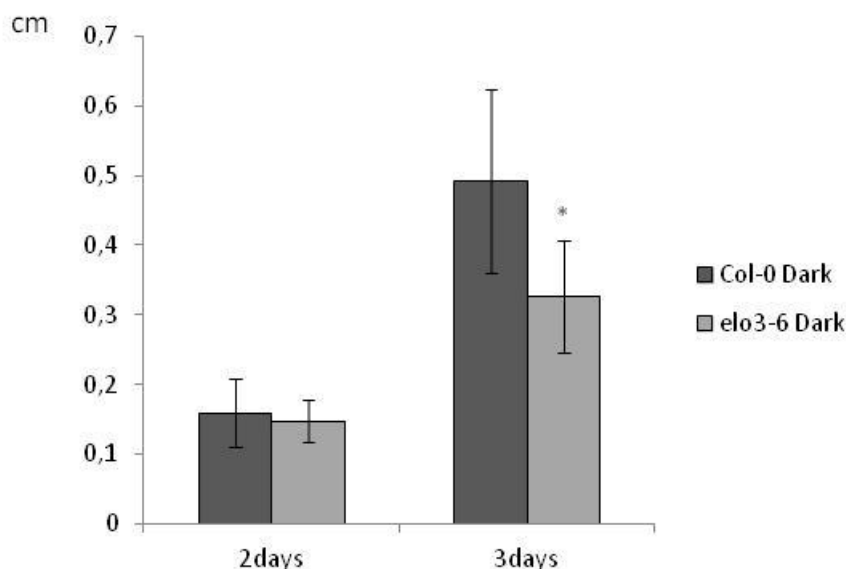

Figure 13. The growth rate of hypocotyl upon 2 to 3 days in darkness. (A)) Two days-old seedling hypocotyl lengths grown in darkness. **(B)** Three days-old seedling hypocotyl lengths grown in darkness. The hypocotyls length were measured by using ImageJ. Error bars represent SD (Standard Deviation) values of at least three repetitions. *, significant difference between wild-type and mutant according to *t*-test (p≤0.05).

The rate of hypocotyl growth is not different between *elo3-6* and wild type after two days (48h) in darkness (Figure 13 (A)). After three days (72h) in darkness the hypocotyl length of *elo3-6* is significantly shorter as compared to wild type (Figure 13 (B)). Therefore, we conclude that in the mutant there is a decline in the growth rate or a reduced ability of hypocotyl cells to elongate. It might suggest that in the *elo3-6* mutant the genes encoding transcription factors involved in skotomorphogenesis are down-regulated or the amount of their transcripts are low explaining the hypocotyl elongation in *elo3-6*.

IIIc1. Hypocotyl assay on Elongator subunit mutants and double mutants

Elongator is a putative interface coupling light signaling to gene expression. The hypocotyl assay is a conventional method to compare the response of wild type and mutant seedlings grown under different light wavelengths or in darkness conditions, and identify signaling pathway(s)

mediated by the product of the mutated gene. In order to verify if whole Elongator complex takes a role in the light signaling pathway and in darkness, the hypocotyl assay was performed on all Elongator mutants. The *elo3-6* (Col-0 background) and, *elo3-1* (L*er* background) were tested under

all light conditions such as red, far-red and blue light, for four and six days. The results of both *elo3* mutations showed the same effect: *elo3* mutants were hyposensitive to all light qualities analyzed. Hypocotyl assay using the mutants of other Elongator's subunits (*elo1, elo2 and elo4)* and a mutant of the putative regulator of the Elongator complex (*drl1-2*) gave similar result as in the case of the *elo3* mutants. So after these results it was possible to conclude that the whole Elongator complex plays a role in light response (Figure 6). In darkness, the *elo* mutants and *drl1-2* had short hypocotyls compared to the respective wild types, indicating that Elongator participates also in the skotomorphogenetic program. Based on these results further analysis was performed to study Elongator in relation to other components of light signaling such as (PHYA, PHYB, HFR1 and PIFs). For this purpose hypocotyl length of double mutants (*elo3-1xphyA-201, elo3-6xphyB9, elo3-1xphyB1, elo3-6xhfr1,*) and triple mutant *elo3-6xpif3,4* and their parental lines were compared after four days of growth in darkness, red and far-red light. The *elo3-6xphyB9, elo3-1xphyB1* and *elo3-6xpif3,4* were analyzed only under red light and darkness, and *elo3-6xhfr1* only under far-red light and darkness. The *elo3-1xphyA-201* double mutant was analyzed only under the far-red light. The analysis of the triple mutant *elo3-1xphyAB*, obtained from a cross between *elo3-1* mutant and *phyA-201B5* double mutant included both red and far-red light. The seedlings were grown under red and/or far-red light and also in darkness for four days. The hypocotyl length was measured with ImageJ software and statistical analysis was performed to identify significant differences between the double mutants and triple mutant and their parental lines.
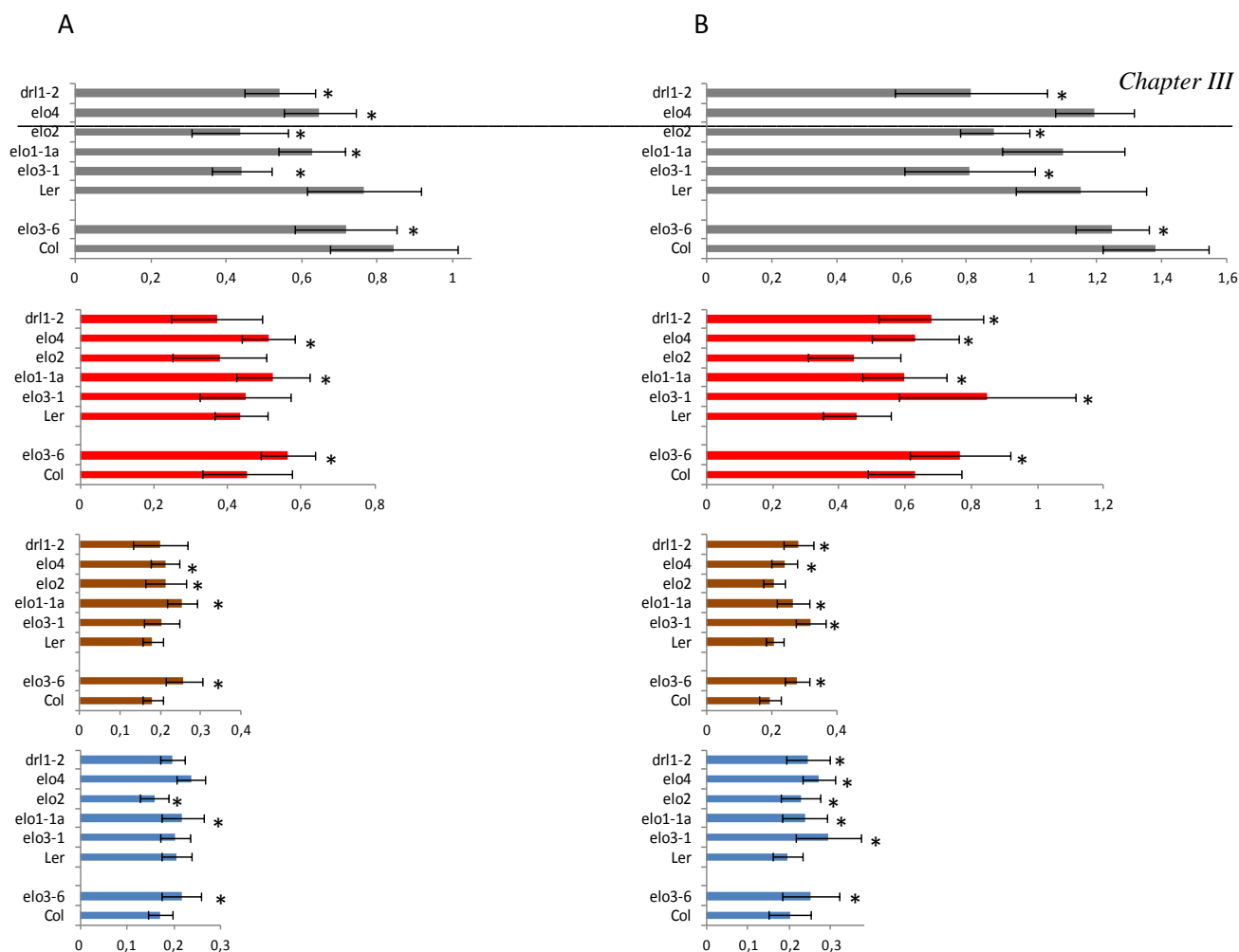
Figure 6. Hypocotyl assay of subunits of the Elongator Complex. Four- and six-day old seedling hypocotyl lengths of wild type Ler, Col-0, and Elongator mutants *elo1-1*, *elo2*, *elo3-1*, *elo3-6*, *elo4* and *drl1-2*, grown in darkness and under red, far-red and blue light. **(A)** Seedlings grown for four days. **(B)** Seedlings grown for six days. The asterisks indicate a statistical significant difference between mutant and wild type (t-test, P<0.05). Error bars represent standard deviation of at least 30 seedlings.

In darkness, the hypocotyl of *hfr1* is the same length as the one of wild type, hence no interaction can be measured in the double mutants *elo3-6xhfr1*. (Figure 7 (a,c)). In red light the hypocotyl length of the double mutant, *elo3-6xpif3,4*, was intermediate to the parental lines, indicating that *elo3-6* hypocotyl phenotype depends on PIF3/PIF4 activity. (Figure 7 (b)). Under far-red light the *elo3-6xhfr1* double mutant is significantly longer than both parental lines *hfr1* and *elo3-6*, showing synergistic or additive genetic interaction, which means that *ELO3* and *HFR1* genes are both involved in response to far-red light but they play independent roles in this process or are independent (Figure 7 (d)).
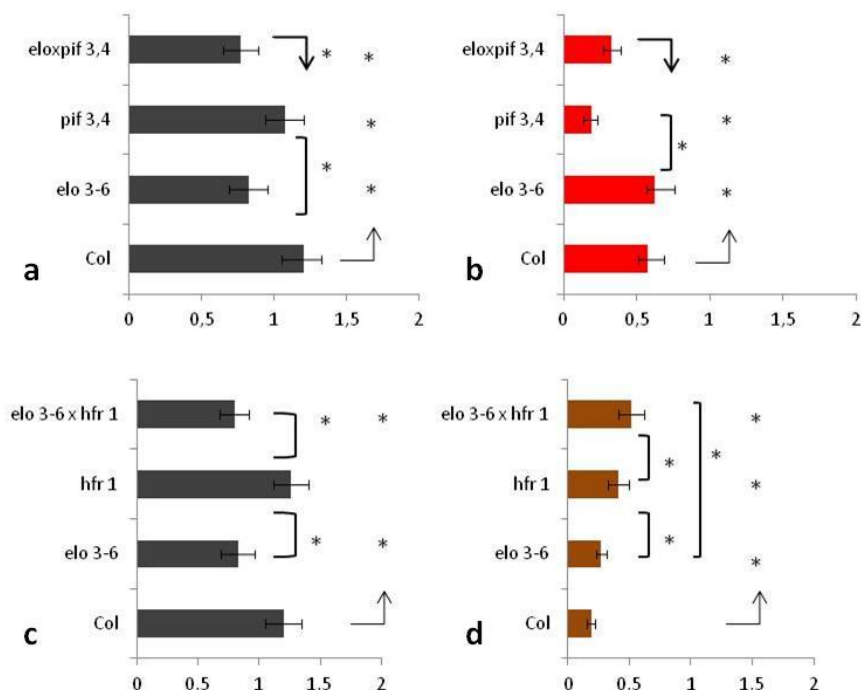
Figure 7. Hypocotyl assay of wild type Col-0 and *pif3,4, hfr1*, *elo3-6* **mutants***, elo3-6xhfr1* **double mutant, and** *elo3-6xpif3,4 triple mutant.*
Hypocotyl lengths of four days-old seedlings of wild type Col-0, *pif3,4*, *hfr1*, *elo3-6, elo3-6xpif3,4, elo3-6xhfr1* grown in darkness, in red or far-red light. The asterisks *, indicate a statistically significant difference between mutant and wild type (P≤0.05).
a-b) Hypocotyl assay of *pif3,4* and *elo3-6* after 4days in darkness and continuous red light;
c-d) Hypocotyl assay of *hfr1* and *elo3-6* after 4days in darkness and continuous far-red light.

In darkness, the double mutants, *elo3-1xphyB1* and *elo3-1xphyA-201*, are intermediate to the parental lines, indicating that *elo3-6* hypocotyl phenotype depends on PHYB and PHYA (Figure 8 (a, c, e)). After four days under red light condition, the hypocotyl lengths of *elo3-6xphyB9 and elo3-1xphyB1* are intermediate compared with the parental lines, which indicates that *elo3-6* hypocotyl length depends on PHYB (Figure 8 (b,d)). In continuous far-red light condition the hypocotyl length of *elo3-1xphyA-201* is intermediate to the parental lines, indicating that *elo3-6* hypocotyl phenotype depends on PHYA (Figure 8 (f)).
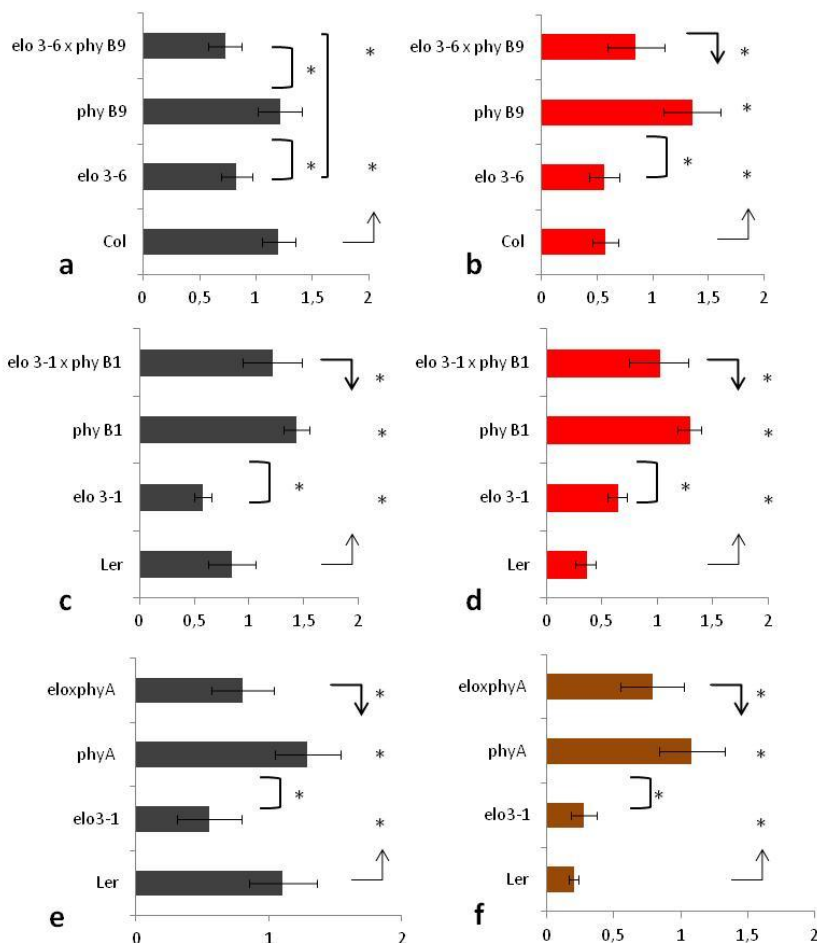
Figure 8. Hypocotyl assay of wild type Col-0 and Ler and *phyA, phyB9, elo3-1, elo3-6* mutants and *elo3-1xphyA-201, elo3-6xphyB9, elo3-1xphyB1* double mutants
Hypocotyl length of four day-old seedlings grown in darkness, red and far-red light. The asterisks indicate a statistically significant difference between mutant and parental lines (P≤0.05).
a-b) Hypocotyl assay of *phyB9* and *elo3-6* after 4days in dark and continuous red light.
c-d) Hypocotyl assay of *phyB1* and *elo3-1* after 4days in dark and continuous red light.
e-f) Hypocotyl assay of *phyA* and *elo3-1* after 4days in dark and continuous far-red light;

The triple mutant, *elo3-6xphyAB*, in darkness and in red and far-red light exhibits an intermediate hypocotyl compared with both parental lines, indicating once more that ELO3 depends on PHA and PHYB in these conditions (Figure 9). Hence, ELO3 is involved in light signaling.
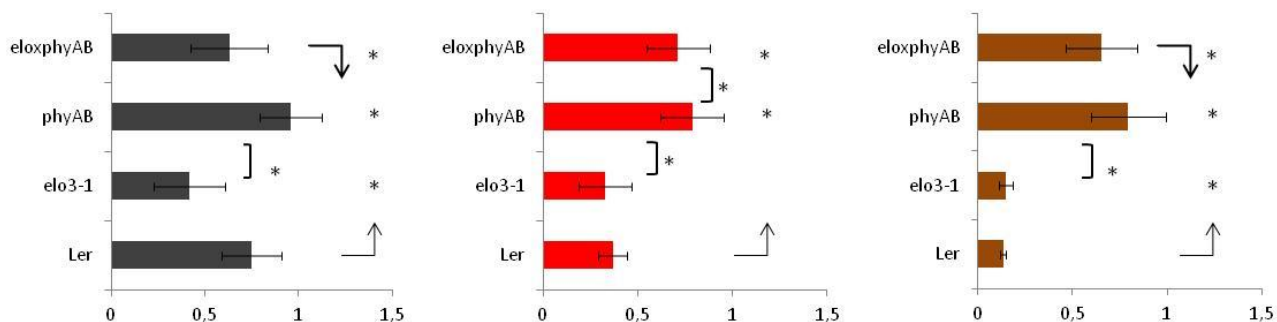
Figure 9. Hypocotyl length of wild type Ler, *elo3-1* **mutant,** *phyAB* **double mutant and** *elo3-1xphyAB* **triple mutant.** Four days-old seedling grown in darkness, red and far-red light. The asterisks indicate a statistically significant difference between mutant and wild type (P≤0.05).

IIIc.2. Chromatin Immunoprecipitation assay (ChIP)

ChIP (Chromatin immunoprecipitation assay) is a conventional method used to understand the interaction between DNA and protein, more specifically we would like to investigate the interaction between Elongator and specific regions of the DNA. To identify light-specific targets of Elongator Magdalena Woloszynska analyzed the transcriptomes of the *elo3-6* mutant grown in darkness for four days or grown in darkness and then exposed for only one hour to red or far-red light. This approach was used to verify if Elongator was involved to modulate the expression of genes earlier responsive to light. Based on the *elo* phenotypes and transcriptomes, we identified a number of genes with reduced expression levels as putative targets of Elongator, i.e: *LHY, HYH, PIF4, HFR1, HY5* and *ELIP2*. Our aim was to investigate if the down-regulation of these genes was related to reduced acetylation levels of histone H3 lysine-14 in their promoter and/or coding region because H3K14 is the predominant substrate of the ELP3 HAT in yeast (Winkler *et al.*, 2002). Chromatin of the *elo3-6* mutant and Col-0 wild-type grown for four days in darkness or for four days in darkness followed by one hour in red light, was immunoprecipitated with an antibody against acetylated H3K14. After immunoprecipitation of chromatin and DNA purification, a qPCR was performed, as a measure of the amount of acetylated H3K14. Primer pairs specific for the 5' end of *ACTIN2* and *UBQ5,* constitutively expressed genes, were used for DNA normalization. Genes in which the acetylation levels are reduced in the mutant compared to wild type, will be considered as a target of Elongator. The qPCR performed after ChIP on sample grown in darkness showed in the *elo* mutant significantly reduced acetylation levels with primers corresponding to *LHY*, *HYH*, *HFR1* and *ELIP2* genes (Figure 14). Acetylation levels of the *LHY* gene is lower in the upstream region from the promoter, in the middle part of the coding region and on the last exon. In *HYH* the acetylation level is lower at the promoter region, the middle part of the coding region and

on the last exon. *HFR1* in darkness shows a significantly reduced acetylation levels with primers corresponding to the promoter region, the middle part of the coding region and also at 3'-untranslated region, while the levels on the promoter region, on middle part of the coding region and on last exon of *ELIP2* gene are lower in *elo* mutant. In darkness the acetylation level of *PIF4* did not differ between the wild type and the *elo3-6* mutant, whereas for *HY5* we can observe a reduction in acetylation levels at the promoter region and on the fourth exon.

Figure 14. ChIP analysis of H3K14 acetylation at *PIF4, LHY, HYH, HY5, HFR1*, and *ELIP2* genes in
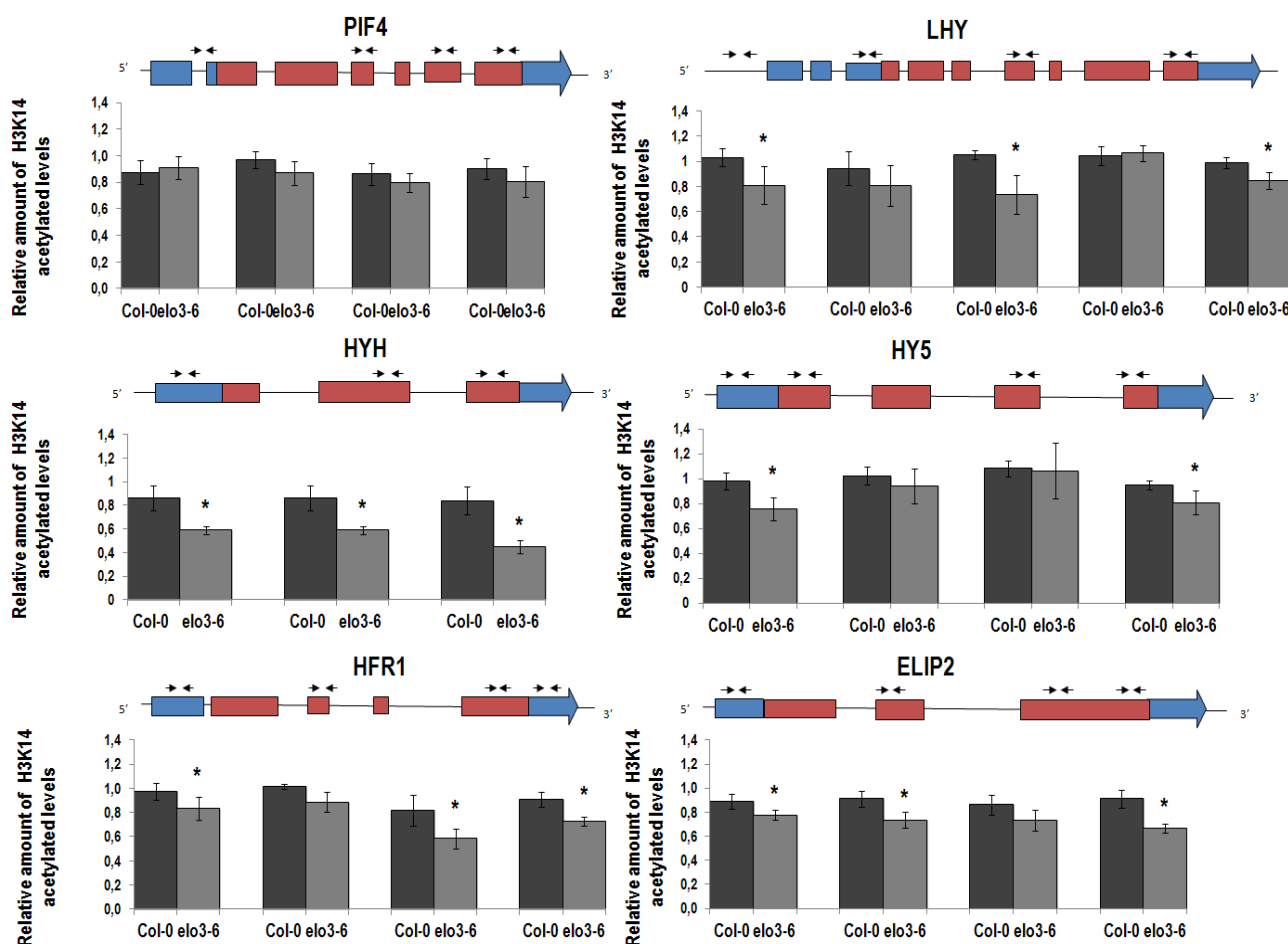
darkness. On top the structure of each gene and the position of primers are indicated. Blue and red boxes indicate untranslated sequence and exons. Relative amount of immunoprecipitation chromatin fragments as determined by real-time PCR compared to wild-type. Error bars represent SD (Standard Deviation) values of at least three repetitions. *, significant difference between wild-type and mutant according to *t*-test (p≤0.05).

Previously ChIP experiment were performed with samples of *elo3-6* and wild type grown in darkness for four days. In order to discover if Elongator plays a specific role under light exposure, a ChiP was performed on samples of *elo3-6* and wild type that were grown for four days in darkness and only one hour under continuous red light. In this case the acetylation level of *HYH* gene (homologue of *HY5)* was analyzed since it is a principal transcription factor involved in the photomorphogenesis pathway. This experiment demonstrated that *HYH* is a target of Elongator in

red light exposure, as indicated by a decrease in acetylation level both in the middle part of the coding region and at 3'-untranslated region of the gene (Figure 15).
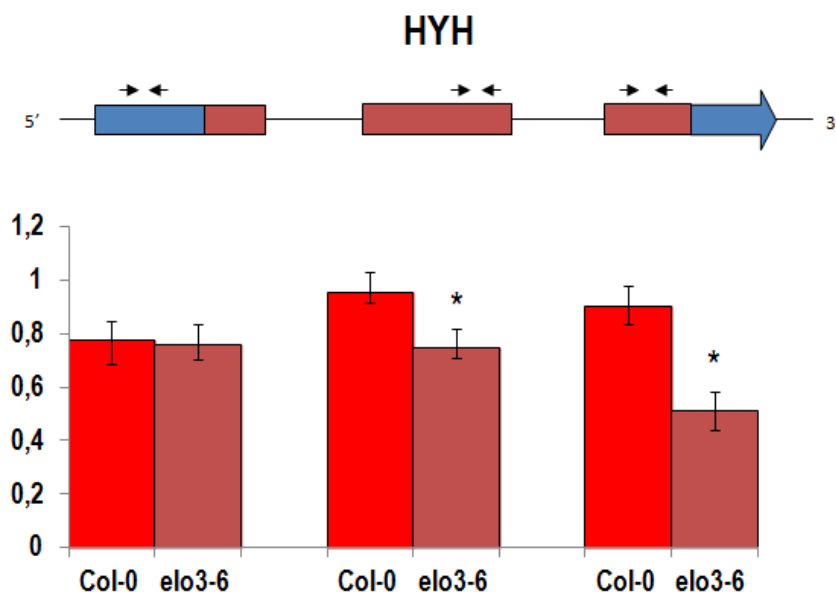

Figure 15. ChIP analysis of H3K14 acetylation at *HYH* genes in darkness 4 days and 1 hour under red light. On top the structure of each gene and the position of primers relative to the promoter and coding regions. Blue and orange boxes indicate untranslated sequence and exons. Relative amount of immunoprecipitation chromatin fragments as determined by real-time PCR compared to wild-type. Error bars represent SD (Standard Deviation) values of at least three repetitions. *, significant difference between wild-type and mutant according to *t*-test (p≤0.05).

IIIc.3. qRT-PCR

The results of the microarray and RNA-seq data addressed the Elongator role in the response to light and darkness. Therefore, we focused on genes differentially expressed in the *elo* mutant relative to the wild type with log2 ratio lower than -0.5 (down-regulated). Using the bioinformatic tool called BINGO, overrepresented gene ontology (GO) categories: response to light stimulus and regulation of transcription were identified in the mutant *elo3-6* grown in darkness and after red and far-red light illumination. In the next step genes down-regulated in the *elo* mutant in red and far-red light but not in darkness were selected and analyzed. Only two GO categories were over represented: response to light stimulus and photosynthesis. Among genes down-regulated only in darkness, but not in red or far-red light, the category response to stimulus was still found as overrepresented. Genes from categories: response to light stimulus, regulation of transcription and photosynthesis down regulated in *elo3-6* in darkness, red or far-red light were analysed in detail. The GO category response to light stimulus contained genes of circadian clock components, related to chloroplast biogenesis and chlorophyll biosynthesis, gene coding for subunits of light harevesting

complex or for transcription factors regulated leaf development, but also genes involved in skotomorphogenesis. These findings represent a good start to explore the role of Elongator in light response and in darkness. In the beginning Magdalena Woloszynska performed a qRT-PCR transcript profiling in wild type and *elo3-6* mutant grown in darkness and in darkness followed by one hour of to red or far-red light, and she analyzed genes belonging to gene category response to light stimulus. The results confirmed down-regulation of genes in *elo* mutant compared to wild type both in darkness, red and far-red light. This suggested that Elongator is not involved in the light specific regulation of those genes, and consequently suggested that it doesn't work in the switch between dark and light conditions. According with these results we confined the BINGO analysis to the genes involved in leaf development, chloroplast biogenesis, positive regulation of skotomorphogenesis, positive regulation of photomorphogenesis (known as specific for response to red light, while other were also engaged in response to blue and far-red light), and on circadian clock genes to test all of them on seedlings of *elo3-6* and wild type grown for four days under different continuous light conditions and also in darkness. For this purpose, we selected and analyzed 25 genes by qRT-PCR (Figure 16 and Figure S1-S8).
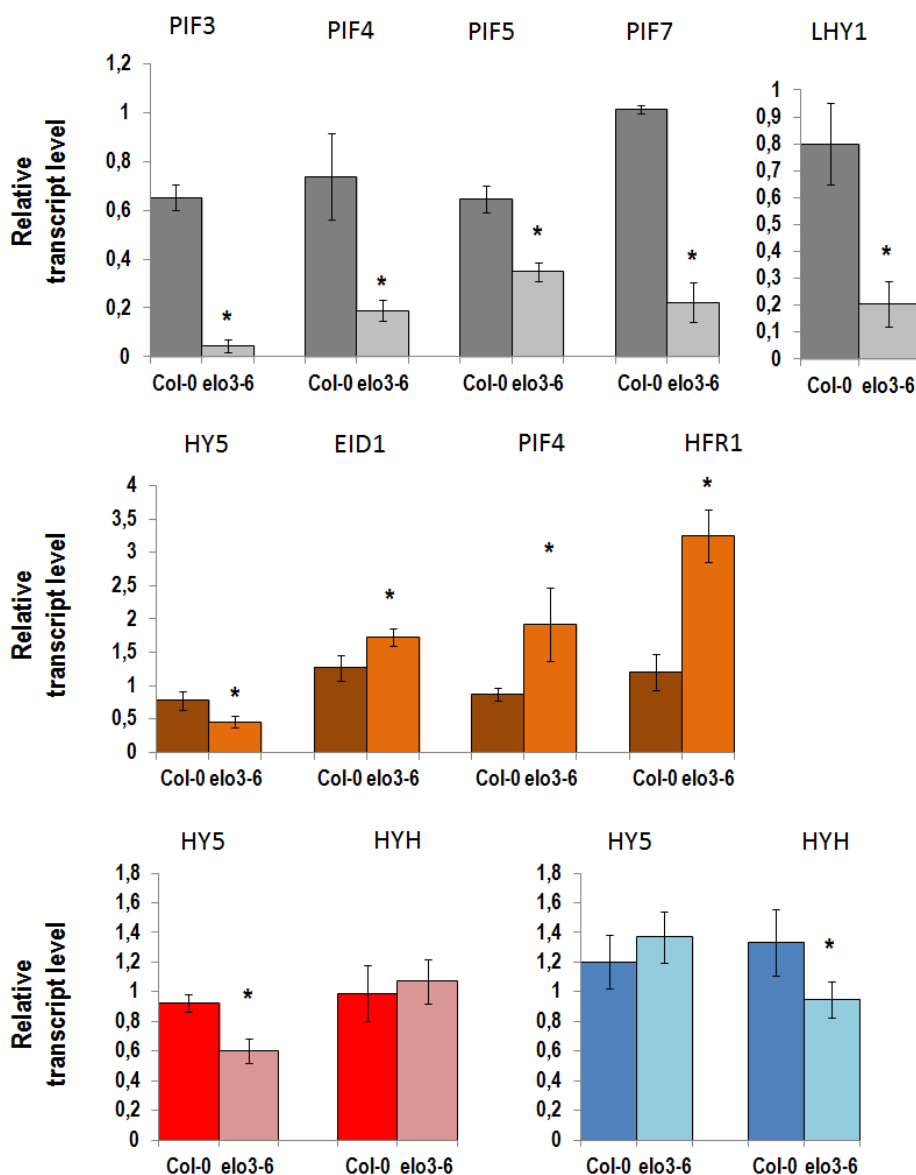
Figure 16. Gene expression analysis by qRT-PCR. Seedlings of *elo3-6* and Col-0 grown for four days in darkness and in red, far-red and blue light. **(A)** Relative transcript level in darkness. **(B)** Relative transcript level in far-red light. **(C)** Relative transcript level in red and blue light. The values were normalized with reference genes and analyzed by qBasePLUS (Hellemans, *et al.*, 2007). The error flags represent the standard deviation of four to six replicates.

The qRT-PCR experiment was performed on sets of genes such as *AS1*, *HEMA*, *PHAV*, *REV*, *STH*, *GNC1*, *GNC2*, *CGA1*, and *CGA2*, involved in leaf development and chloroplast biosynthesis, on positive regulators of photomorphogenesis, *HY5*, *HYH*, *HFR1*, on positive regulators of skotomorphogenesis, *PIF3*, *PIF4*, *PIF5*, *PIF7*, *EID1*, and genes of circadian clock, *LHY1*, *SPA1*, *CCA1*, *TOC1*, *PPR7*, *PRR5*, *PRR8*, *PRR9* (Supplemental data). Figure 16 shows the most representative results of gene expression in the *elo3-6* mutant compared with the wild type. Microarray and RNA-seq showed that *PIF4* and *PIF7* genes are down-regulated in darkness, but in

our experiment we included also the expression analysis of other PIF genes because it's known that almost the whole Pifs family is involved in the skotomorphogenesis pathway. The results confirmed that in the *elo3-6* mutant not only the transcript level of *PIF4* and *PIF7* is reduced but also the amounts of *PIF3* and *PIF5* transcripts were low (Figure 15 (A)). Circadian clock genes regulate sets of genes implicated in the skotomorphogenesis program, in particular *LHY* gene acts to regulate *PIF4* and only some of PIFs genes. In order to identify a putative target of Elongator the transcript level of *LHY* gene was studied in the *elo3-6* mutant grown in darkness and it revealed that its transcript is reduced. HFR1 is a principal transcription factor positively regulating response to far-red light, it is involved in a mechanism that prevents an excessive shade avoidance response by inhibiting hypocotyl elongation under far-red light. HFR1 interacts with another positive photomorphogenesis transcription factor HY5 in order to regulate together the activity of transcription factors involved in skotomorphogenesis program. HFR1works to inhibit PIFs by forming non-DNA-binding dimers with PIF4 and PIF5. In far-red light *EID1* gene is active that encodes a nuclear F-box protein which acts as a negative regulator of light signaling under far-red light and it promotes hypocotyl elongation. The results obtained by qRT-PCR demonstrated that in *elo3-6* mutant there are high levels of *PIF4* and *EID1*, involved in hypocotyl elongation under far-red light. HFR1 needs the interaction with HY5 to contrast the activity of genes that stimulate long hypocotyl under this light condition. On this line the phenotype of *elo3-6* with long hypocotyl under far-red light could be explained by less interaction between HY5 and HFR1 due to lower transcript level of HY5 under far-red light. (Figure 15 (B)). Among these transcription factors, HY5 and HYH homolog of HY5 are required for hypocotyls growth inhibition in light in fact they are known as a positive regulators of photomorphogenesis. HY5 and HYH form a heterodimer and mediate light-regulated expression of overlapping as well as distinct target genes. In particular HY5 is predominantly involved in red light-mediated development whereas HYH plays a role in blue light. Accordingly, the transcript level of HY5 is lower in the *elo* mutant in red light, while transcript level of HYH is lower in blue light corresponding to the hyposensitivity of *elo* to this light conditions.

IIId.- Discussion

In this thesis a study was performed on the putative role of Elongator complex as interface between light/darkness signaling and gene expression during transcription elongation. Starting from skoto/photomorphogenesis response of *elo3-6* mutant in darkness and under different light qualities

we noticed that the mutant compared with wild type showed a specific phenotype both in darkness and in light. This encouraged us to examine one by one the light and darkness conditions, first by using microarray and RNA-seq data from which we selected a group of genes, then by using a qRT-PCR on these genes to determine the transcript level of *elo3-6* mutant, in order to find an explanation about the *elo* phenotype in all conditions. In darkness wild type plants are characterized by long hypocotyls resulting from high expression of the *Pifs* genes, products of which stimulate hypocotyls elongation in darkness. The *Pif* genes are regulated by circadian clock, specifically by CCA1 and LHY1 transcription factors. PIF4 interacts with BZR1, a brassinosteroid regulated gene also involved in hypocotyl elongation in darkness. Interestingly, in both microarray and RNA-seq data BSU1, a gene of brassinosteroid pathway that induces the activation of BZR1 in darkness, is down-regulated. Our qRT-PCR results confirmed the data present in microarray and RNA-seq on PIF4, PIF7 and LHY, but on the other hand we found that other PIFs genes such as PIF5 and PIF7 are also lower expressed in the *elo3-6* mutant. All data taken together can explain the *elo3-6* phenotype in darkness, therefore the reduction of hypocotyls elongation might be related to reduction in transcript level of *Pifs* genes that induce in *elo* mutant less accumulation of PIF3/PIF4 proteins, lower interaction with BZR1 and lower inhibition of positive photomorphogenesis transcription factors (HY5 and HFR1). In contrast to the darkness related phenotype, the *elo3-6* mutant had longer hypocotyls under all light conditions as compared to the wild type. HY5, HYH and HFR1 are the most important transcription factors involved in the photomorphogenesis. Their function is to inhibit hypocotyls elongation under light exposure and in some cases they work together to perform such activity. Our qRT-PCR results showed that in red light and blue light the long hypocotyls of elo mutant maybe is a consequence of a reduction in the transcript level of *HY5* and *HYH* genes respectively. In far-red light the long hypocotyl is stimulated by less interaction between HFR1 and HY5 protein due to a lower transcript level of *HY5* in *elo3-6* mutant, indeed, HFR1 under far-red light needs the help of HY5 protein to contrast the activity of other genes involved in the promotion of hypocotyl elongation in far-red light (Jang, *et al*., 2013). The results

from hypocotyls assay suggested that Elongator complex takes part in the skotomorphogenesis and photomorphogenesis and is dependent on photoreceptors PHYA and PHYB.

In summary microarray, RNA-seq, qPCR and ChIP-qPCR analyses displayed that Elongator regulates transcription of some genes both in light and in darkness. Through gene expression analysis putative targets of Elongator were identified such as circadian clock components, genes involved in skoto/photomorphogenesis, genes coding for transcription factors. A biological model is proposed, in which the Elongator complex is positioned in the skoto- and photomorphogenetic pathways (Figure 17).
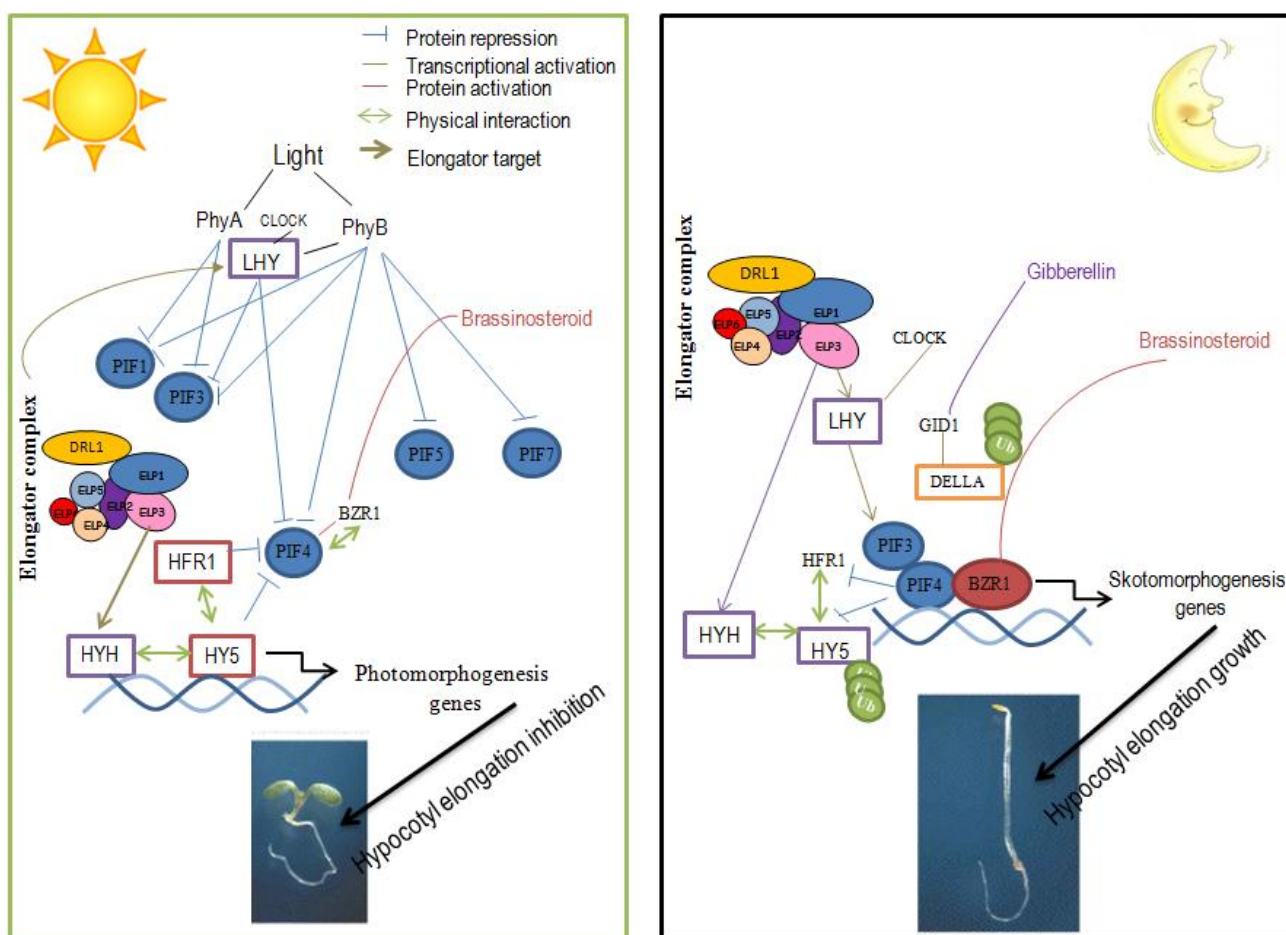

Figure 17. Model of Elongator role in skoto/photomorpogenic pathway.

In this biological model the Elongator complex participates in the skoto/photomorphogenic pathways by binding target genes such as *HYH* and *LHY* in light and darkness condition respectively. Whereas in line with the qRT-PCR results it can regulate the activity of other putative targets as *Pifs* gene (*PIF4*) in darkness and *HY5* or *HFR1* under light condition,

Acknowledgements

Now that I'm reaching the end of my PhD, I start to be sentimental about the time I spent in the laboratories of Prof Maria Beatrice Bitonti and Prof Mieke Van Lijsebettens. It was a great time and a good mixture between excellent but also tough moments.

I would like to take this opportunity to express my gratitude to the people that supported me in the achievement of this degree. Foremost my supervisor Maria Beatrice Bitonti for proving me a possibility both to work in her lab and to have a scientific experience abroad in the VIB-Plant System Biology institute (Belgium). I thank her for this opportunity and for her support. She was always ready to help me whatever the problem was. I'm grateful for everything I learned in her lab.

It gives me great pleasure in acknowledging the support and help of my co-promoter Prof Mieke Van Lijsebettens I consider it a good opportunity to have had the chance to work with her and her research group at Plant Systems Biology, UGent (PSB). I would like to express my gratitude for her continuous support of my PhD study in Ghent and research, for her patience, motivation, and immense knowledge.

My deepest words of gratitude go also to Magdalena Woloszynska for friendly support and scientific advice. Thank you, for the offered time, for your continuous availability and for allowing me to learn from you. I have always appreciated your determination to work, your scientific background and the desire to put questions and try to find the answers, I hope to treasure of all of this.

During my PhD, I had the opportunity to meet many different people. Working on this thesis has been a great journey and I have enjoyed the company and support of many people. My gratitude goes out to these people who contributed to this learning experience. The time spent in Gent was truly great this surely for the special collegues and friends that I found during my travel, each of you gave me a pleasant memory of my stay in Belgium. Would like to thank my Italians colleagues for their affection, disponibility and for the good atmosphere that they are able to create also in hard moments.

A huge thanks goes out to all the members of my family who have always encouraged me to go on with grit and determination, and supported my choices during these three years. Thank you from the bottom of my heart.

References

Alberini Cristina M. (2009). Transcription Factors in Long-Term Memory and Synaptic Plasticity. Physiological Reviews January. Vol. 89no. 1,121-145DOI: 10.1152.

Anderson SL., Coli R., Daly IW., Kichula EA., Rork MJ., Volpi SA., Ekstein J., Rubin BY. (2001). Familial dysautonomia is a caused by mutation of the IKAP gene.. Am J Hum Genet, 68:753-758.

Antonny, B., Madden, D., Hamamoto, S., Orci, L. and Schekman, R. (2001). Dynamics of the COPII coat with GTP and stable analogues. Nat. Cell Biol. 3, 531-537.

Archacki Rafal, Sarnowski Tomasz J., Halibart-Puzio Joanna, Brzeska Katarzyna, Buszewicz Daniel, Prymakowska-Bosak Marta, Koncz Csaba, Jerzmanowski Andrzej. (2009). Genetic analysis of functional redundancy of BRM ATPase and ATSWI3C subunits of Arabidopsis SWI/SNF chromatin remodelling complexes. Planta 1281-1292.

Aridor, M., S.I. Bannykh, T. Rowe, and W.E. Balch. 1995. Sequential coupling between COPII and COPI vesicle coats in endoplasmic reticulum to Golgi transport. J. Cell Biol. 131:875–893. doi:10.1083/jcb.131.4.875

Arsovsk Andrej A., Galstyan Anahit, Guseman Jessica M., and Nemhauser Jennifer L.. (2012). Photomorphogenesis. American Society of Plant Biologists. doi: 10.1199/tab.0147

Bannykh SI, Balch WE. Membrane dynamics at the endoplasmic reticulum-Golgi interface. J Cell Biol.1997;138:1–4.

Barlowe, C., L. Orci, T. Yeung, M. Hosobuchi, S. Hamamoto, N. Salama, M.F. Rexach, M. Ravazzola, M. Amherdt, and R. Schekman. 1994. COPII: a membrane coat formed by Sec proteins that drive vesicle budding from the endoplasmic reticulum. Cell. 77:895–907. doi:10.1016/ 0092-8674(94)90138-4

Berná G, Robles P, Micol JL (1999) A mutational analysis of leaf morphogenesis in Arabidopsis thaliana. Genetics 152: 729-742

Bertrand, C., Bergounioux, C., Domenichini, S., Delarue, M., and Zhou, D.- X. (2003). Arabidopsis histone acetyltransferase AtGCN5 regulates the floral meristem activity through the WUSCHEL/AGAMOUS pathway. J. Biol. Chem. 278: 28246–28251.

Bi, X., Corpina, R. A. and Goldberg, J. (2002). Structure of the Sec23/24-Sar1 pre-budding complex of the COPII vesicle coat. Nature 419, 271-277.

Bielli, A., Haney, C. J., Gabreski, G., Watkins, S. C., Bannykh, S. I. and Aridor, M. (2005). Regulation of Sar1 NH2 terminus by GTP binding and hydrolysis promotes membrane deformation to control COPII vesicle fission. J. Cell Biol. 171, 919-924

Bonifacino, J.S. and Glick, B.S. (2004) The mechanisms of vesicle budding and fusion. Cell 116, 153-166.

Bonifacino, J.S. and Glick, B.S. (2004) The mechanisms of vesicle budding and fusion. Cell 116, 153-166.

Bowler, C., Benvenuto, G., Laflamme, P., Molino, D., Probst, A.V.,Tariq, M., and Paszkowski, J.(2004). Chromatin techniques for plant cells. Plant J. 39:776-789

Brandizzi Federica and Barlowe Charles. (2013). Organization of the ER–Golgi interface for membrane traffic control. Nature Reviews Molecular Cell Biology. 14, 382-392 doi:10.1038/nrm3588

Brandizzi, F., Saint-Jore, C., Moore, I., and Hawes, C. 2003. The relationship between endomembranes and the plant cytoskeleton. Cell Biol Int. 27: 177– 179.

Brandizzi, F., Snapp, E. L., Roberts, A. G., Lippincott-Schwartz, J., and Hawes, C. 2002. Membrane protein transport between the endoplasmic reticulum and the Golgi in tobacco leaves is energy dependent but cytoskeleton independent: evidence from selective photobleaching. Plant Cell. 14: 1293– 1309.

Brownell, J.E., and Allis, C.D. (1996). Special HATs for special occa sions: linking histone acetylation to chromatin assembly and gen activation. Curr. Opin. Genet. Dev. 6, 176–184.

Butler, A. R., Porter, M., and Stark, M. J. (1991). Intracellular expression of Kluyveromyces lactis toxin gamma subunit mimics treatment with exogenous toxin and distinguishes two classes of toxin-resistant mutant. Yeast 7, 617–625

Butler, A.R., White, J.H., Folawiyo, Y., Edlin, A., Gardiner, D., and Stark, M.J. 1994. Two Saccharomyces cerevisiae genes which control sensitivity to G1 arrest induced by Kluyveromyces lactis toxin. Mol. Cell. Biol. 14: 6306–6316.

Butler, W.L., Norris, K.H., Seigelman, H.W., and Hendricks, S.B. (1959). Detection, assay, and preliminary purification of the pigment controlling photoresponsive development of plants. Proc. Natl. Acad. Sci. USA 45, 1703–1708.

Cao H, Glazebrook J, Clark JD, Volko S, Dong X. The Arabidopsis NPR1 gene that controls systemic acquired resistance encodes a novel protein containing ankyrin repeats. Cell 1997; 88:57-63.

Casal, J.J., and Mazzella, M.A. (1998). Conditional synergism between cryptochrome 1 and phytochrome B is shown by the analysis of phyA, phyB, and hy4 simple, double, and triple mutants in Arabidopsis. Plant Physiol. 118: 19-25.

Chan, H. M. & La Thangue, N. B. (2001). p300/CBP proteins: HATs for transcriptional bridges and scaffolds. J. Cell Sci. 114, 2363–2373.

Chen, C., Tuck, S., and Bystrom, A.S. (2009) Defects in tRNA modification associated with neurological and developmental dysfunctions in Caenorhabditis elegans elongator mutants. PLoS Genet 5: e1000561.

Cho, H., Orphanides, G., Sun, X., Yang, X.J., Ogryzko, V., Lees, E., Nakatani, Y., and Reinberg, D. (1998). A human RNA polymerase II complex containing factors that modify chromatin structure. Mol. Cell. Biol. 18, 5355–5363.

Chory J, Nagpal P, Peto C (1991) Phenotypic and genetic analysis of det2, a new mutant that affects light-regulated seedling development in Arabidopsis. Plant Cell 3 445-459

Clack, T., Mathews, S., and Sharrock, R.A. (1994). The phytochrome apoprotein family in Arabidopsis is encoded by five genes: the sequences and expression of PHYD and PHYE. Plant Mol. Biol. 25: 413-427.

Coˆteˊ, J., J. Quinn, J. L. Workman, and C. L. Peterson. (1994). Stimulation of GAL4 derivative binding to nucleosomal DNA by the yeast SWI/SNF complex. Science 265:53–60.

Connelly S, Manley JL. (1988) A functional mRNA polyadenylation signal is required for transcription termination by RNA polymerase II. Genes & Dev 2:440–452.

Courey AJ, Jia S. (2001). Transcriptional repression: the long and the short of it. Genes Dev 15: 2786-2796

Cramer P. (2002). Multisubunit RNA polymerases. Curr Opin Struct Biol 12: 89-97.

Creppe C, Malinouskaya L, Volvert ML, Gillard M, Close P, Malaise O, Laguesse S, Cornez I, Rahmouni S, Ormenese S, Belachew S, Malgrange B, Chapelle JP, Siebenlist U, Moonen G, Chariot A, Nguyen L (2009) Elongator controls the migration and differentiation of cortical neurons through acetylation of alpha-tubulin. Cell 136: 551-564

De Bodt, S., Hollunder, J., Nelissen, H., Meulemeester, N., and Inze, D. (2012). CORNET 2.0, integrating plant coexpression, protein-protein interactions, regulatory interactions, gene associations and functional annotations. New Phytol. 195, 707–720.

De Craene1Johan-Owen., Courte Fanny, Rinaldi Bruno, Fitterer Chantal, Herranz Mari Carmen, Schmitt-Keichinger Corinne, Ritzenthaler Christophe, Friant Sylvie. (2014). Study of the Plant COPII Vesicle Coat Subunits by Functional Complementation of Yeast Saccharomyces cerevisiae Mutants. PLoS ONE 9(2): e90072. doi:10.1371/journal.pone.0090072

De Grauwe L, Vandenbussche F, Tietz O, Palme K, Van Der Straeten D. (2005). Auxin, ethylene and brassinosteroids: tripartite control of growth in the Arabidopsis hypocotyl. Plant Cell Physiol.;46:827–836.

Defraia CT, Zhang X, Mou Z. (2010). Elongator subunit 2 is an accelerator of immune responses in Arabidopsis thaliana. Plant J; 64:511-23.

Dehesh, K., Franci, C., Parks, B.M., Seeley, K.A., Short, T.W., Tepperman, J.M., and Quail, P.H. (1993). Arabidopsis HY8 locus encodes phytochrome A. Plant Cell 5: 1081-1088.

Dello Ioio Raffaele, Scaglia Linhares Francisco, Scacchi Emanuele, Casamitjana-Martinez Eva , Heidstra, Costantino Paolo, Sabrina Sabatini. (2007). Cytokinins determine Arabidopsis root-meristem size by controlling cell differentiation. Curr. Biol. 17:678-682.

Deng, X.W., and Quail, P.H. (1999). Signalling in light-controlled development. Semin. Cell Dev. Biol. 10: 121-129.

Denu, J. M. 2003. Linking chromatin function with metabolic networks: Sir2 family of NAD+-dependent deacetylases. Trends Biochem. Sci. 28: 41–48.

Di Santo R, Bandau S, Stark MJ. (2014). A conserved and essential basic region mediates tRNA binding to the Elp1 subunit of the Saccharomyces cerevisiae Elongator complex. Mol Microbiol. 92(6):1227-42

Dong X. NPR1. (2004). All things considered. Curr Opin Plant Biol; 7:547-52.

Dubos C, Le Gourrierec J, Baudry A, Huep G, Lanet E, Debeaujon I, Routaboul JM, Alboresi A, Weisshaar B, Lepiniec L (2008) MYBL2 is a new regulator of flavonoid biosynthesis in Arabidopsis thaliana. Plant J 55: 940-953

Dürr, J., Lolas, I. B., Sørensen, B. B., Schubert, V. et al. (2014). The transcript elongation factor SPT4/SPT5 is involved in auxinrelated gene expression in Arabidopsis. Nucleic Acids Res., 42, 4332–4347.

Earley KW, Shook MS, Brower-Toland B, Hicks L, Pikaard CS. (2007). In vitro specificities of Arabidopsis co-activator histone acetyltransferases: implications for histone hyperacetylation in gene activation. Plant J 52: 615-626

Eisen, J. A., K. S. Sweder, and P. C. Hanawalt. (1995). Evolution of the SNF2 family of proteins: subfamilies with distinct sequences and functions. Nucleic Acids Res. 23:2715–2723.

Esberg, A., Huang, B., Johansson, M.J. and Byström, A.S. (2006) Elevated levels of two tRNA species bypass the requirement for elongator complex in transcription and exocytosis. Mol Cell, 24, 139-148.

Feinberg AP, Tycko B. (2004). The history of cancer epigenetics. Nat Rev Cancer. 2004 Feb;4(2):143-53.

Fellows, J., Erdjument-Bromage, H., Tempst, P. & Svejstrup, J. (2000). The Elp2 Subunit of Elongator and Elongating RNA Polymerase II Holoenzyme Is a WD40 Repeat Protein. J. Biol. Chem. 275, 12896–12899.

Fichtner L, Frohloff F, Jablonowski D, Stark MJ, Schaffrath R (2002) Protein interactions within Saccharomyces cerevisiae Elongator, a complex essential for Kluyveromyces lactis zymocicity. Mol Microbiol 45: 817-826

Fichtner, L., Frohloff, F., Bürkner, K., Larsen, M., Breunig, K.D., and Schaffrath, R. (2002). Molecular analysis of KTI12/TOT4, a Saccharomyces cerevisiae gene required for Kluyveromyces lactis zymocin action. Mol. Microbiol. 43, 783–791.

Frohloff, F., Fichtner, L., Jablonowski, D., Breunig, K. D., and Schaffrath, R. (2001). Saccharomyces cerevisiae Elongator mutations confer resistance to the Kluyveromyces lactis zymocin.EMBO J. 20, 1993–2003

George Orphanides, Danny Reinberg. (2000). RNA polymerase II elongation through chromatin. Nature.. 28;407(6803):471-5.

Glick, B.S. (2001) ER export: more than one way out. Curr. Biol. 11, R361-3.

Guenther MG, Levine SS, Boyer LA, Jaenisch R, Young RA: A chromatin landmark and transcription initiation at most promoters in human cells. Cell, 130:77-88.

Gustilo, E.M., Vendeix, F.A.P., and Agris, P.F. (2008) tRNA's modifications bring order to gene expression. Curr Opin Microbiol 11: 134–140.

Haag, J.R., and Pikaard, C.S. (2011). Multisubunit RNA polymerases IV and V: purveyors of non-coding RNA for plant gene silencing. Nat. Rev. Mol. Cell Biol. 12, 483–492.

Hahn S. (2004). Structure and mechanism of the RNA polymerase II transcription machinery. Nat Struct Mol Biol. 11(5):394-403.

Hartzog, G. A., Fu, J. (2013). The Spt4–Spt5 complex: amulti-faceted regulator of transcription elongation. Biochim. Biophys. Acta, 1829, 105–115.

Haseloff, J. (2003). Old botanical techniques for new microscopes. Biotechniques 34: 1174–1178, 1180, 1182.

Heijde Marc , Ulm .(2012). UV-B photoreceptor-mediated signalling in plants. Volume 17, Issue 4, Pages 230–237

Hejátko J, Blilou I, Brewer PB, Friml J, Scheres B, Benková E, (2006). In situ hybridization technique for mRNA detection in whole mount Arabidopsis samples. Nat Prot. 4: 1939-1946.

Hellemans J, Mortier G, De Paepe A, Speleman F, Vandesompele J. 2007 qBase relative quantification framework and software for management and automated analysis of real-time quantitative PCR data. Genome Biol,8(2)

Hepher, A. and Roberts, J.A. (1985) The control of seed germination in Trollius ledebouri: the breaking of dormancy. Planta 166: 314–320

Herr, A.J., Jensen, M.B., Dalmay, T., and Baulcombe, D.C. (2005). RNA polymerase IV directs silencing of endogenous DNA. Science 308, 118–120.

Hirschfeld, M., Tepperman, J.M., Clack, T., Quail, P.H., and Sharrock, R.A. (1998). Coordination of phytochrome levels in phyB mutants of Arabidopsis as revealed by apoprotein-specific monoclonal antibodies. Genetics 149: 523-535.

Hsieh, T.F., and Fischer, R.L. (2005). Biology of chromatin dynamics. Annu Rev Plant Biol 56, 327-351.

Huang Jiaqiang, Fan Tao, Yan Qingsheng, Zhu Heming, Fox Stephen, Issaq Haleem J., Best Lionel, Gangi Lisa, Munroe Muegge David and Kathrin. (2004). Lsh, an epigenetic guardian of repetitive elements. Nucleic Acids Res. 2004;32:5019–5028.

Huang, B., Johansson, M.J.O., and Byström, A.S. (2005) An early step in wobble uridine tRNA modification requires the Elongator complex. RNA 11: 424–436.

Hubert, J.C., Guyonvarch, A., Kammerer, B., Exinger, F., Liljelund, P., and Lacroute, F. (1983). Complete sequence of a eukaryotic regulatory gene. EMBO J. 2, 2071–2073.

Jablonowski, D., Frohloff, F., Fichtner, L., Stark, M. J., and Schaffrath, R. (2001). Kluyveromyces lactis zymocin mode of action is linked to RNA polymerase II function via Elongator. Mol. Microbiol. 42, 1095–1105

Jang In-Cheol, Henriques Rossana, and Chua Nam-Hai. (2013). Three Transcription Factors, HFR1, LAF1 and HY5, Regulate Largely Independent Signaling Pathways Downstream of Phytochrome A. Plant Cell Physiol. Jun 2013; 54(6): 907–916.

Jelinsky SA, Estep P, Church GM, Samson LD. (2000) Regulatory networks revealed by transcriptional profiling of damaged Saccharomyces cerevisiae cells: Rpn4 links base excision repair with proteasomes. Mol Cell Biol 20: 8157-8167

Jenuwein and Allis, 2001 Translating the histone code. Science. 293 pp. 1074–1080

Jiao, Y., Lau, O.S., and Deng, X.W. (2007). Light-regulated transcriptional networks in higher plants. Nat. Rev. Genet. 8: 217-230.

Johansson MJ, Bystrom AS (2002) Dual function of the tRNA(m(5)U54)methyltransferase in tRNA maturation. RNA 8: 324-335

Kanno, T., Huettel, B., Mette, M.F., Aufsatz, W., Jaligot, E., Daxinger, L., Kreil, D.P., Matzke, M., and Matzke, A.J. (2005). Atypical RNA polymerase subunits required for RNA-directed DNA methylation. Nat. Genet. 37, 761–765.

Karam CS, Kellner WA, Takenaka N, Clemmons AW, Corces VG (2010) 14-3-3 mediates histone cross-talk during transcription elongation in Drosophila. PLoS Genet 6: e1000975

Karssen, C.M. (1976) Uptake and effect of abscisic acid during induction and progress of radicle growth in seeds of Chenopodium album. Physiol Plant 36: 259–263.

Kasten Margaret, Szerlong Heather, Erdjument-Bromage Hediye, Tempst Paul, Werner Michel and Cairns Bradley R. (2004) Tandem bromodomains in the chromatin remodeler RSC recognize acetylated histone H3 Lys14 The EMBO Journal 23, 1348–1359.

Kirchhausen T, (2000). Three ways to make a vesicle. Nat. Rev.Mol.Cel.Biol. 1: 187-198.

Kitamoto, H. K., Jablonowski, D., Nagase, J., and Schaffrath, R. (2002) Mol. Genet. Genomics 268, 49–55

Kleine-Vehn J. Kleine-Vehn, F. Huang, S. Naramoto, J. Zhang, M. Michniewicz, R. Offringa, J. Friml. (2009). PIN auxin efflux carrier polarity is regulated by PINOID kinase-mediated recruitment into GNOM-independent trafficking in Arabidopsis Plant Cell, 21, pp. 3839–3849

Klug, W.S. and Cummings M. R. (1997). "Concepts of Genetics". Fifth Edition. Prentice-Hall, Inc.

Koch CM, Andrews RM, Flicek P, Dillon SC, Karaöz U, Clelland GK, Wilcox S, Beare DM, Fowler JC, Couttet P, James KD, Lefebvre GC, Bruce AW, Dovey OM,Ellis PD, Dhami P, Langford CF, Weng Z, Birney E, Carter NP, Vetrie D, Dunham I. (2007). The landscape of histone modifications across 1% of the human genome in five human cell lines. Genome Res. June;17(6):691-707.

Koornneef, M., Rolf, E. and Spruit, C. J. P. (1980). Genetic control of lightinhibited hypocotyl elongation in Arabidopsis thaliana (L.) Heynh.Pflanzenphysiol. 100, 147-160

Kornberg and Lorch. (1999). Twenty-five years of the nucleosome, fundamental particle of the eukaryote chromosome. Cell, 98 (1999), pp. 285–294.

Kouzarides T. (2007). Chromatin modifications and their function. Cell, 128, 693-705.

Kuge, O., C. Dascher, L. Orci, T. Rowe, M. Amherdt, H. Plutner, M. Ravazzola, G. Tanigawa, J.E. Rothman, and W.E. Balch. 1994. Sar1 promotes vesicle budding from the endoplasmic reticulum but not Golgi compartments. J. Cell Biol. 125:51–65. doi:10.1083/jcb.125.1.51

Kurihara T, Hamamoto S, Gimeno RE, Kaiser CA, Schekman R, et al. (2000) Sec24p and Iss1p function interchangeably in transport vesicle formation from the endoplasmic reticulum in Saccharomyces cerevisiae. Mol Biol Cell 11: 983– 998.

Kwon, C.S., Hibara, K.I., Pfluger, J., Bezhani, S., Metha, H., Aida, M., Tasaka, M., and Wagner, D. (2006). A role for chromatin remodeling in regulation of CUC gene expression in the Arabidopsis cotyledon boundary. Development 133: 3223–3230.

Lee, M. C. and Miller, E. A. (2007). Molecular mechanisms of COPII vesicle formation. Semin. Cell Dev. Biol. 18, 424-434.

Lee, M.C., E.A. Miller, J. Goldberg, L. Orci, and R. Schekman. 2004. Bi-directional protein transport between the ER and Golgi. Annu. Rev. Cell Dev. Biol. 20:87 123.doi:10.1146/annurev.cellbio.20.010403.105307

Leonardo Bruno, Antonella Muto, Natasha D. Spadafora, Domenico Iaria, Adriana Chiappetta, Mieke Van Lijsebettens and Maria B. Bitonti. (2011). Multi-probe in situ hybridization to whole mount Arabidopsis seedlings. Int. J. Dev. Biol. 55: 197-203.

Leubner-Metzger, G., Fru¨ ndt, C., Vo¨ geli-Lange, R. and Meins, F.Jr (1995) Class I b-1,3-glucanase in the endosperm of tobacco during germination. Plant Physiol 109: 751–759.

Li Bing, Carey Michael, Workman Jerry L.(2007). The Role of Chromatin during Transcription. Cell. 23;128(4):707-19.

Li J, Li G, Wang H, Deng XW. (2011). Phytochrome signaling mechanisms. The Arabidopsis book e0148.. doi:10.1199/tab.0148

Li, Y., Takagi, Y., Jiang, Y., Tokunaga, M., Erdjument-Bromage, H., Tempst, P. & Kornberg, R. D. (2001). A Multiprotein Complex That Interacts with RNA PolymeraseII ElongatorJ. Biol. Chem. 276, 29628–29631.

Logan J, Falck-Pedersen E, Darnell JE, Jr, Shenk T. (1987) A poly(A) addition site and a downstream termination region are required for efficient cessation of transcription by RNA polymerase II in the mouse β maj-globin gene. Proc Natl Acad Sci 84:8306–8310.

Lorincz MC, Schubeler D: (2007). RNA polymerase II: just stopping by. Cell. 130:16-18.

Lu J, Huang B, Esberg A, Johansson MJ, Bystrom AS (2005) The Kluyveromyces lactis gamma-toxin targets tRNA anticodons. RNA 11: 1648-1654

Luger Karolin, Mäder Armin W., Richmond Robin K., Sargent David F. and Richmond Timothy J. (1997). Crystal structure of the nucleosome core particle at 2.8 Å resolution. Nature 389, 251-260 September

Lusser, L., Brosch, G., Loidl, A., Haas, H., and Loidl, P. (1997). Identification of maize histone deacetylase HD2 as an acidic nucleolar phosphoprotein. Science 277: 88–91.

Lykke-Andersen, S. & Jensen, T. H. (2007). Overlapping pathways dictate termination of RNA polymerase II transcription. Biochimie 89, 1177–1182.

Macdonald N, Welburn JP, Noble ME, Nguyen A, Yaffe MB, et al. (2005) Molecular basis for the recognition of phosphorylated and phosphoacetylated histone h3 by 14-3-3. Mol Cell 20: 199–211.

Marti L, Fornaciari S, Renna L, Stefano G, Brandizzi F (2010) COPII-mediated traffic in plants. Trends Plant Sci 15: 522–528.

Matsui K, Umemura Y, Ohme-Takagi M (2008) AtMYBL2, a protein with a single MYB domain, acts as a negative regulator of anthocyanin biosynthesis in Arabidopsis. Plant J 55: 954-967

Mazzella A.M., Casal J.J., Muschietti J:P:, Fox A.R. (2014). Hormonal networks involved in apical hook development in darkness and their response to light. Plant Science. Review. Volume 5, Article 52.

Moreno, N., Bougourd, S., Haseloff, J., and Feijo, J. (2006). Imaging plant cells. In Handbook of Biological Confocal Microscopy, J. Pawley, ed (New York: SpringerScience and Business Media), pp. 769–787.

Moubayidin L., Perilli S., Dello Ioio R., Di Mambro R., Costantino P., Sabatini S. (2010). The rate of cell differentiation controls the Arabidopsis root meristem growth phase. Curr. Biol. 1138–1143.

Neff, M.M., and Chory, J. (1998). Genetic interactions between phytochrome A, phytochrome B, and cryptochrome 1 during Arabidopsis development. Plant Physiol. 118: 27-35.

Neff, M.M., and Van Volkenburgh, E. (1994). Light-stimulated cotyledon expansion in Arabidopsis seedlings (the role of phytochrome B). Plant Physiol. 104: 1027-1032.

Nelissen H, Clarke JH, De Block M, De Block S, Vanderhaeghen R, Zielinski RE, Dyer T, Lust S, Inze D, Van Lijsebettens M (2003) DRL1, a homolog of the yeast TOT4/KTI12 protein, has a function in meristem activity and organ growth in plants. Plant Cell 15: 639-654

Nelissen H, De Groeve S, Fleury D, Neyt P, Bruno L, Bitonti MB, Vandenbussche F, Van der Straeten D, Yamaguchi T, Tsukaya H, Witters E, De Jaeger G, Houben A, Van Lijsebettens M (2010) Plant Elongator regulates auxin-related genes during RNA polymerase II transcription elongation. Proc Natl Acad Sci U S A 107: 1678-1683

Nelissen H, Fleury D, Bruno L, Robles P, De Veylder L, Traas J, Micol JL, Van Montagu M, Inze D, Van Lijsebettens M (2005) The elongata mutants identify a functional Elongator complex in plants with a role in cell proliferation during organ growth. Proc Natl Acad Sci U S A 102: 7754-7759

North, B.J., and Verdin, E. (2007). Mitotic regulation of SIRT2 by cyclin-dependent kinase 1-dependent phosphorylation. J. Biol. Chem. 282, 19546–19555.

Novick P, Ferro S, Schekman R (1981) Order of events in the yeast secretory pathway. Cell 25: 461–469.

Novick P, Field C, Schekman R (1980) Identification of 23 complementation groups required for post-translational events in the yeast secretory pathway. Cell 21: 205–215.

Onodera, Y., Haag, J.R., Ream, T., Costa Nunes, P., Pontes, O., and Pikaard, C.S. (2005). Plant nuclear RNA polymerase IV mediates siRNA and DNA methylation-dependent heterochromatin formation. Cell 120, 613–622.

Orci, L., Ravazzola, M., Meda, P., Holcomb, C., Moore, H. P., Hicke, L., and Schekman, R.. 1991. Mammalian Sec23p homologue is restricted to the endoplasmic reticulum transitional cytoplasm. Proc Natl Acad Sci U S A. 88: 8611–8615.

Otero G, Fellows J, Li Y, de Bizemont T, Dirac AM, Gustafsson CM, Erdjument-Bromage H, Tempst P, Svejstrup JQ (1999) Elongator, a multisubunit component of a novel RNA polymerase II holoenzyme for transcriptional elongation. Mol Cell 3: 109-118

Palade, G. 1975. Intracellular aspects of the process of protein synthesis. Science. 189: 347–358.

Pandey R, Muller A, Napoli CA, Selinger DA, Pikaard CS, Richards EJ, Bender J, Mount DW, Jorgensen RA. (2002). Analysis of histone acetyltransferase and histone deacetylase families of Arabidopsis thaliana suggests functional diversification of chromatin modification among multicellular eukaryotes. Nucleic Acids Res 30: 5036-5055

Parks, B.M., and Quail, P.H. (1993). hy8, a new class of Arabidopsis long hypocotyl mutants deficient in functional phytochrome A. Plant Cell 5: 39-48.

Pontier, D., Yahubyan, G., Vega, D., Bulski, A., Saez-Vasquez, J., Hakimi, M.A., Lerbs-Mache, S., Colot, V., and Lagrange, T. (2005). Reinforcement of silencing at transposons and highly repeated sequences requires the concerted action of two distinct RNA polymerases IV in Arabidopsis. Genes Dev. 19, 2030–2040.

Ponting Chris P. (2002). Novel domains and orthologues of eukaryotic transcription elongation factors. Nucl. Acids Res. 30(17):3643-3652.

Pucadyil, T. J. and Schmid, S. L. (2009). Conserved functions of membrane active GTPases in coated vesicle formation. Science 325, 1217-1220.

Rasmussen EB, Lis JT: (1993). In vivo transcriptional pausing and cap formation on three Drosophila heat shock genes. Proc Natl Acad Sci USA, 90:7923-7927.

Ream, T., Haag, J., and Pikaard, C.S. (2014). Plant multisubunit RNA polymerases IV and V. In Nucleic Acid Polymerases, K. Murakami and M. Trakselis, eds. (Berlin, Heidelberg: Springer-Verlag), pp. 289–308.

Reed, J.W., Nagatani, A., Elich, T.D., Fagan, M., and Chory, J. (1994). Phytochrome A and phytochrome B have overlapping but distinct functions in Arabidopsis development. Plant Physiol. 104: 1139-1149.

Reik W. (2007). Stability and flexibility of epigenetic gene regulation in mammalian development. Nature. 2007 May 24;447(7143):425-32.

Richard, P. & Manley, J. L. (2009). Transcription termination by nuclear RNA polymerases. Genes Dev. 23, 1247–1269.

Rizzini, L., Favory, J.J., Cloix, C., Faggionato, D., O'Hara, A., Kaiserli, E., Baumeister, R., Schafer, E., Nagy, F., Jenkins, G.I., and Ulm, R. (2011). Perception of UV-B by the Arabidopsis UVR8 protein. Science 332: 103-106.

Roberg, K.J. Crotwell, M. Espenshade, P. Gimeno, R. and Kaiser, C. A. (1999) LST1 is a SEC24 homologue used for selective export of the plasma membrane ATPase from the endoplasmic reticulum. J. Cell Biol. 145, 659–672

Robinson DG, Herranz MC, Bubeck J, Pepperkok R, Ritzenthaler C (2007) Membrane Dynamics in the Early Secretory Pathway. Crit Rev Plant Sci 26: 199–225.

Robinson DG, Herranz M-C, Bubeck J, Pepperkok R, Ritzenthaler C: Membrane dynamics in the early secretory pathway. Crit Rev Plant Sci 2007, 26:199-225.

Rondon, A. G., Mischo, H. E. & Proudfoot, N. J. (2008).Terminating transcription in yeast: whether to be a 'nerd' or a 'rat'. Nature Struct. Mol. Biol. 15, 775–776.

Rossanese, O.W., Soderholm, J., Bevis, B.J., Sears, I.B., O'Connor, J., Williamson, E.K. and Glick. B.S. (1999) Golgi structure correlates with transitional endoplasmic reticulum organization in Pichia pastoris and Saccharomyces cerevisiae. J. Cell Biol. 145, 69–81.

Roth SY, Denu JM, Allis CD. (2001). Histone acetyltransferases. Annu Rev Biochem. 70:81-120.

Saltzman, A. G., and Weinmann, R. (1989). FASEB J. 3, 1723-1728

Sanderfoot A, Raikhel. (2003) The secretory system of Arabidopsis. In The Arabidopsis Book. American Society of Plant Biologists, Rockville, MD, doi/

Saunders A, Core LJ, Lis JT. (2006). Breaking barriers to transcription elongation.Nat Rev Mol Cell Biol, 7:557-567.

Sharrock RA, Quail PH. (1989). Novel phytochrome sequences in Arabidopsis thaliana: structure, evolution and differential expression of a plant photoreceptor family. Genes and Development 3, 1745–1757.

Sharrock, R.A., and Clack, T. (2002). Patterns of expression and normalized levels of the five Arabidopsis phytochromes. Plant Physiol. 130: 442-456.

Shiba, Y. & Randazzo, P. A. (2012). ArfGAP1 function in COPI mediated membrane traffic: currently debated models and comparison to other coat-binding ArfGAPs. Histol. Histopathol. 27, 1143–1153

Simpson CL, Lemmens R, Miskiewicz K, Broom WJ, Hansen VK, van Vught PW, Landers JE, Sapp P, Van Den Bosch L, Knight J, Neale BM, Turner MR, Veldink JH, Ophoff RA, Tripathi VB, Beleza A, Shah MN, Proitsi P, Van Hoecke A, Carmeliet P, Horvitz HR, Leigh

PN, Shaw CE, van den Berg LH, Sham PC, Powell JF, Verstreken P, Brown RH, Jr., Robberecht W, Al-Chalabi A (2009) Variants of the elongator protein 3 (ELP3) gene are associated with motor neuron degeneration. Hum Mol Genet 18: 472-481

Sims RJ 3rd, Belotserkovskaya R, Reinberg D. (2004). Elongation by RNA polymerase II: the short and long of it. Genes Dev, 18:2437-2468.

Slaugenhaupt S.A. and Guasella J.F. (2002). Familial dysautonomia. Current Opinion in Genetic & Development 12:307-311.

Stephens, D. J., and Pepperkok, R. 2001. Illuminating the secretory pathway: when do we need vesicles? J Cell Sci. 114: 1053–1059.

Stockinger, E. J., Mao, Y., Regier, M. K., Triezenberg, S. J., and Thomashow, M. F. (2001). Transcriptional adaptor and histone acetyltransferase proteins in Arabidopsis and their interactions with CBF1, a transcriptional activator involved in cold-regulated gene expression. Nucleic Acids Res. 29: 1524– 1533.

Szul, T. & Sztul, (2011). E. COPII and COPI traffic at the ER–Golgi interface. Physiol. (Bethesda) 26, 348–364

Takase T, Nakazawa M, Ishikawa A, Manabe K, Matsui M. (2003). DFL2, a new member of the Arabidopsis GH3 gene family, is involved in red light-specific hypocotyl elongation. Plant Cell Physiol. 44(10):1071-80.

Talbert PB, Henikoff S. (2006). Spreading of silent chromatin: inaction at a distance. Nat Rev Genet. Oct;7(10):793-803.

Tang, B.L., Zhang, T., Low, D.Y., Wong, E.T., Horstmann, H., and Hong, W. (2000). Mammalian homologues of yeast sec31p. An ubiquitously expressed form is localized to endoplasmic reticulum (ER) exit sites and is essential for ER-Golgi transport. J Biol Chem 275, 13597-13604.

The ENCODE Project Consortium. (2007). Identification and analysis of functional elements in 1% of the human genome by the pilot project. Nature, June;447, 799-816.

Traas J, (2008). Whole-Mount In situ Hybridization of RNA Probes to Plant Tissues. Cold Spring Harb Protoc pdb prot. 4944.

Travers, A.A. (1992). The reprogramming of transcriptional competence. Cell 69, 573–575.

Truernit, E., Siemering, K.R., Hodge, S., Grbic, V., and Haseloff, J. (2006). A map of KNAT gene expression in the Arabidopsis root. Plant Mol. Biol. 60: 1–20.

Utley, R. T., Ikeda, K., Grant, P. A., Cote, J., Steger, D. J., Eberharter, A., John, S. & Workman, J. L. (1998). ranscriptional activators direct histone acetyltransferase complexes to nucleosomes. Nature 394, 498–502.

Van Lijsebettens Mieke and Grasser Klaus D. (2014). Transcript elongation factors: shaping transcriptomes after transcript initiation. Trends in Plant Sci.. 360-1385(14)00192-7.

Van Lijsebettens Mieke, Dürr3 Julius, Woloszynska Magdalena Grasser and Klaus D. (2014). Elongator and SPT4/SPT5 complexes as proxy to study RNA polymerase II transcript elongation control of plant development. Proteomics. 00, 1–6

Vaquero, A., Scher, M.B., Lee, D.H., Sutton, A., Cheng, H.L., Alt, F.W., Serrano, L., Sternglanz, R., and Reinberg, D. (2006). SirT2 is a histone deacetylase with preference for histone H4 Lys 16 during mitosis. Genes Dev. 20, 1256–1261.

Verséees, W., De Groeve, S., Van Lijsebettens, M.. (2010). Elongator, a conserved multitasking complex? Mol. Microbiol., 76, 1065–1069.

Vert, G., Walcher, C.L., Chory, J., and Nemhauser, J.L. (2008). Integration of auxin and brassinosteroid pathways by Auxin Response Factor 2. Proc. Natl. Acad. Sci. USA 105: 9829–9834.

Wagner D. and Meyerowitz, E.M. (2002). SPLAYED, a novel SWI/SNF ATPase homolog, controls reproductive development in Arabidopsis. Curr. Biol. 12: 85-94.

Walker Jane, Kwon So Yeon, Badenhorst Paul, East Phil, McNeill Helen and Svejstrup Jesper Q. (2011). Role of Elongator Subunit Elp3 in Drosophila melanogaster Larval Development and Immunity. Genetics Society of America 10.1534/genetics.110.123893.

Wang, H., and Deng, X.W. (2003). Dissecting the phytochrome A-dependent signaling network in higher plants. Trends Plant Sci. 8: 172-178.

Weissman, J. T., Plutner, H. and Balch, W. E. (2001). The mammalian guanine nucleotide exchange factor mSec12 is essential for activation of the Sar1 GTPase directing endoplasmic reticulum export. Traffic 2, 465-475.

Wendeler MW, Paccaud JP, Hauri HP (2007) Role of Sec24 isoforms in selective export of membrane proteins from the endoplasmic reticulum. EMBO Rep 8: 258–264.

Whitelam, G.C., Johnson, E., Peng, J., Carol, P., Anderson, M.L., Cowl, J.S., and Harberd, N.P. (1993). Phytochrome A null mutants of Arabidopsis display a wild-type phenotype in white light. Plant Cell 5: 757-768.

Wieland, F. & Harter, C. (1999). Mechanisms of vesicle formation: insights from the COP system. Curr. Opin. Cell Biol. 4, 440–446

Winkler, G. S., Kristjuhan, A., Erdjument-Bromage, H., Tempst, P., Svejstrup, J. Q. (2002). Elongator is a histone H3 and H4 acetyltransferase important for normal histone acetylation levels in vivo. Proc. Natl. Acad. Sci. USA, 99, 3517–3522.

Winkler, G. S., Petrakis, T. G., Ethelberg, S., Tokunaga, M., Erdjument-Bromage, H., Tempst, P. & Svejstrup, J. Q. (2001). Molecular Architecture, Structure-Function Relationship, and Importance of the Elp3 Subunit for the RNA Binding of Holo-Elongator. J. Biol. Chem. 276, 32743–32749.

Wittschieben, B. O., Otero, G., de Bizemont, T., Fellows, J., Erdjument- Bromage, H., Ohba, R., Li, Y., Allis, C. D., Tempst, P. & Svejstrup, J. Q. (1999). A novel histone acetyltransferase is an integral subunit of elongatin RNA polymerase II holoenzyme. Mol. Cell 4, 123–128.

Wynshaw-Boris A (2009) Elongator bridges tubulin acetylation and neuronal migration. Cell 136: 393-394

Yoshihisa, T., Barlowe, C. and Schekman, R. (1993). Requirement for a GTPase-activating protein in vesicle budding from the endoplasmic reticulum. Science 259, 1466-1468.

Yuling J., On Sun L. & Xing W. D. (2007). Light-regulated transcriptional networks in higher plants. Nat. Rev. Gen. 8, 217-230.

Zeitlinger Julia, Stark Alexander, Kellis Manolis, Hong Joung-Woo, Nechaev Sergei, Adelman Karen, Levine Michael & Young Richard A. 2007. RNA polymerase stalling at developmental control genes in the Drosophila melanogaster embryo. Nature Genetics. Vol. 39 Issue 12, p1512.

Zhang K, Sridhar VV, Zhu J, Kapoor A, Zhu JK. (2007). Distinctive core histone post-translational modification patterns in Arabidopsis thaliana. PLoS One 2: e1210

Zhou X, Hua D, Chen Z, Zhou Z, Gong Z. (2009). Elongator mediates ABA responses, oxidative stress resistance and anthocyanin biosynthesis in Arabidopsis. Plant J; 60:79-90.

Zippo A, Serafini R, Rocchigiani M, Pennacchini S, Krepelova A, et al. (2009) Histone crosstalk between H3S10ph and H4K16ac generates a histone code that mediates transcription elongation. Cell 138: 1122–1136.

web site:

http://arabidopsis.info/NASC

http://bar.utoronto.ca/efp

https://bioinformatics.psb.ugent.be/cornet

A. Supplemental Material for Chapter 2

A.1 Table S1. List of interactors in between ELO3 and Sec31

Table S1. List of interactors in between ELO3 and Sec31

Gene code	Protein name	Function
AT5G15550	transducin family protein	nucleotide binding
AT3G46040	RPS15AD	translation
AT5G14050	transducin family protein	nucleotide binding
AT4G31480	COPI vesicle coat;	vesicle-mediated transport COPI vesicle coat
AT4G02730	transducin family protein	signalling.G-proteins
AT2G36160	40S ribosomal protein S14 (RPS14A)	cell wall modification
AT5G15200	40S ribosomal protein S9 (RPS9B)	RNA methylation, translation
AT1G29310	SecY	protein secretion, protein transport
AT3G62310	RNA helicase, putative	RNA helicase activity, ATP-dependent helicase activity
AT4G09800	RPS18C	RNA methylation, ribosome biogenesis, translation
AT5G05010	clathrin adaptor complexes	intracellular protein transport, transport, vesicle-mediated transport
AT5G43900	MYA2	Golgi vesicle transport,
AT1G04600	XIA	actin cytoskeleton organization
AT4G10710	GLOBAL TRANSCRIPTION FACTOR C, SPT16	positive regulation of cell proliferation
AT4G04940	transducin family protein	mRNA splicing, via spliceosome
AT4G31490	coatomer beta subunit, putative	vesicle-mediated transport COPI vesicle coat
AT1G65030	transducin family protein	CUL4-RING ubiquitin ligase complex
AT1G34030	40S ribosomal protein S18 (RPS18B)	translation
AT1G16030	Hsp70b	response to endoplasmic reticulum stress, response to high light intensity
AT1G44900	ATP binding	cell proliferation
AT1G55150	DEAD box RNA helicase, putative (RH20)	helicase activity, ATP-dependent helicase activity,
AT1G59760	ATP-dependent RNA helicase	histone methylation, photomorphogenesis, positive regulation of transcription
AT3G10950	Zinc-binding ribosomal prote	ribosome biogenesis, translation
AT4G14160	ER to Golgi vesicle-mediated transport	ER to Golgi vesicle-mediated transport
AT5G02490	heat shock protein 2 (HSC70-2) (HSP70-2)	endoplasmic reticulum unfolded protein response
AT3G11510	40S ribosomal protein S14 (RPS14B)	RNA methylation, translation
AT1G72550	tRNA synthetase beta subunit	phenylalanyl-tRNA aminoacylation
AT3G60245	60S ribosomal protein L37a (RPL37aC)	ribosome biogenesis, translation
AT1G49540	ELONGATOR SUBUNIT 2, ELP2	histone acetylation, DNA-dependent DNA replication
AT1G34130	STT3B	protein glycosylation
AT3G21540	transducin family protein	RNA methylation, mRNA export from nucleus, protein import into nucleus
AT5G60670	60S ribosomal protein L12 (RPL12C)	ribosome biogenesis, translation
AT3G52580	40S ribosomal protein S14 (RPS14C)	translation
AT5G59850	40S ribosomal protein S15A	translation
AT3G21060	RBBP5 LIKE, RBL	vegetative to reproductive phase transition of meristem
AT1G20970	RPS15A	biological_process
AT1G07770	EDA7	translation
AT3G56990	EDA7, EMBRYO SAC DEVELOPMENT ARREST 7	megagametogenesis

AT3G12580	HEAT SHOCK PROTEIN 70, HSP70	response to endoplasmic reticulum stress, response to high light intensity
AT1G78720	SecY protein transport family protein	protein secretion, protein transport
AT1G63660	GMP synthase	asparagine synthase (glutamine-hydrolyzing) activity
AT2G40360	Transducin/WD40 repeat-like superfamily protein	protein maturation, rRNA processing, regulation of cell cycle
AT1G22780	PFL,	ribosome biogenesis, translation, translational initiation
AT1G26450	protein transport protein sec61	transport
AT2G34250	SecY protein transport family protein	ER to Golgi vesicle-mediated transport,
AT4G05410	YAO, YAOZHE	RNA methylation, acceptance of pollen
AT3G49660	WDR5A	G-protein coupled receptor signaling pathway
AT2G37190	Ribosomal protein L11 family protein	RNA methylation, response to cold, ribosome biogenesis, translation
AT2G47250	RNA helicase family protein	chloroplast envelope, membrane, nucleus

B. Supplemental Material for Chapter 3

B.1. Figure of qRT-PCR results (first biological replicate)
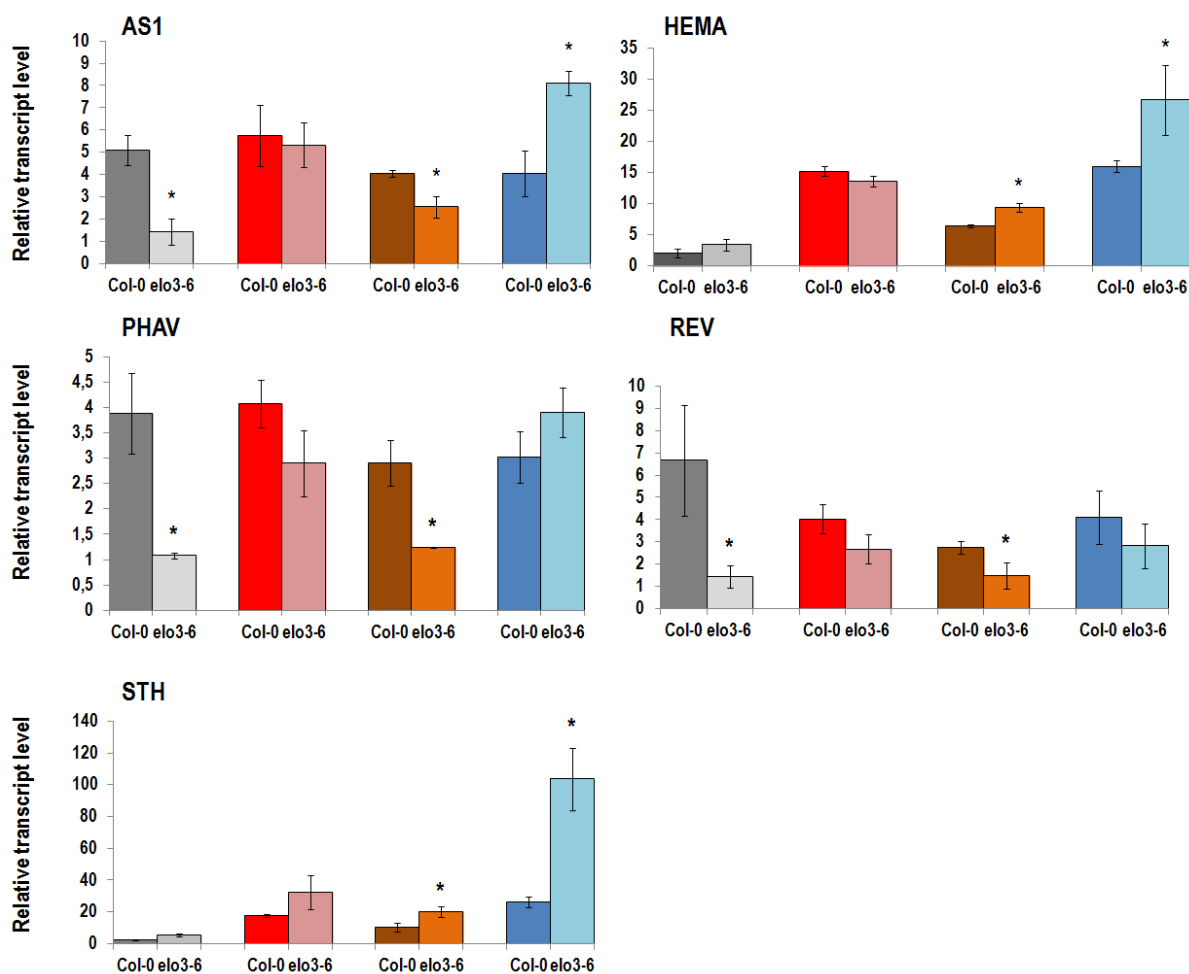
Figure S1 (exp1.) Gene expression analysis by qRT-PCR on gene involved in leaf development and chloroplast biosinthesys. Seedlings of *elo3-6* and Col-0 grown for four days in darkness and in red, far-red and blue light. The values were normalized with reference genes and analyzed by qBasePLUS. The error flags represent the standard deviation of four to six replicates. These data represent the first biological replicate.
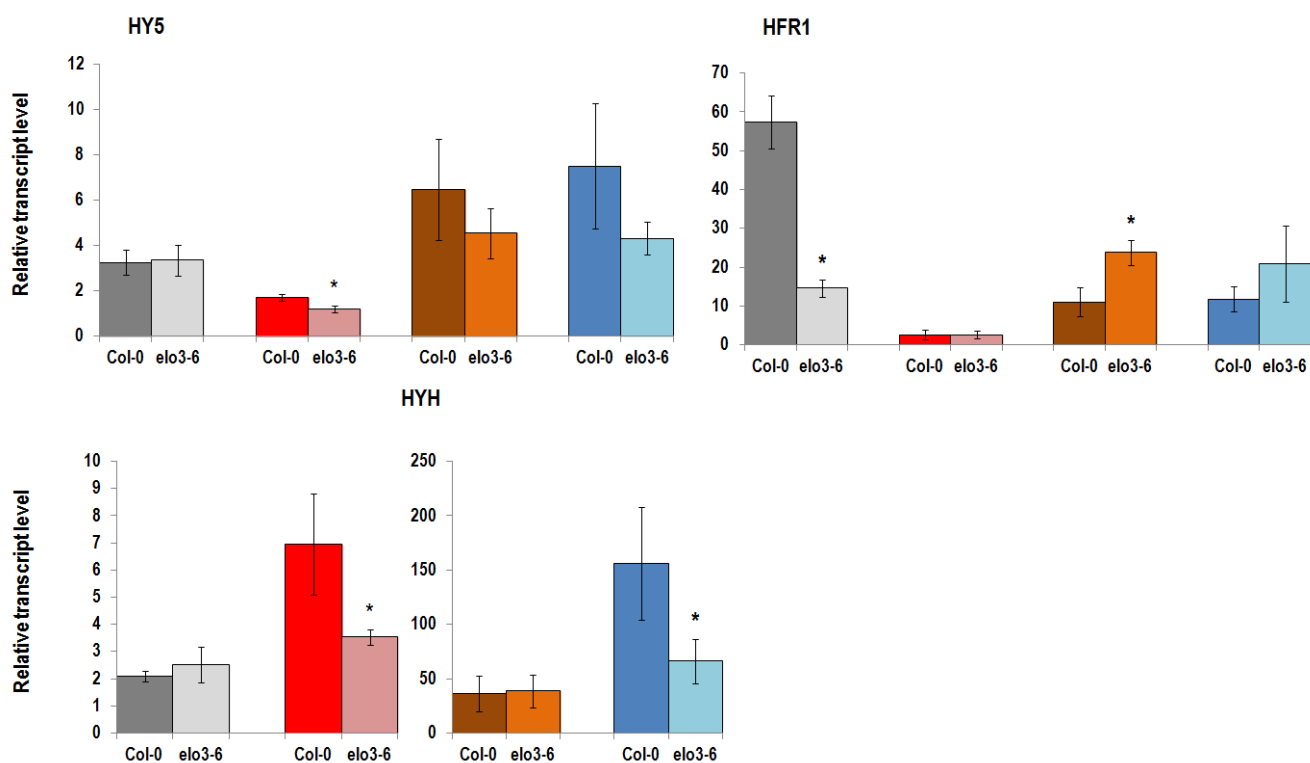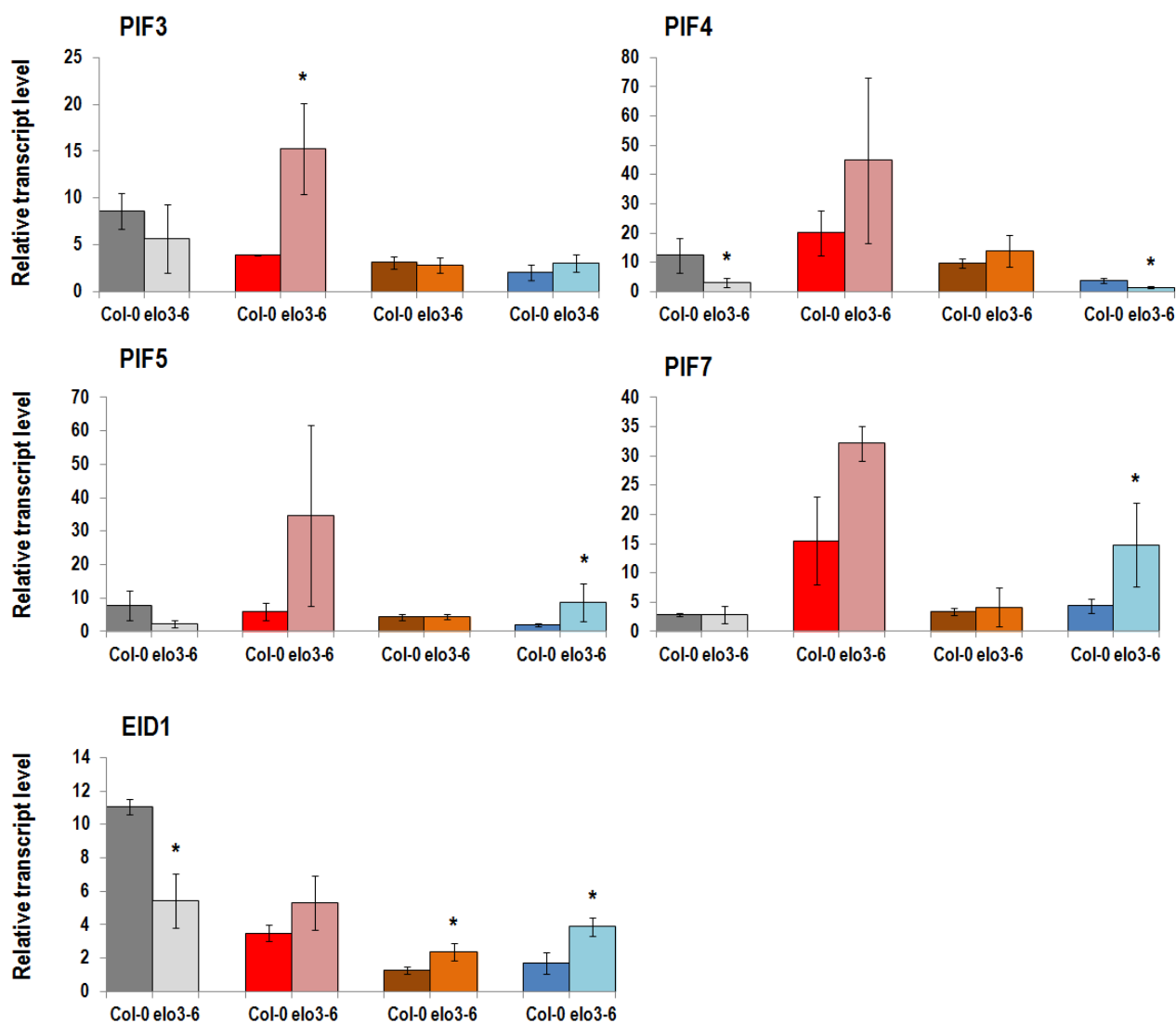
Figure S2 (exp1.) Gene expression analysis by qRT-PCR on positive regulator of photomorphogenesis. Seedlings of *elo3-6* and Col-0 grown for four days in darkness and in red, far-red and blue light. The values were normalized with reference genes and analyzed by qBasePLUS. The error flags represent the standard deviation of four to six replicates. These data represent the first biological replicate.
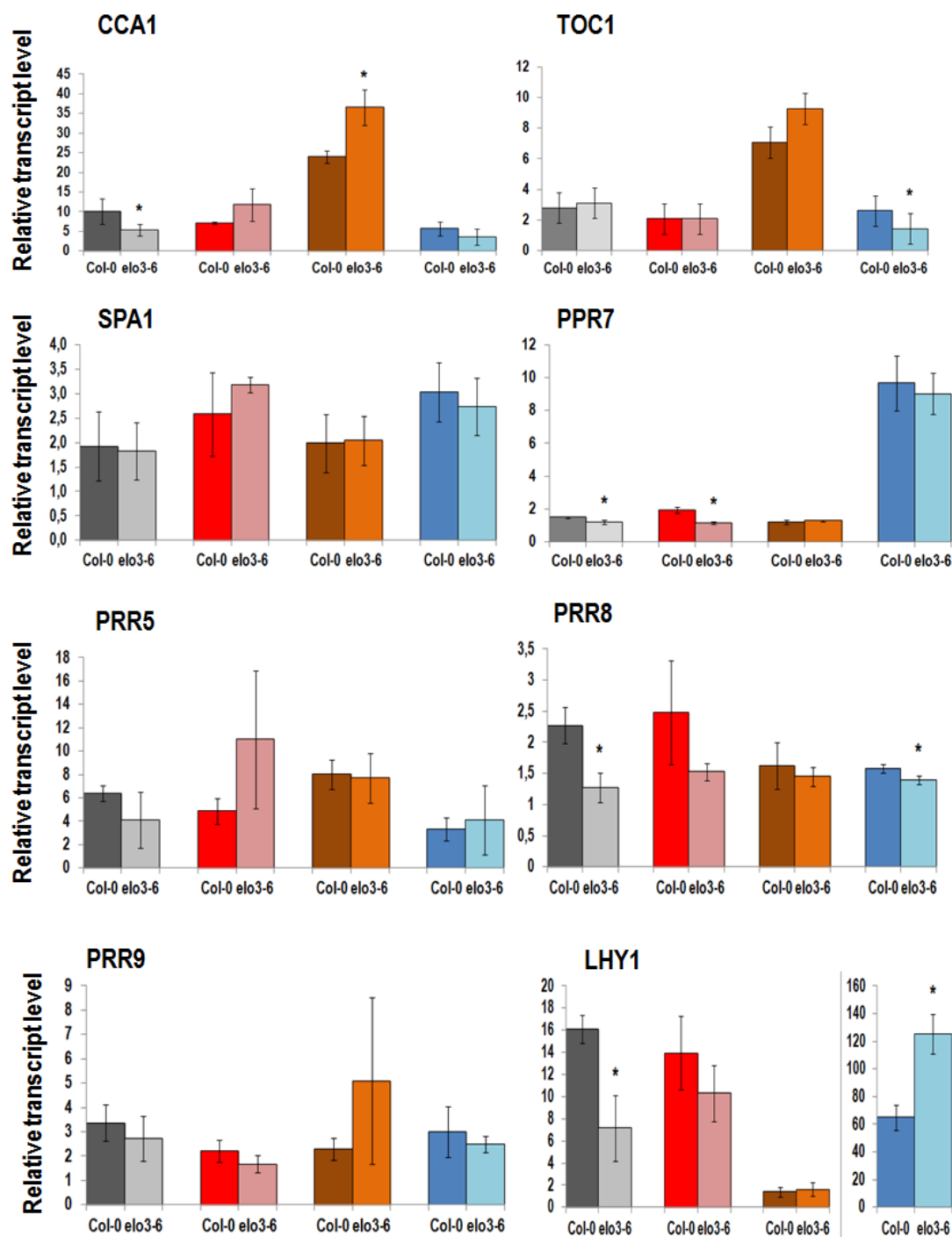
Figure S3 (exp1.) Gene expression analysis by qRT-PCR on positive regulator of skotomorphogenesis. Seedlings of *elo3-6* and Col-0 grown for four days in darkness and in red, far-red and blue light. The values were normalized with reference genes and analyzed by qBasePLUS. The error flags represent the standard deviation of four to six replicates. These data represent the first biological replicate.

Figure S4 (exp1.) Gene expression analysis by qRT-PCR on circadian clock genes. Seedlings of *elo3-6* and Col-0 grown for four days in darkness and in red, far-red and blue light. The values were normalized with reference genes and analyzed by qBasePLUS. The error flags represent the standard deviation of four to six replicates. These data represent the first biological replicate.

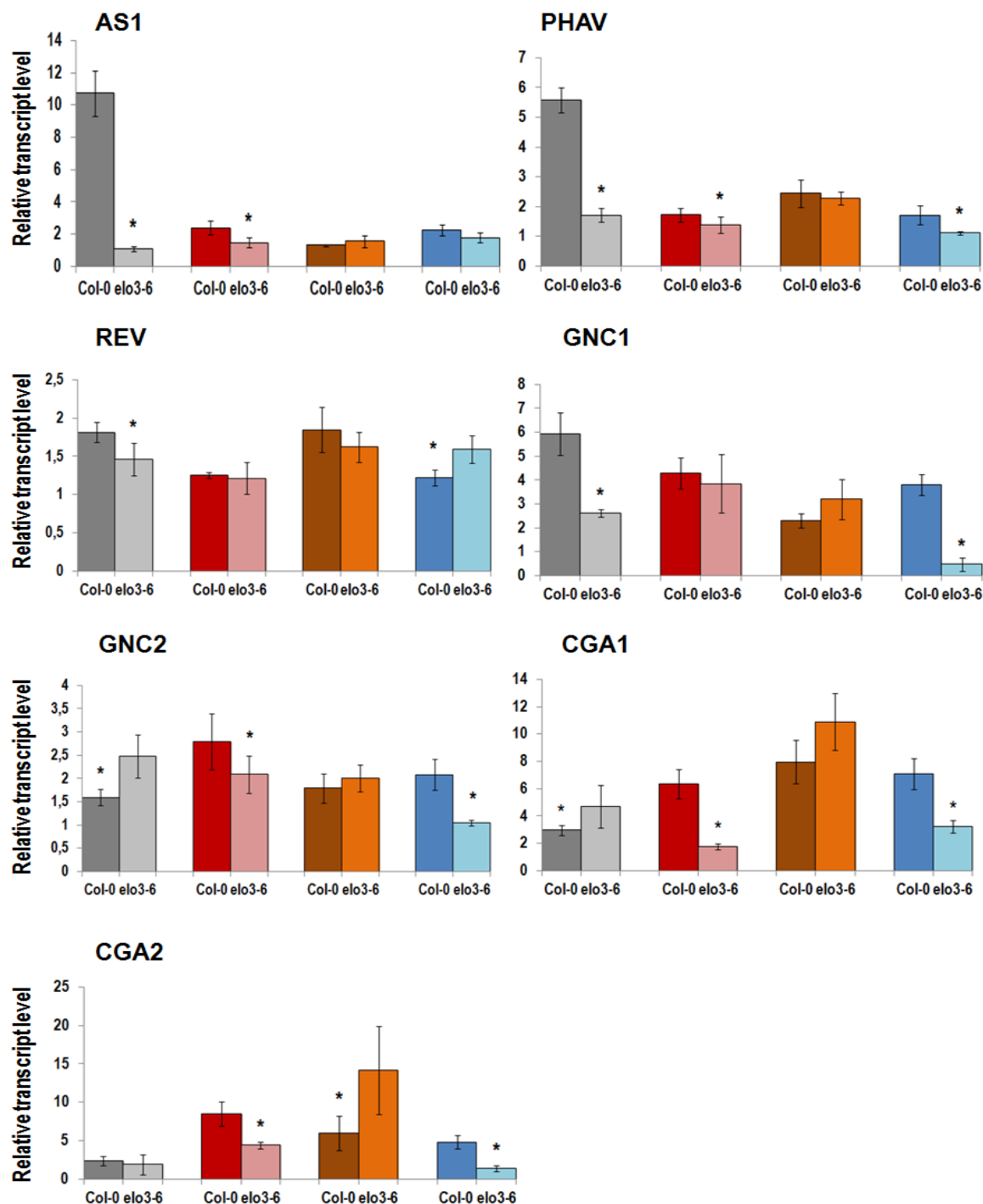## B.2. Figure of qRT-PCR results (second biological replicate)

Figure S5 (exp2.) Gene expression analysis by qRT-PCR on gene involved in leaf development and chloroplast biosinthesys. Seedlings of *elo3-6* and Col-0 grown for four days in darkness and in red, far-red and blue light. The values were normalized with reference genes and analyzed by qBasePLUS. The error flags represent the standard deviation of four to six replicates. These data represent the second biological replicate.
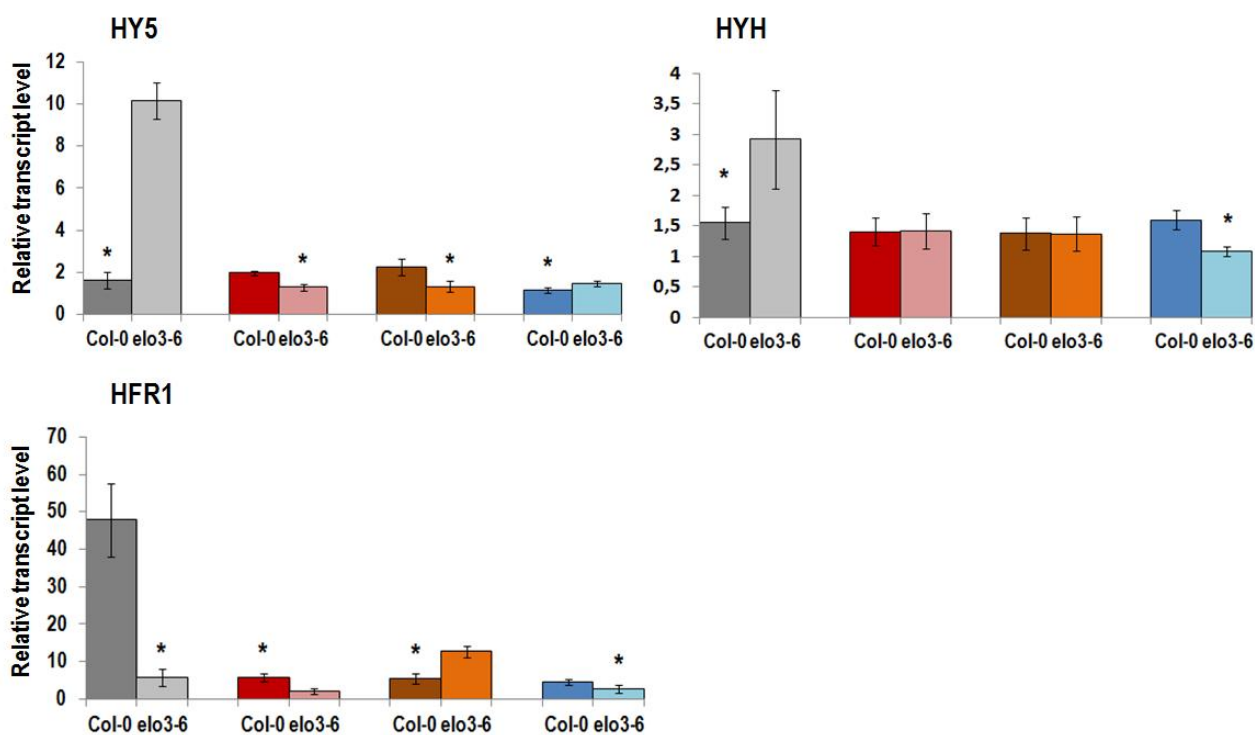
Figure S6 (exp2.) Gene expression analysis by qRT-PCR on positive regulator of photomorphogenesis. Seedlings of *elo3-6* and Col-0 grown for four days in darkness and in red, far-red and blue light. The values were normalized with reference genes and analyzed by qBasePLUS. The error flags represent the standard deviation of four to six replicates. These data represent the second biological replicate.
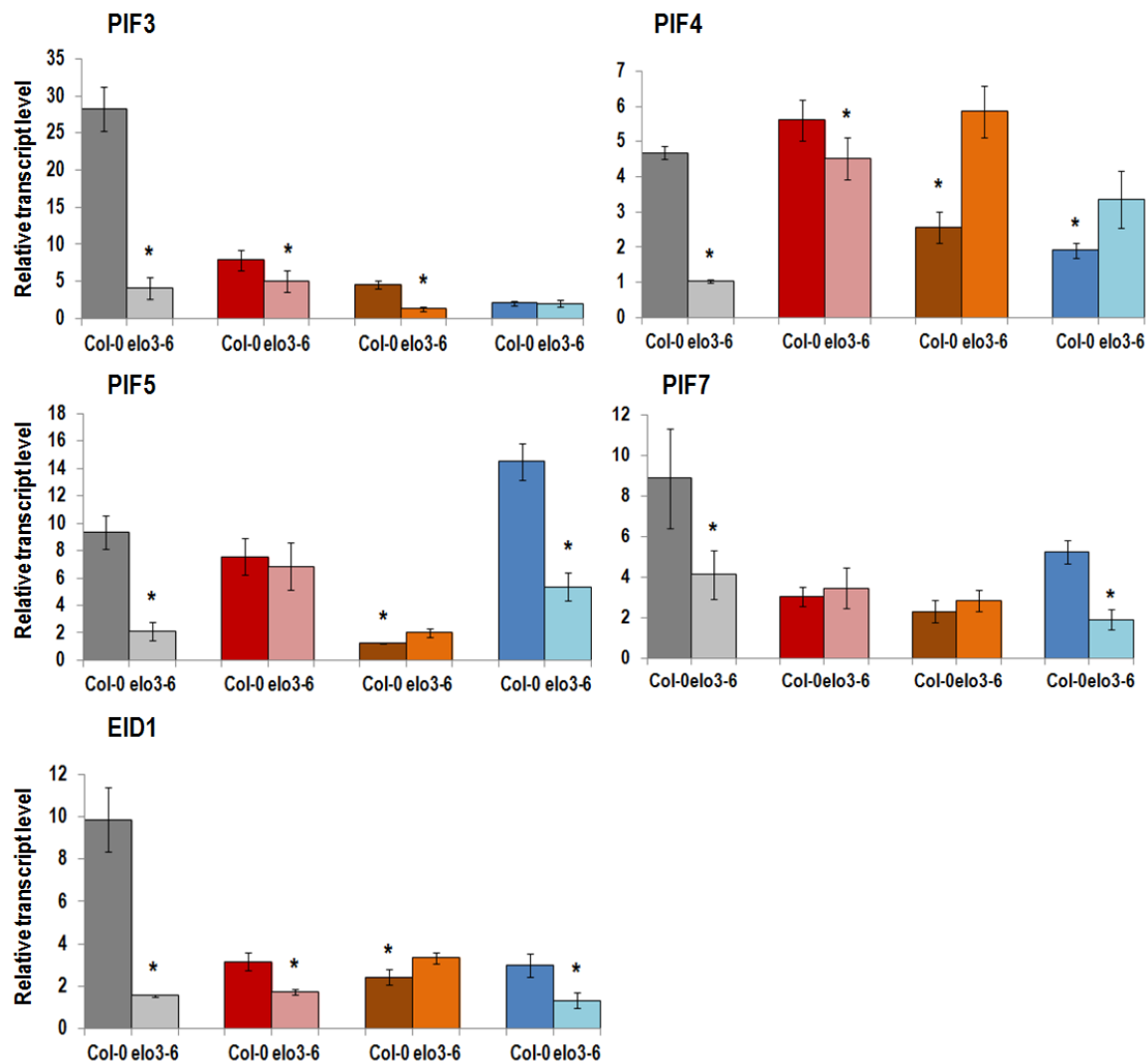
Figure S7 (exp2.) Gene expression analysis by qRT-PCR on positive regulator of skotomorphogenesis. Seedlings of *elo3-6* and Col-0 grown for four days in darkness and in red, far-red and blue light. The values were normalized with reference genes and analyzed by qBasePLUS. The error flags represent the standard deviation of four to six replicates. These data represent the second biological replicate.
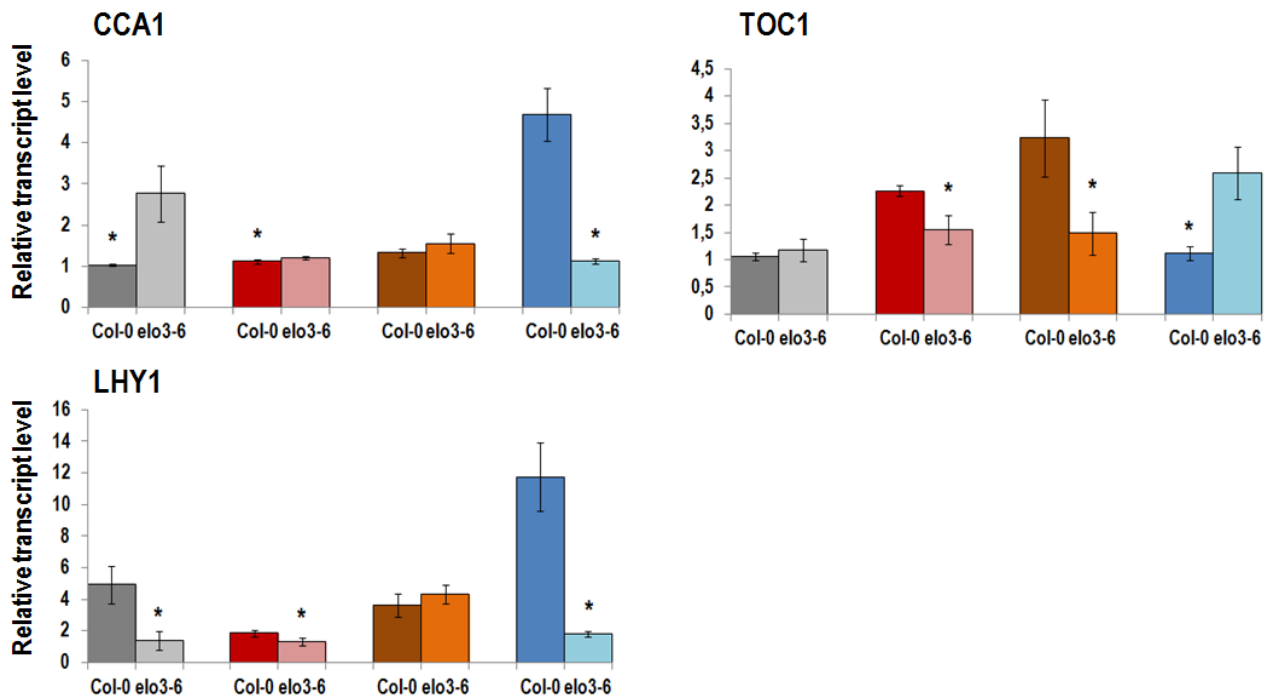
Figure S8 (exp2.) Gene expression analysis by qRT-PCR on circadian clock genes. Seedlings of *elo3-6* and Col-0 grown for four days in darkness and in red, far-red and blue light. The values were normalized with reference genes and analyzed by qBasePLUS. The error flags represent the standard deviation of four to six replicates. These data represent the second biological replicate.